Computer-Integrated Surgery (CIS) I
October 4, 2022
Hackerman B17

Bringing “the sixth sense” for surgeons using light and sound

Jeeun Kang, Ph.D.

Evolution of my personal interest

- **One-dimensional advances towards smaller clinical ultrasound (US) imaging**

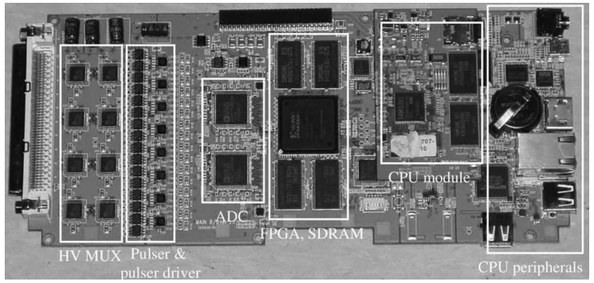

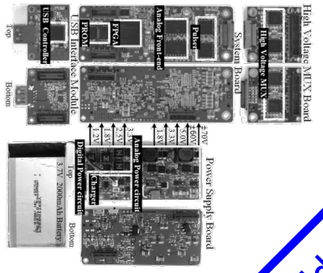

Could be nimbler in catching subtle temporal changes?

- **Higher spatiotemporal-spectral contrast**

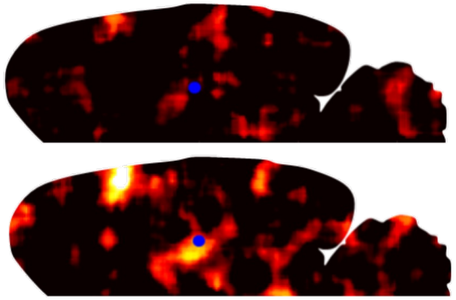

Neuroimaging

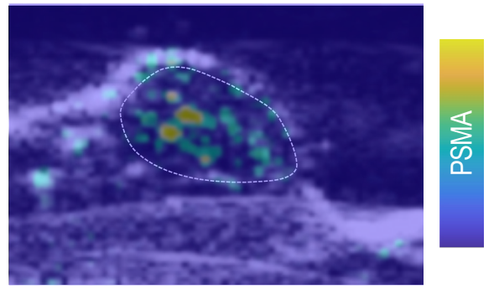

Tumor-targeted imaging

Could be more colorful?

- **Multi-modal imaging**

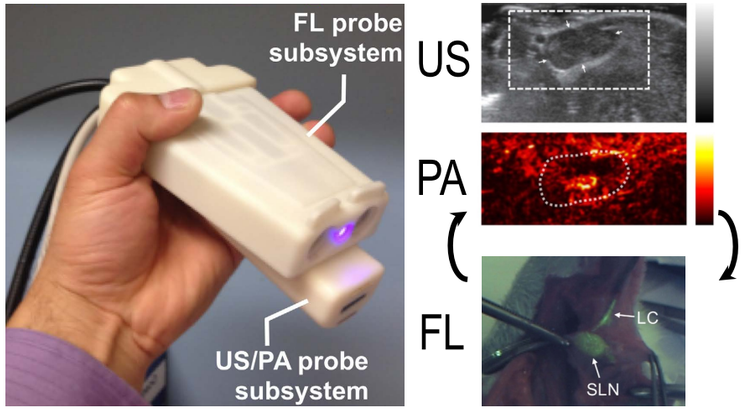

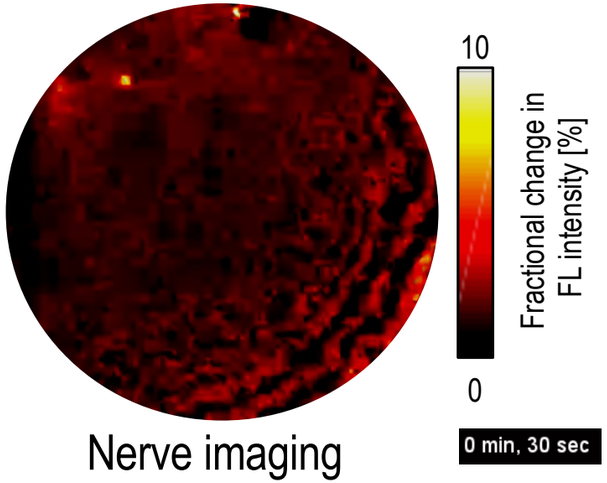

Nerve imaging

Defining the right form of “the sixth sense”

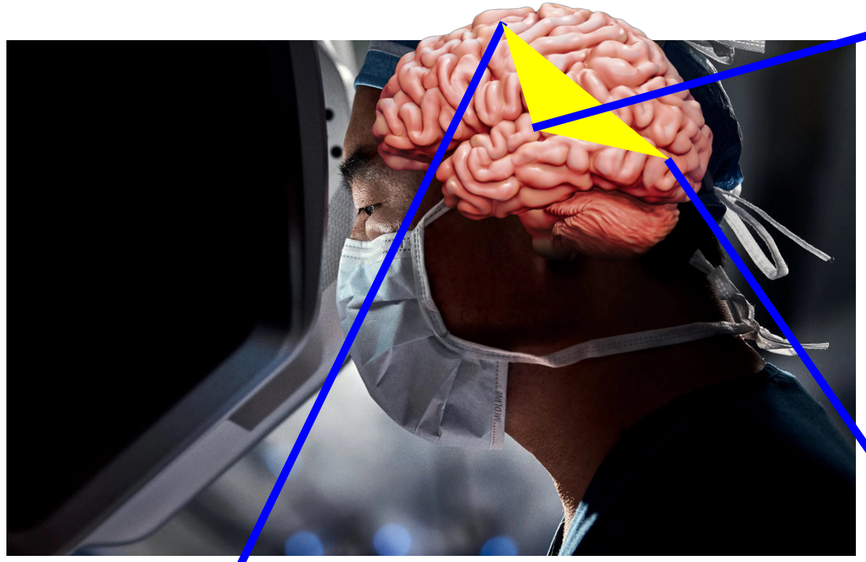

Knowledge in human anatomy &
body memory of surgical procedures

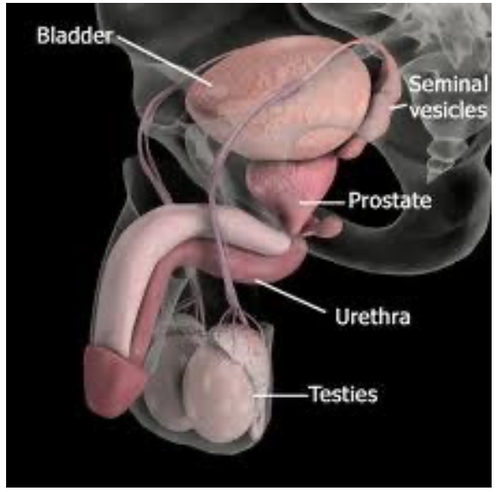

Vision: a dynamic input

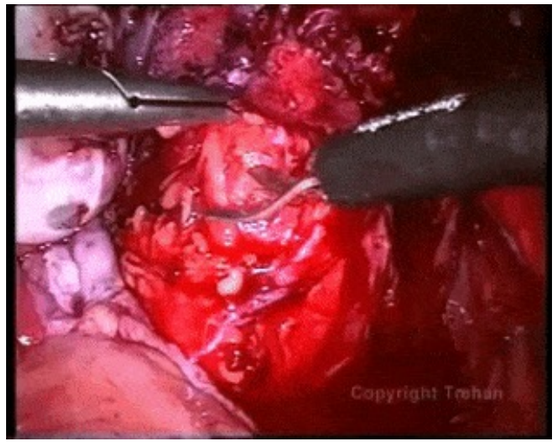

Crisp perception is a must for the new sixth sense

- High spatiotemporal resolution
- High contrast resolution
- Wide volumetric field-of-view
- Real-time feedback
- No surgical interruption

Current state-of-the-art in intra-operative guidance

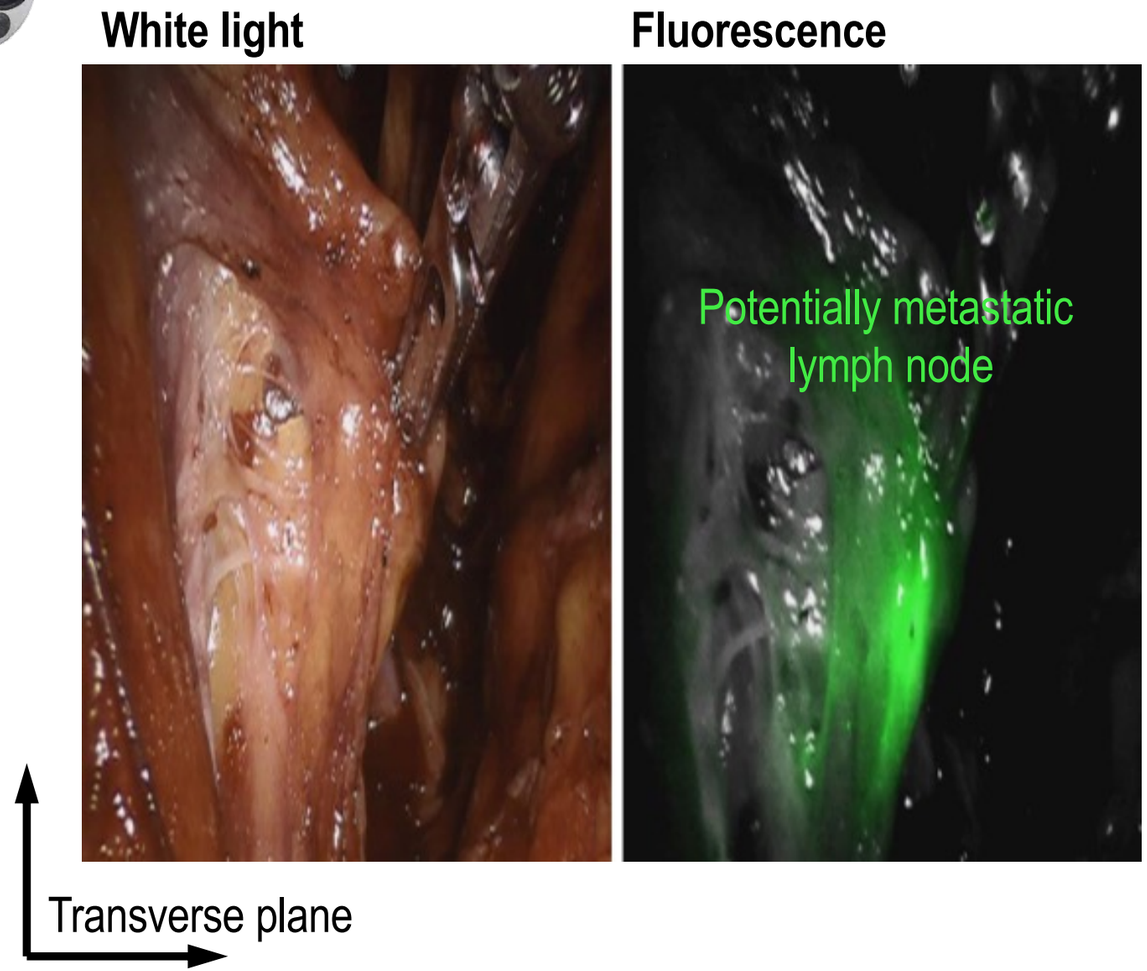

† Manny, T. B., Patel, M. & Hemal, A. K. *Eur Urol* **65**, 1162–1168 (2014).

Current state-of-the-art in intra-operative guidance

Fluorescence imaging †

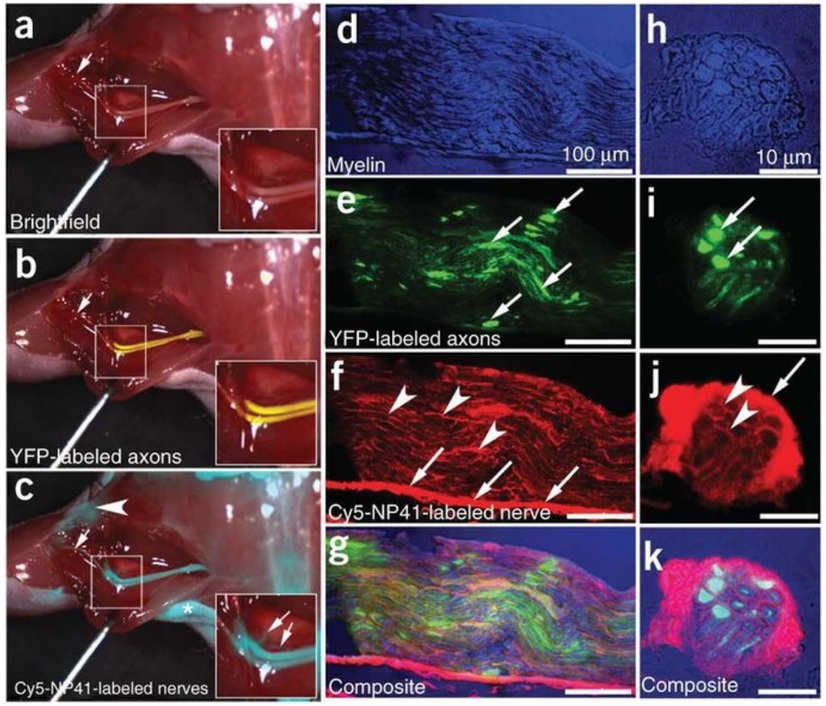

- Only 2-dimensional perception with *en face* imaging FOV

Confocal / multiphoton microscopy & Raman spectroscopy

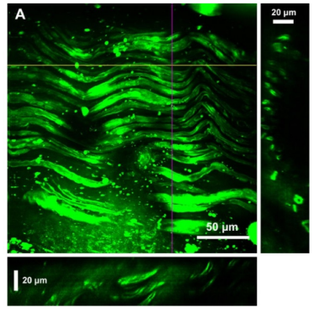

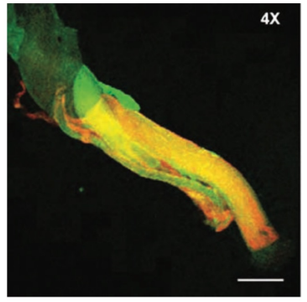

- Slow imaging
- Limited imaging depth & FOV

Optical coherence tomography (OCT) ‡

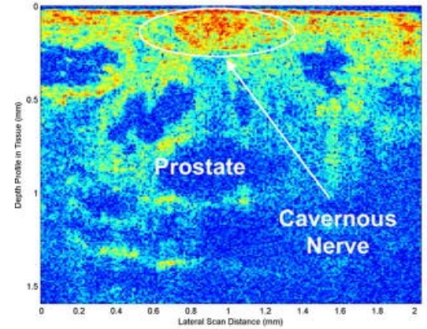

- Small FOV in few mm diameter
- Limited contrast resolution

X-ray §

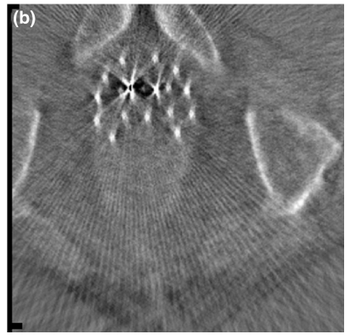

- Ionizing effect
- Interrupt the surgical procedure

Prostate MRI §

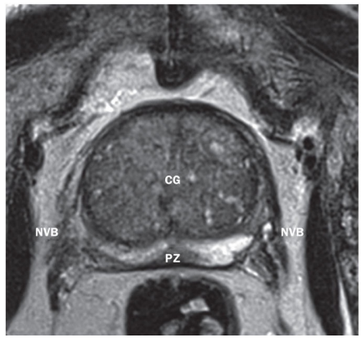

- Challenging for intra-operative use

† Whitney, M. A. et al. Nat Biotechnol 29, 352–356 (2011).
‡ Chitchian, S., et al., J. Biomed. Opt. 14, 014031-14-6 (2009).
§ A. L. Burnett, Nat. Rev. Urol. 12, 451-460 (2015).

Medical ultrasound

Anatomical

A-Scan

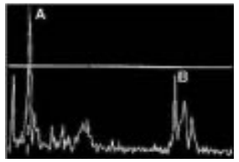

Static 2D compound

1D array (e-scan)

2D Dynamic focusing

3D/4D imaging

Synthetic aperture focusing

1950 1960 1970 1980 1990 2000 2010 2020

Functional & Molecular

Flow

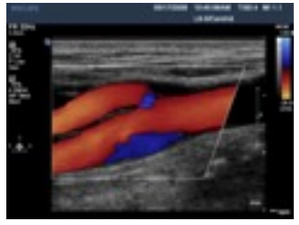

CA

Elastography

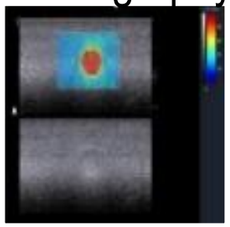

Photoacoustics

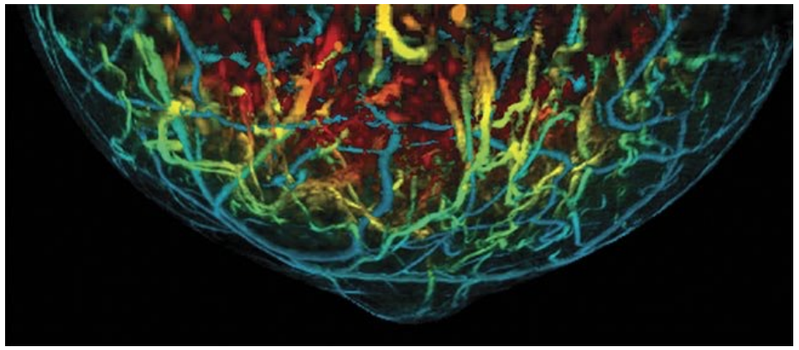

Prostate Cancer (PCa)

- PCa is a **leading organ for new cancer cases** for males, (21% in total cancer diagnosis) resulting **second highest cancer deaths** †
- High survival rate when localized, but **survival rate drops with metastasis**
- **Early PCa detection & accurate surgery for negative tumor margin** are the best defense strategy

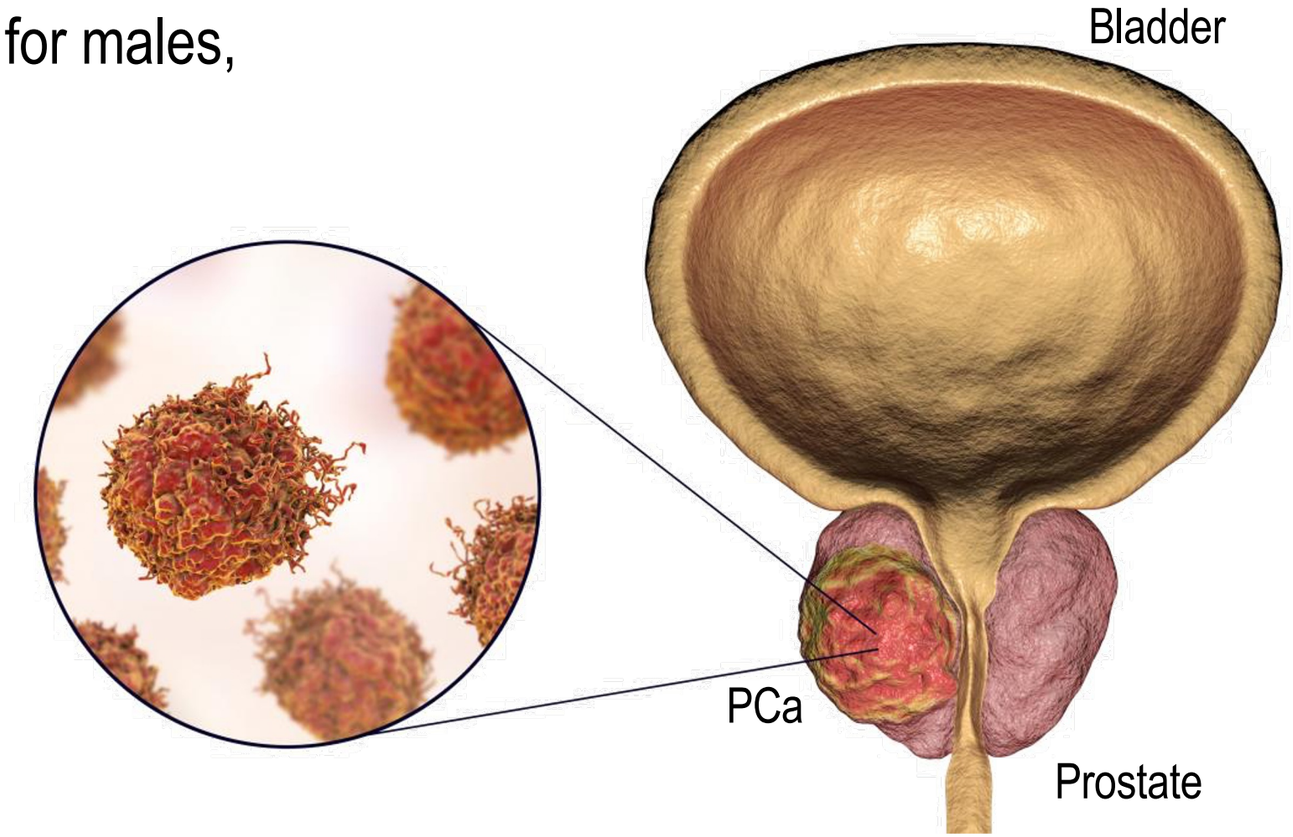

† Siegel, R. L., *et al.*, Cancer statistics, 2016. *CA: A Cancer Journal for Clinicians* **66**, 7 30 (2016).

Clinical US imaging of PCa

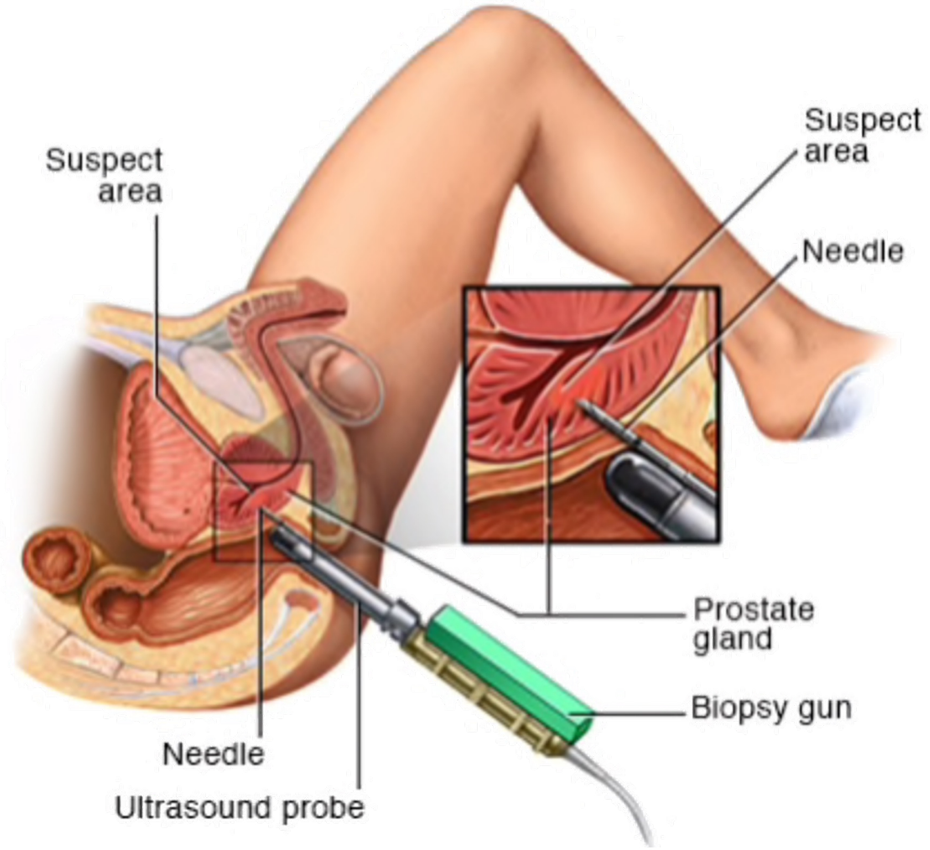

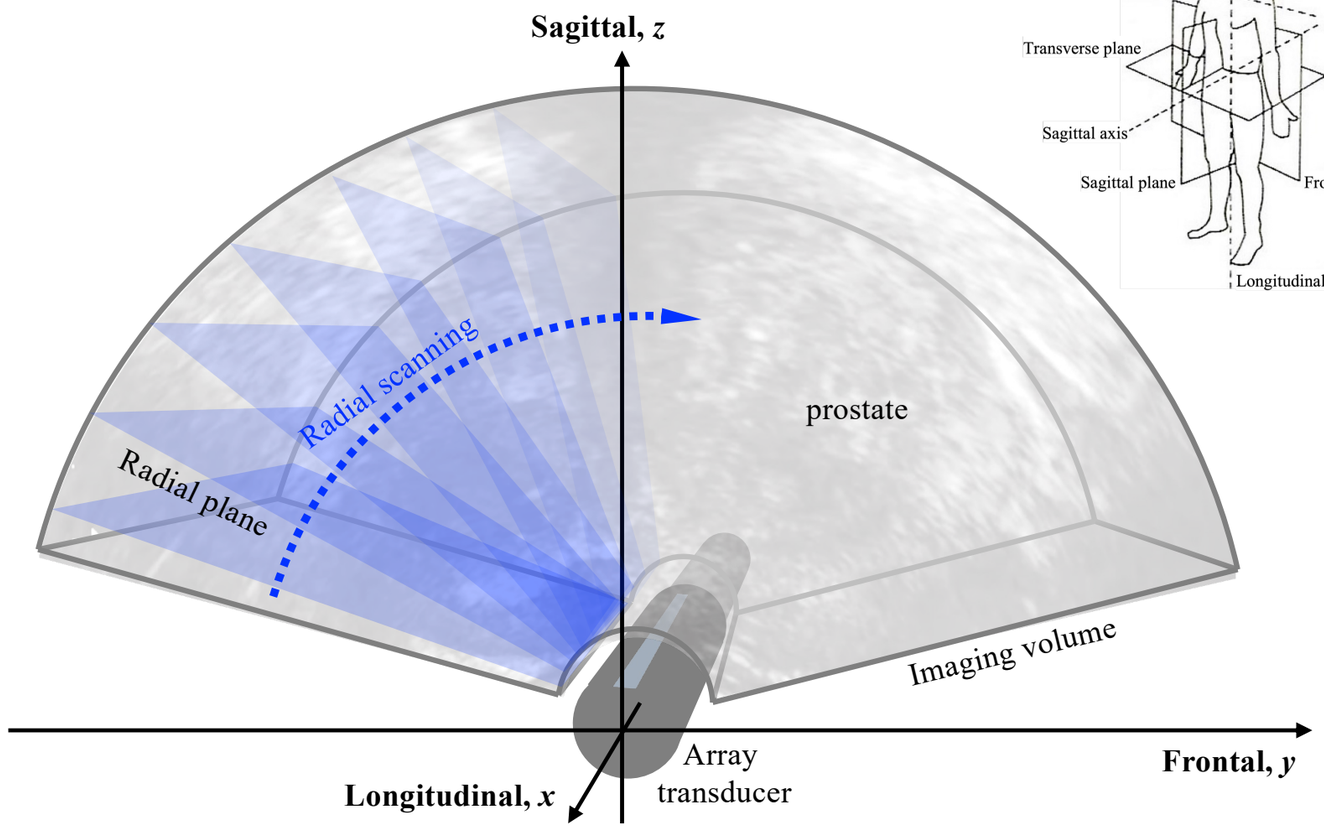

PCa management in healthcare

Prostate-Specific Antigen (PSA) †

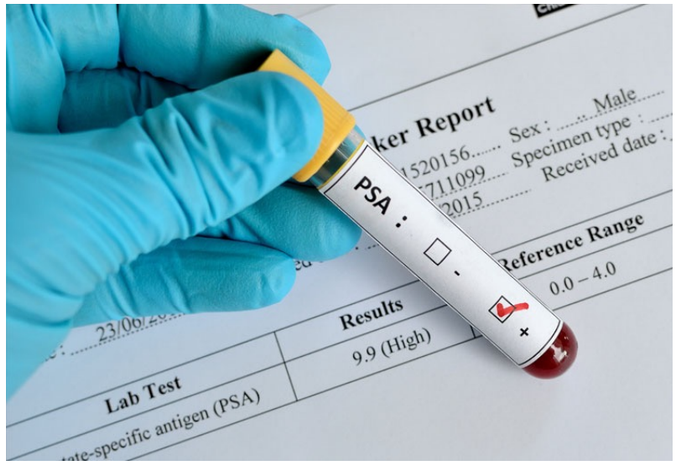

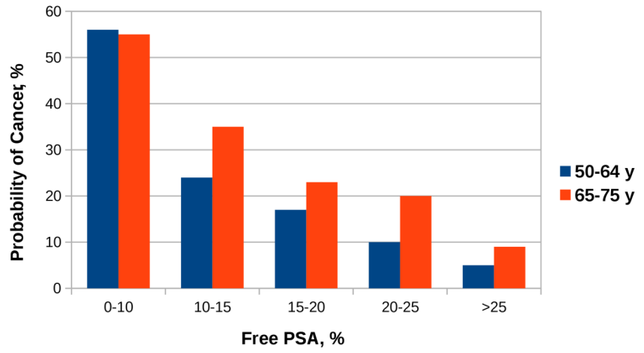

- High false-positive rate (75%) †

MRI
PET/CT

Transrectal US-guided biopsy

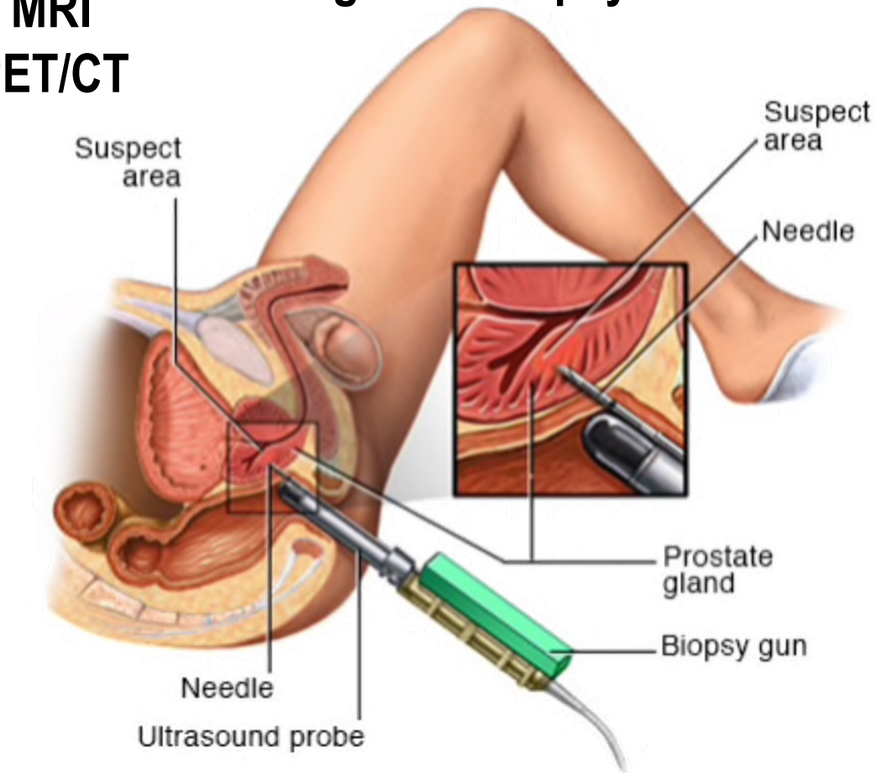

- The prevalence of nearly invisible PCa on TRUS ranges from 25 to 42% ♀

Histopathology

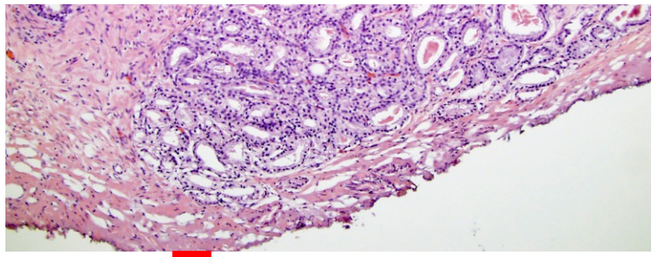

Prostatectomy guidance

- Post-operative complications: erectile dysfunction (59.9% at 18M); incontinence (8.4% at 18M)

† Catalona W, *et al.*, *JAMA*. **279** (19): 1542 – 7 (1998).
‡ Slatkoff S., et al., *J. Fam. Pract.* **60** (6): 357 – 60 (2011).
♀ Piao D., *et al.*, *IEEE J. Selec. Topics in Quantum. Electron.*, **16** (4): 715 – 29 (2009).

Mission

Prostate-Specific Antigen (PSA) †

- High false-positive rate (75%) †

MRI
PET/CT

Transrectal
US-guided biopsy

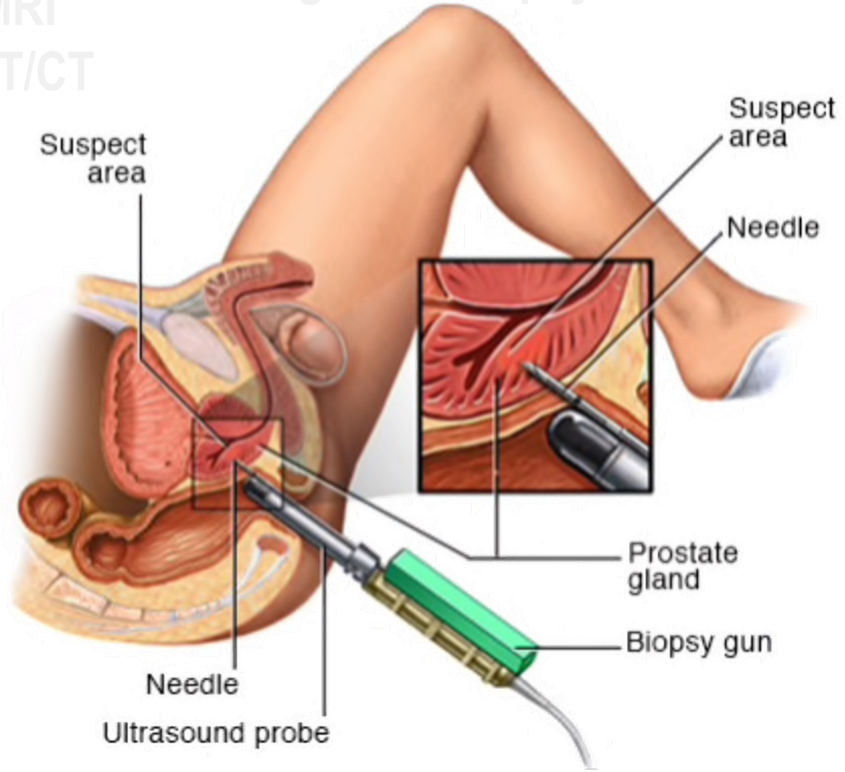

- The prevalence of nearly invisible PCa on TRUS ranges from 25 to 42% ♀

Histopathology

- **Higher spatial resolution**

Prostatectomy guidance

- **Molecular contrast**

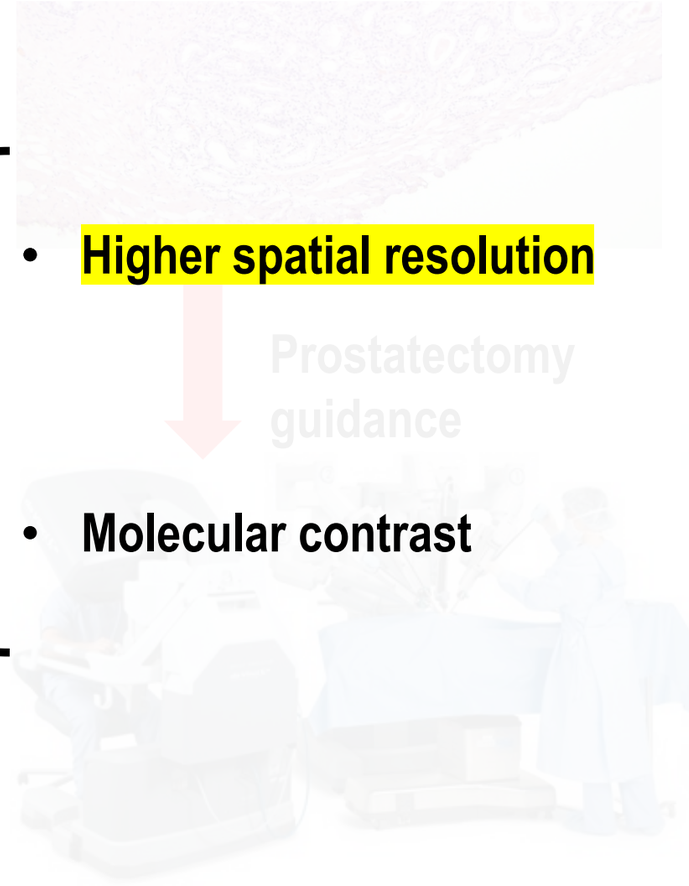

- Post-operative complications: erectile dysfunction (59.9% at 18M); incontinence (8.4% at 18M)

† Catalona W, *et al.*, *JAMA*. **279** (19): 1542 – 7 (1998).
† Slatkoff S., et al., *J. Fam. Pract.* **60** (6): 357 – 60 (2011).
♀ Piao D., *et al.*, *IEEE J. Selec. Topics in Quantum. Electron.*, **16** (4): 715 – 29 (2009).

Limited aperture, but desire to see more – What shall we do?

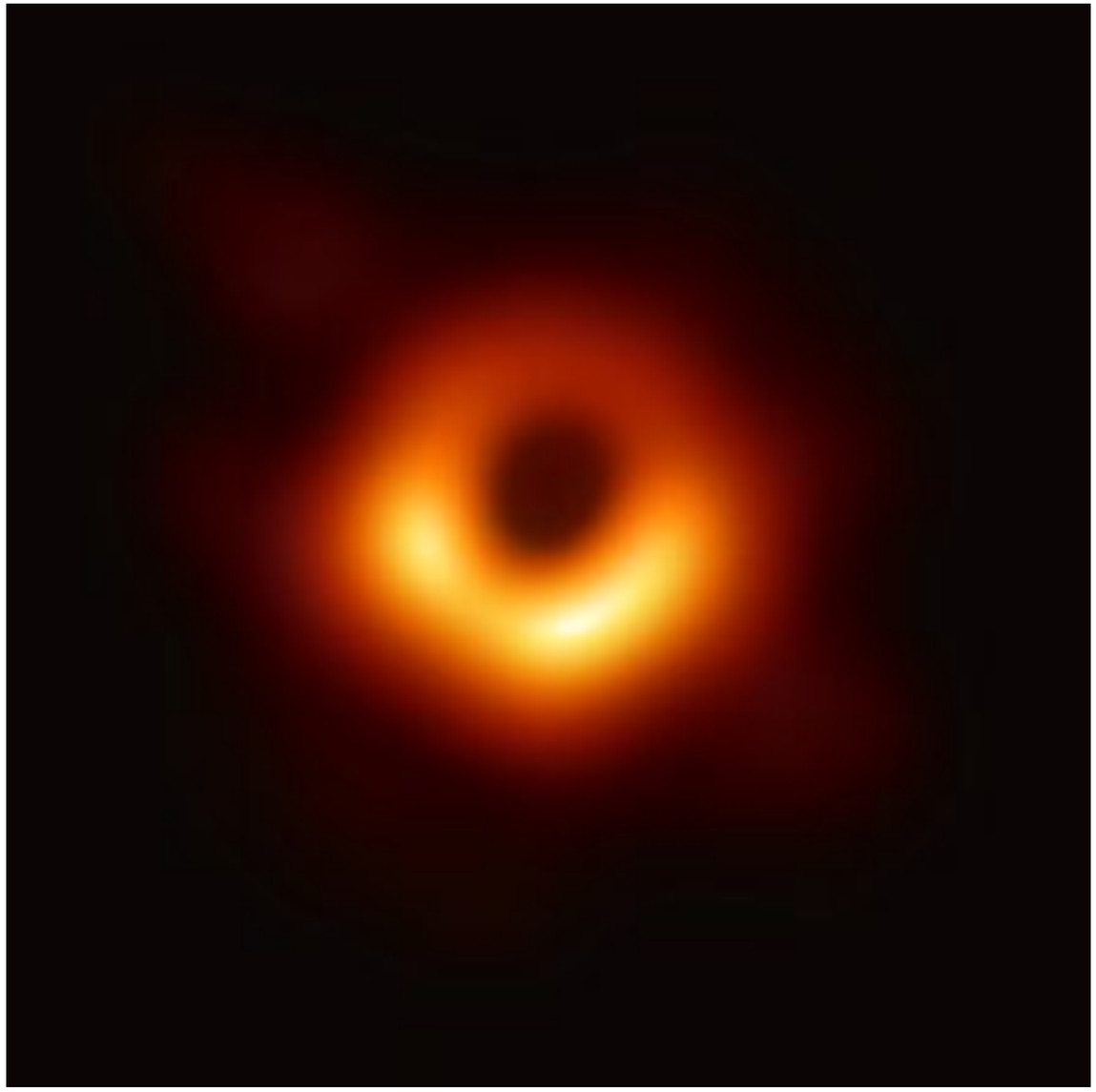

Synthetic aperture focusing?

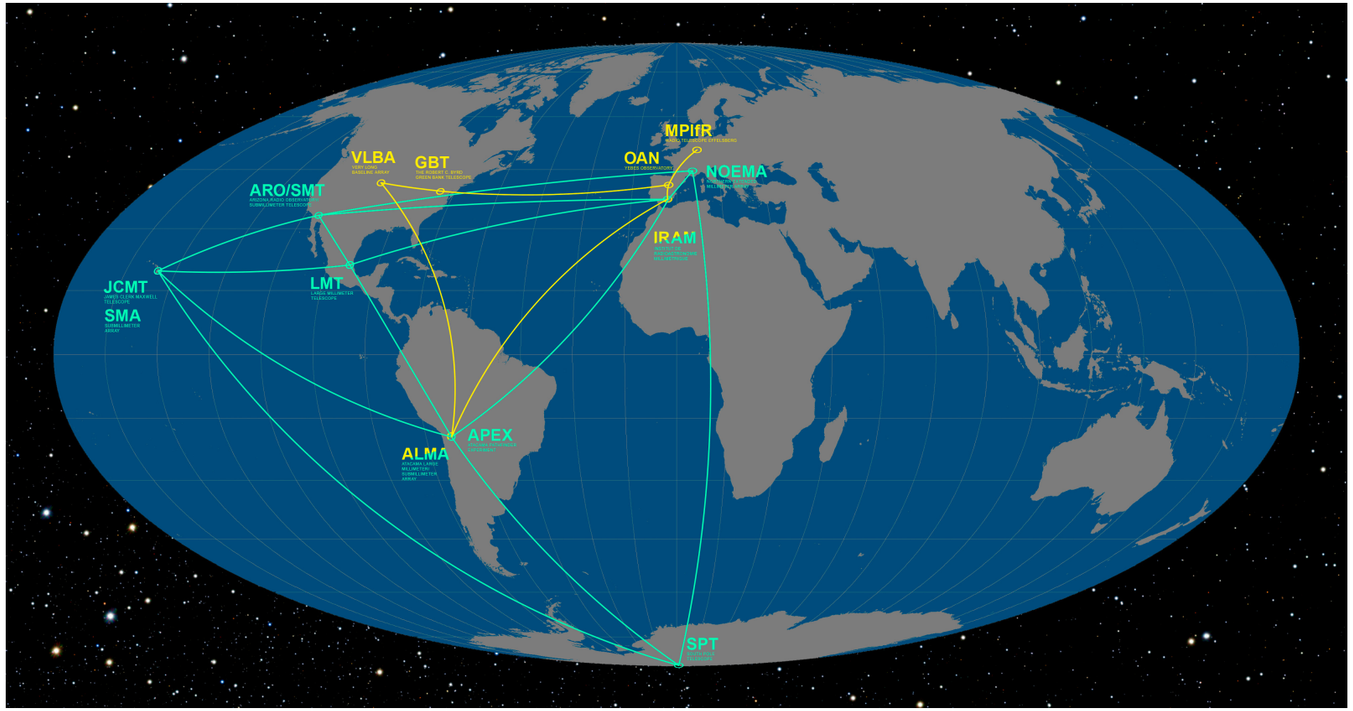

Event Horizon Telescope

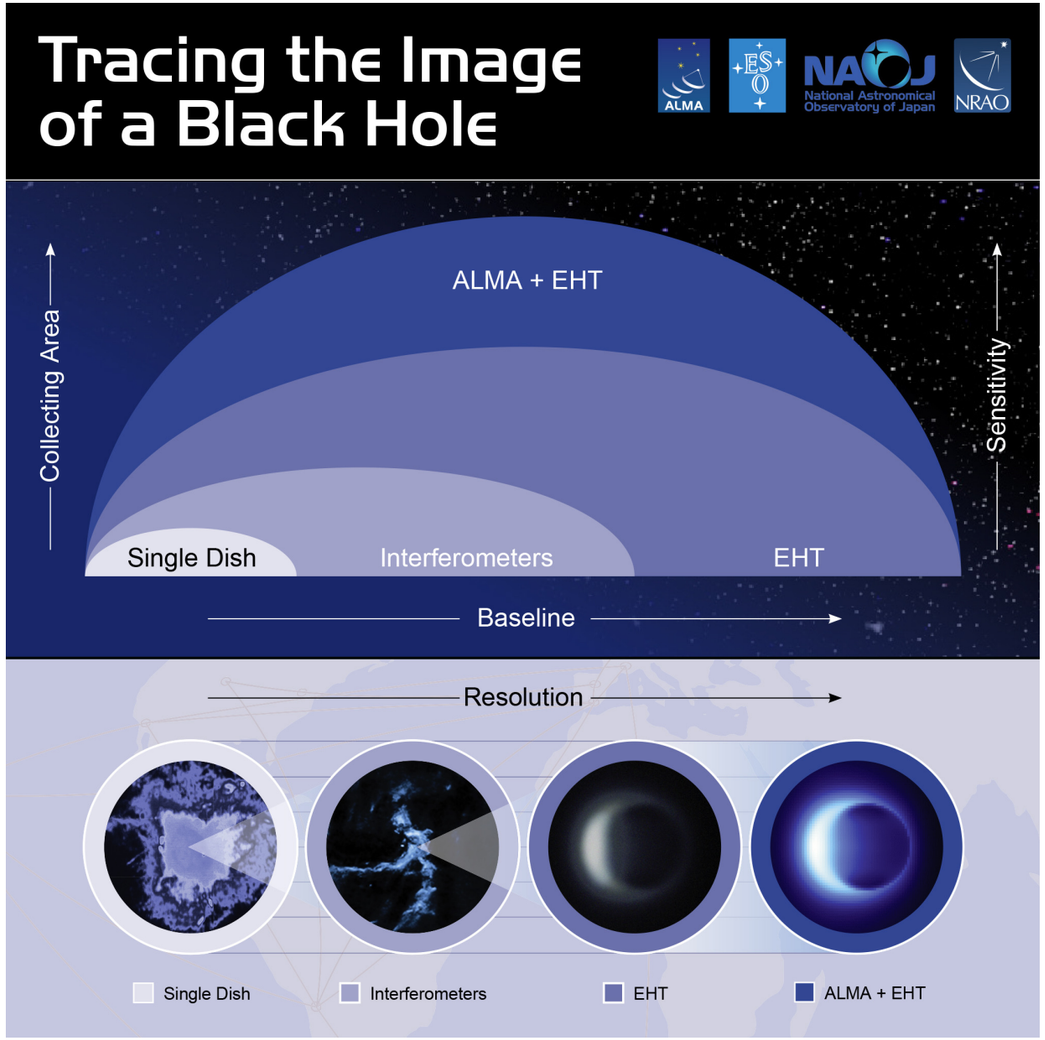

Synthetic “lateral” aperture focusing in medical ultrasound

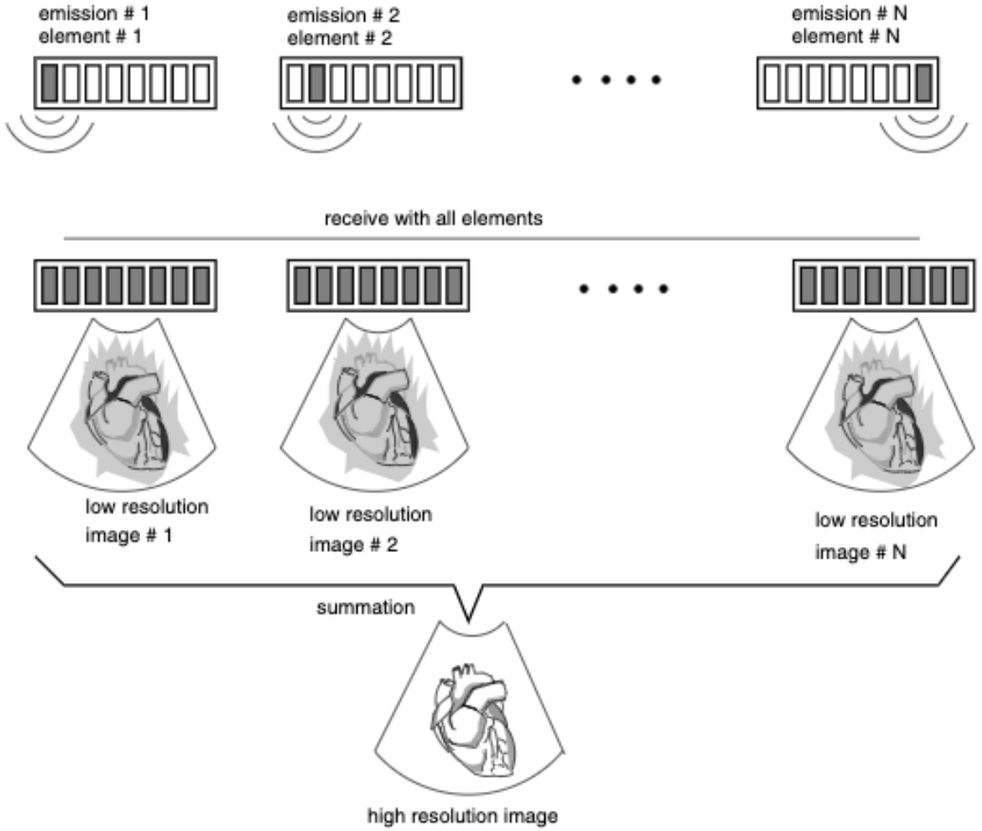

Fig. 1. Basic principle of synthetic aperture ultrasound imaging (from [25]).

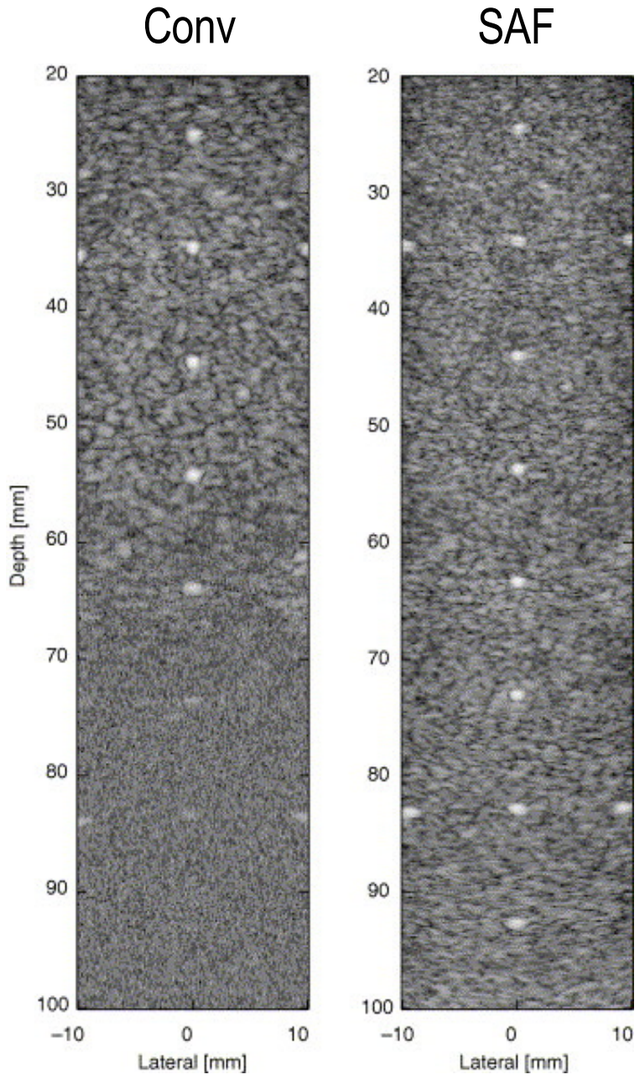

† Bae, S., Kim, P., Song, T. K., *J Acou Soc Am* **144**(5), 2627-2644 (2018).
Chang, J. H., Song, T. K., *IEEE Trans Ultrason Ferroelect, Freq Control* **58**(2), 327-337 (2011).

Forget about something?

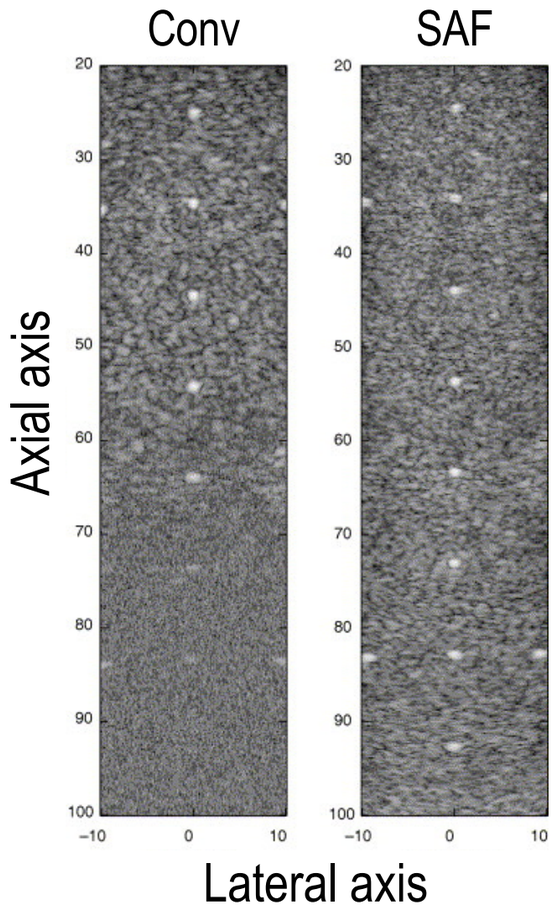

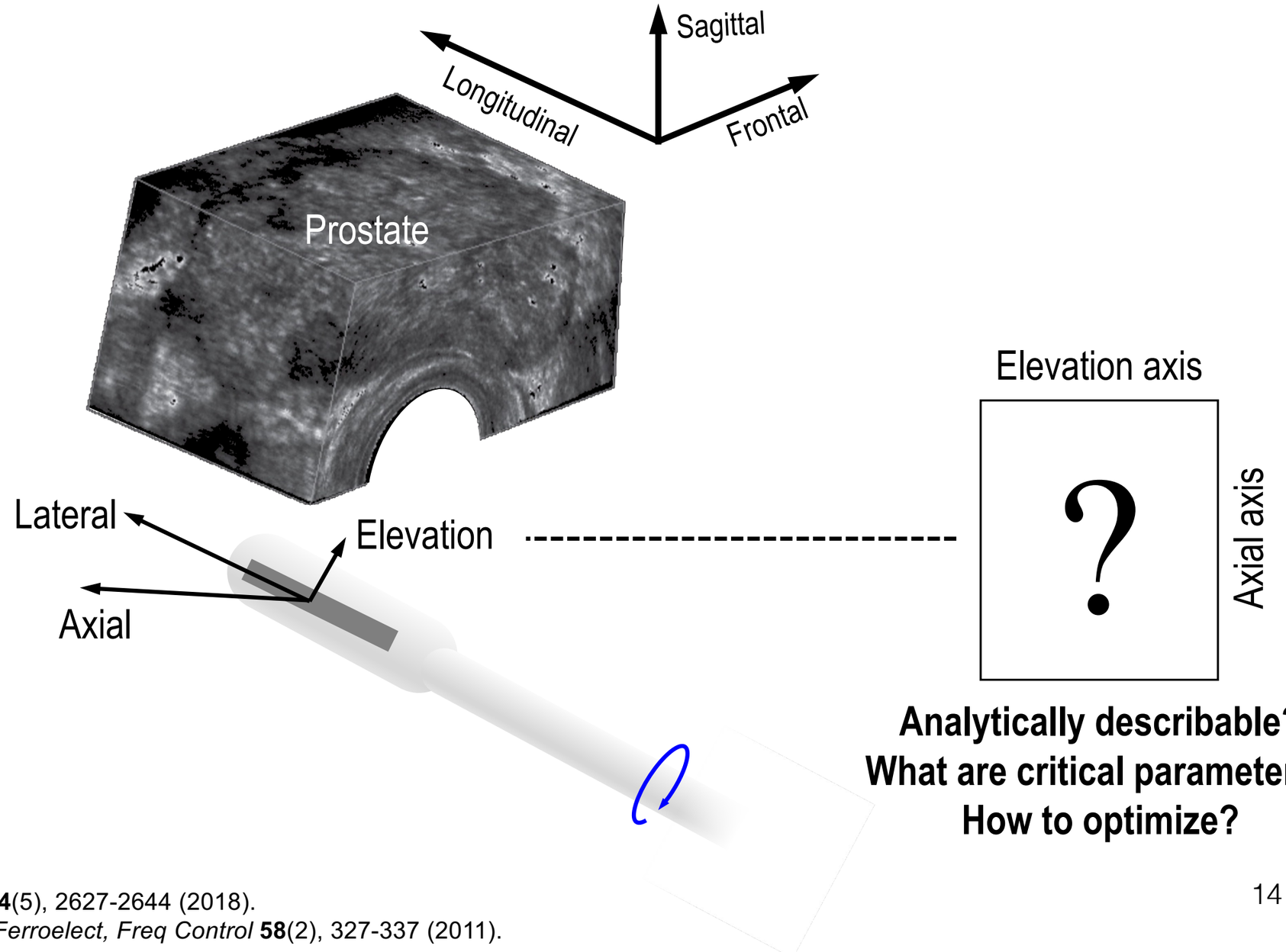

Analytically describable?
What are critical parameters?
How to optimize?

† Bae, S., Kim, P., Song, T. K., *J Acou Soc Am* **144**(5), 2627-2644 (2018).
Chang, J. H., Song, T. K., *IEEE Trans Ultrason Ferroelect, Freq Control* **58**(2), 327-337 (2011).

Synthetic “radial” aperture focusing (rSAF)

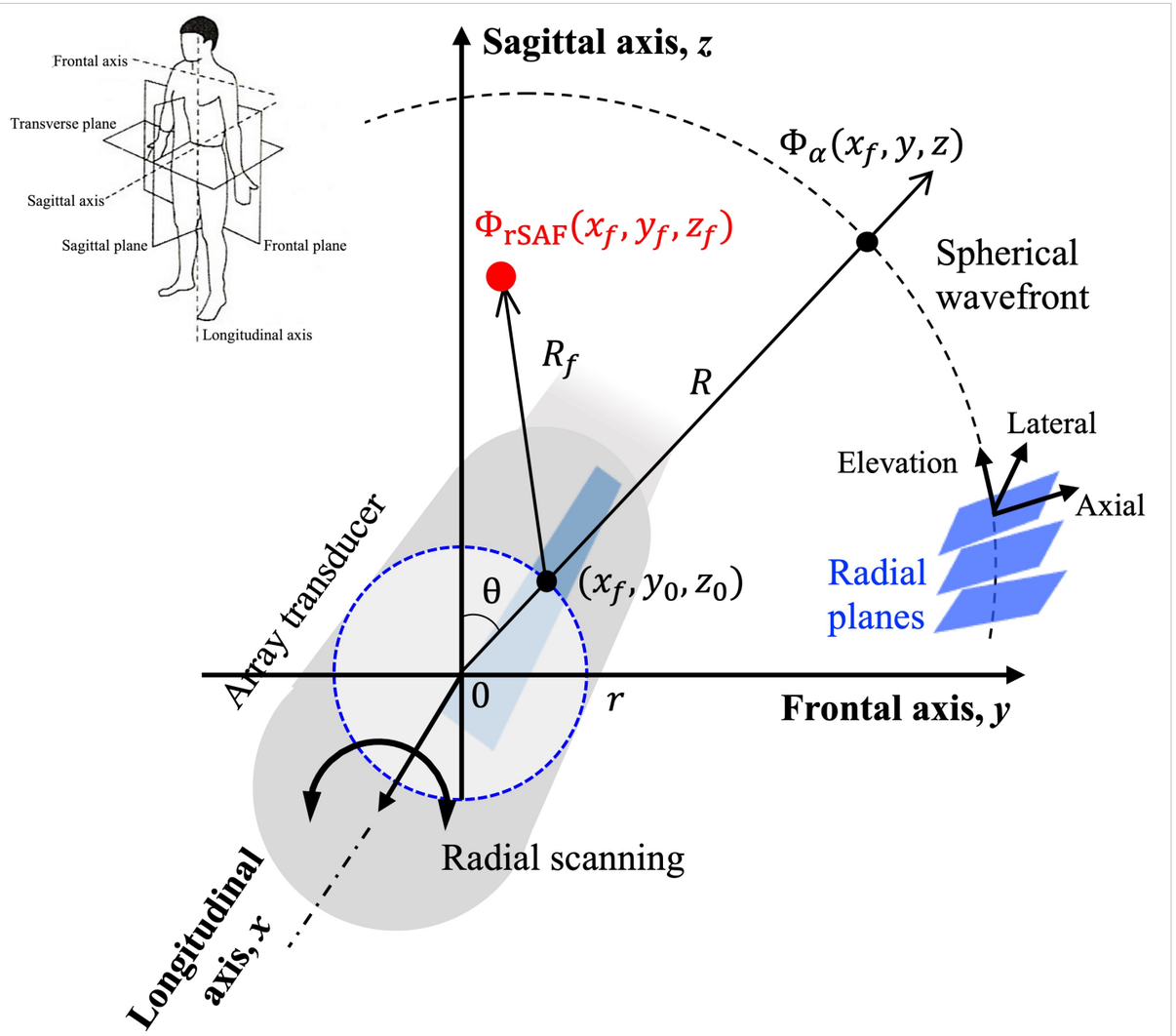

Acoustic field expression of single transmission

$$\Phi_\alpha(y,z,t) = \frac{e^{-j\omega t}}{j\lambda\|R\|_2}\Psi_\alpha(y,z)$$

Continuous transmit beam pattern at a depth of R

$$\Psi_\alpha(y,z) = e^{jkR} = e^{jk\sqrt{(y-r\alpha)^2+(z-r\beta)^2}}$$

Transducer parameters: $r = \sqrt{y_o^2 + z_0^2}$, $k = 2\pi/\lambda$

Scanning parameters: $\theta = \sin^{-1}\alpha$, $\beta = \cos\theta$

Synthetic transmit aperture focused beam pattern at (y_f, z_f)

$$\Psi_{\mathrm{rSAF}}(y_f, z_f) = c_0 \int_{-\infty}^{\infty} p_s(\alpha)\tau(\alpha)\Psi_\alpha(y,z)\,d\alpha$$

Scale factor

$$c_0 = \frac{1}{j\lambda\|R\|_2}$$

Synthetic focusing delay

$$\tau(\alpha) = e^{-jk\sqrt{(y_f-r\alpha)^2+(z_f-r\beta)^2}}$$

† H. Song, **J. Kang***, *J Comput Des Eng* **9**, 1774-1787 (2022).
J. Kang, et al., US Patent 63/355,525 (2022).

Analytical solution for synthetic radial aperture focusing (rSAF)

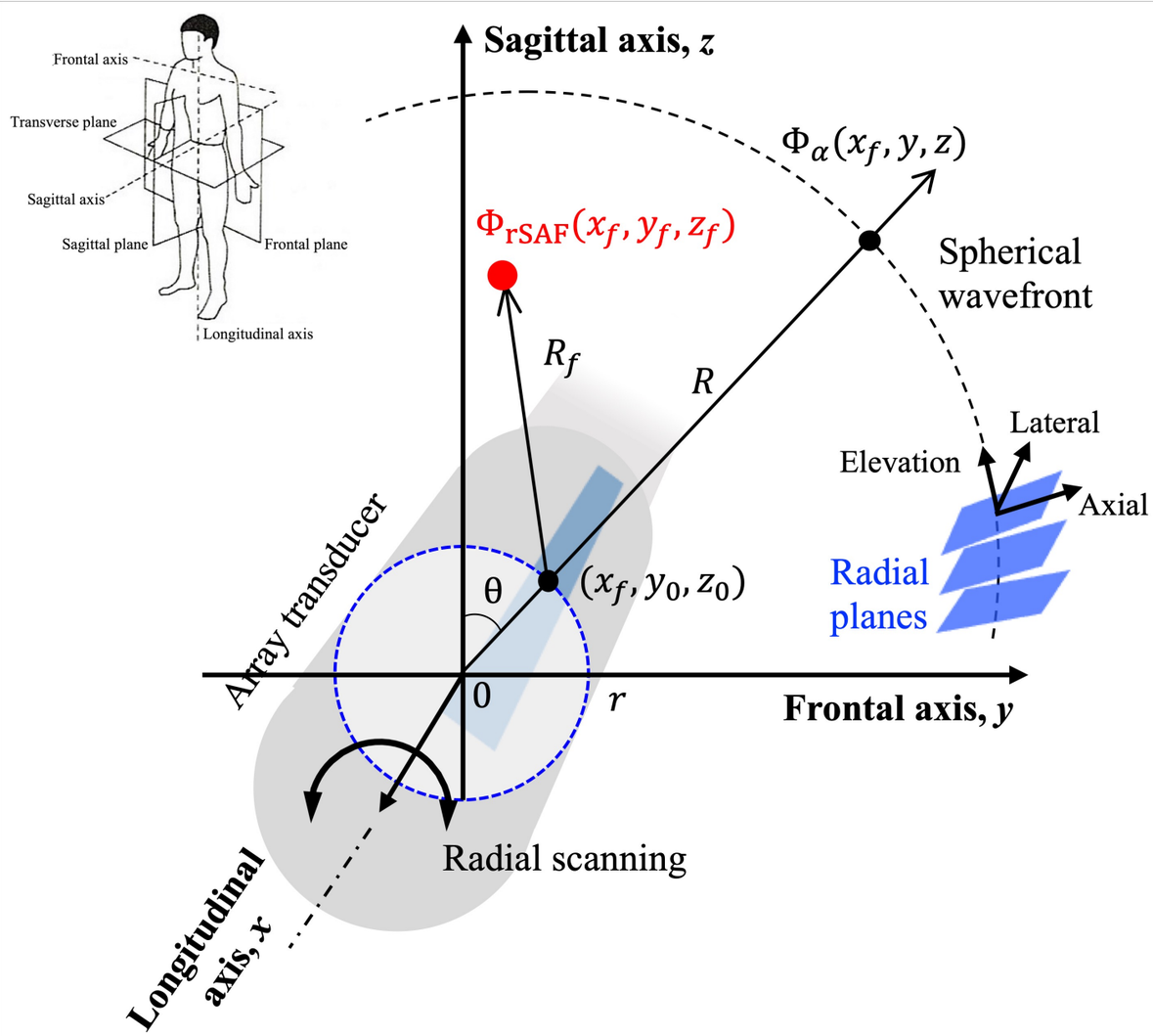

Synthetic transmit aperture focused beam pattern

$$\Psi_{\mathrm{rSAF}}(y_f, z_f) = c_0 \int_{-\infty}^{\infty} p_s(\alpha)\tau(\alpha)\Psi_\alpha(y, z)d\alpha,$$

$$\tau(\alpha) = e^{-jk\sqrt{(y_f - r\alpha)^2 + (z_f - r\beta)^2}}$$

$$\Psi_\alpha(y, z) = e^{jkR} = e^{jk\sqrt{(y-r\alpha)^2 + (z-r\beta)^2}}$$

$$\Psi_{\mathrm{rSAF}}(y_f, z_f) = c_0 \int_{-\infty}^{\infty} p_s(\alpha) e^{jk(R - R_f)} d\alpha.$$

Fresnel approximation

$$R - R_f = \frac{y^2 - y_f^2}{2z_f} + \frac{r(y - y_f)}{z_f}\alpha$$

$$\Psi_{\mathrm{rSAF}}(y_f, z_f) = c_0 e^{jk\frac{y^2 - y_f^2}{2z_f}} \mathcal{F}[p_s(\alpha)]_{f_y = \frac{ry'}{\lambda z_f}} \qquad y' = y - y_f$$

† H. Song, **J. Kang***, *J Comput Des Eng* **9**, 1774-1787 (2022).
J. Kang, et al., US Patent 63/355,525 (2022).

Analytical solution for synthetic radial aperture focusing (rSAF)

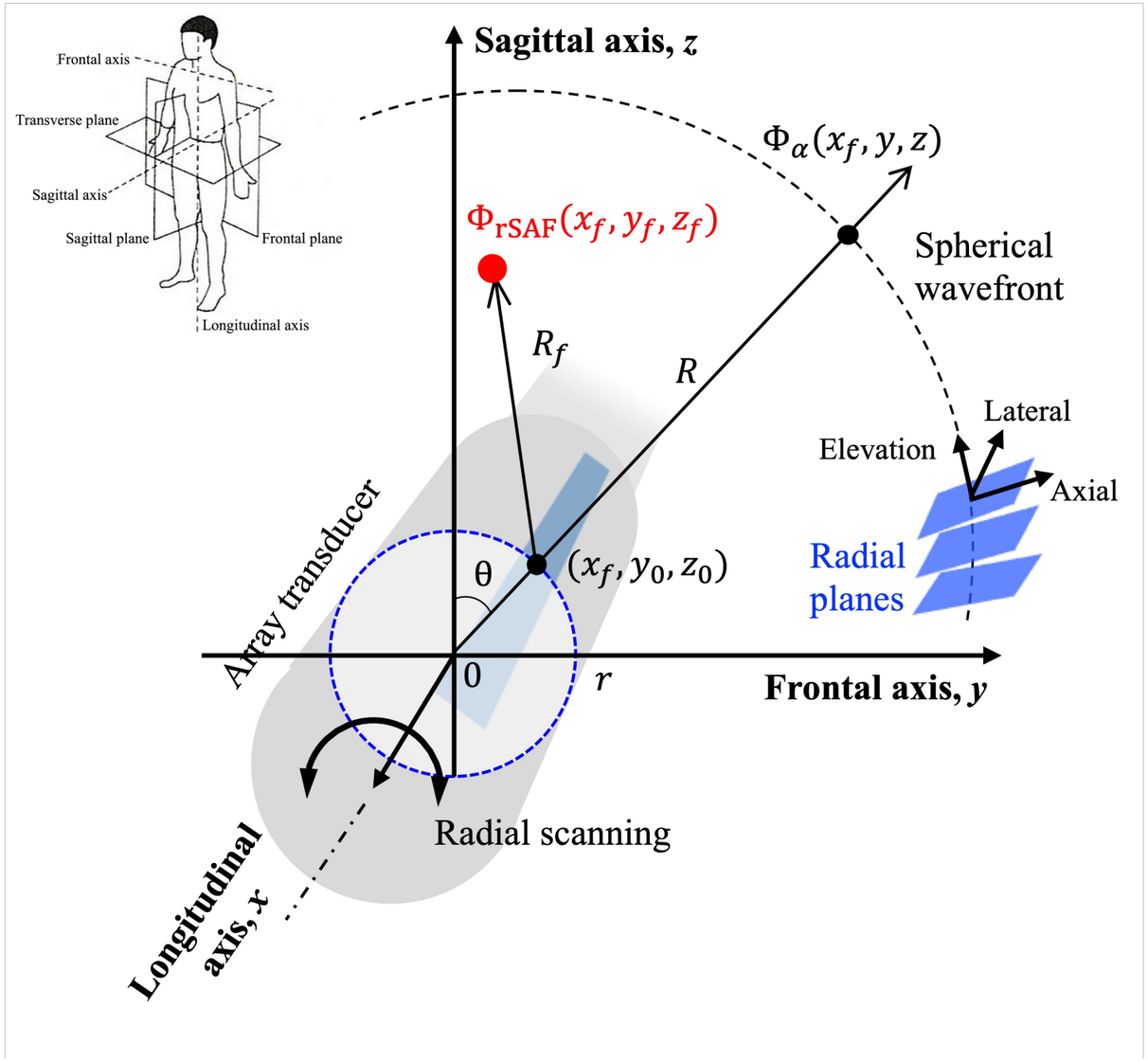

Discrete synthetic transmit aperture focused beam pattern

$$\Psi_{\mathrm{rSAF}}(y_f, z_f) = c_0 e^{jk\frac{y^2 - y_f^2}{2z_f}} \mathcal{F}[p_s(\alpha)]_{f_y = \frac{ry'}{\lambda z_f}}$$

$$p'_s(\alpha) = \sum_{n=0}^{N-1} \delta(\alpha - \alpha_n)$$

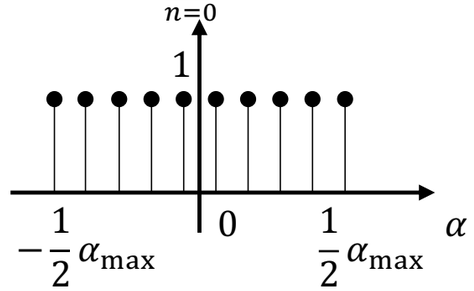

$$\Psi_{\mathrm{rSAF}}(y_f, z_f) = c_1' \frac{\sin \pi \frac{rN\Delta\alpha}{\lambda z_f} y}{\sin \pi \frac{r\Delta\alpha}{\lambda z_f} y}$$

Revised scale factor

$$c_1' = c_0 \cdot e^{jk\frac{y^2 - y_f^2 + r\alpha_{\max}}{2z_f} y}$$

Null-to-null beam width

$$y'_{s\,\mathrm{ML}} = \frac{\lambda z_f}{rN\Delta\alpha} = \frac{\lambda z_f}{r\alpha_{\max}}$$

Grating lobe positions

$$y'_{s\,\mathrm{GL}} = \frac{\lambda z_f}{r\Delta\alpha} n \quad (n = 1, 2, \ldots)$$

† H. Song, **J. Kang***, *J Comput Des Eng* **9**, 1774-1787 (2022).
J. Kang, et al., US Patent 63/355,525 (2022).

Practical implementation strategy

Virtual source-based SAF technique✢

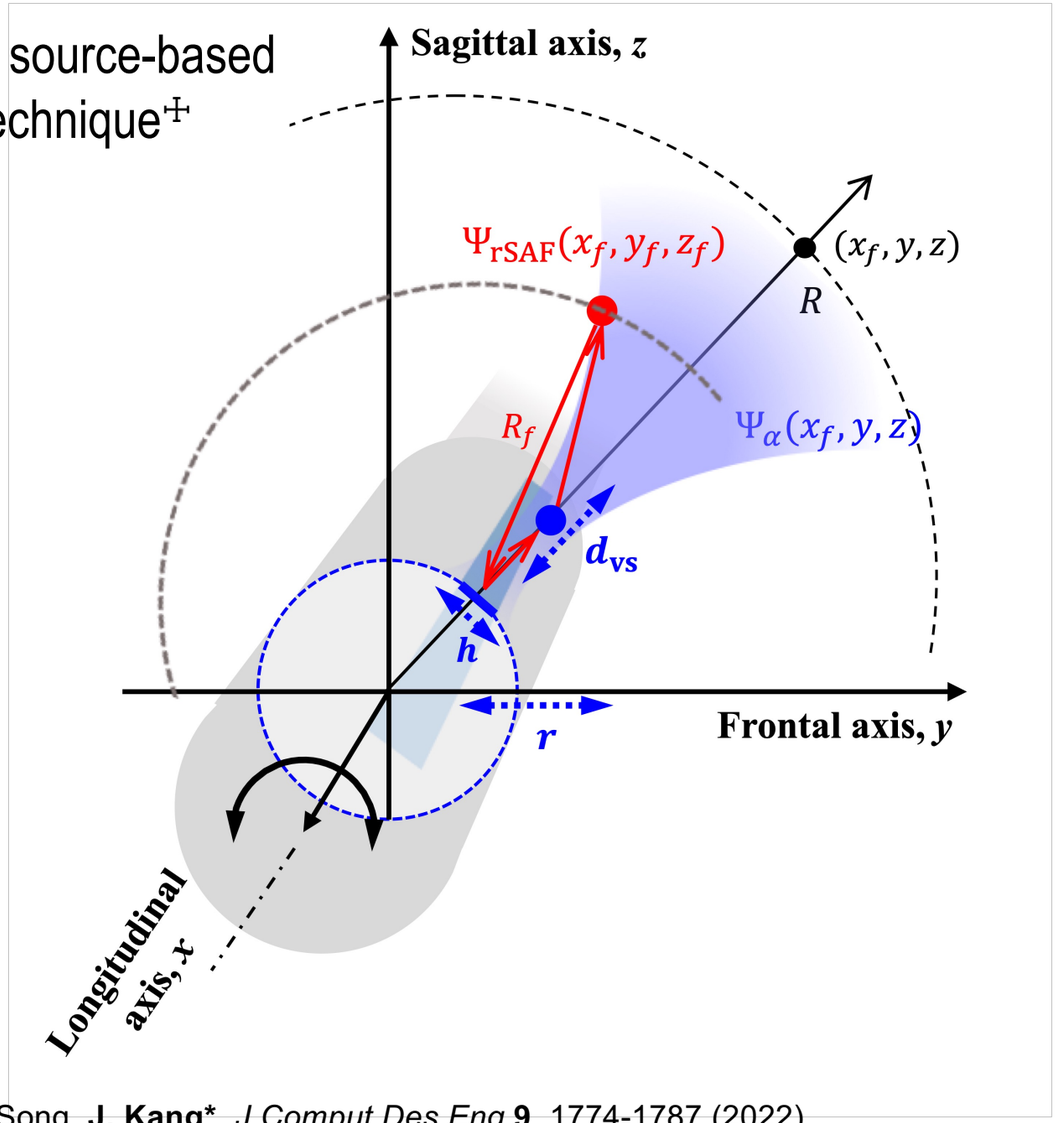

Synthetic aperture focusing delay calculation

Transmit

$$d_t(i,z) = d_{VS} + d_{tf}(i,z)$$

$$\tau_t(i,z) = d_t(i,z)/c$$

Receive

$$\tau_r(z) = d_r(z)/c \quad \text{(i.e., } R_f\text{)}$$

$$\tau_f(i,z) = \tau_t(i,z) + \tau_r(z)$$

Radial aperture synthesis

$$I_{\mathrm{rSAF}}(\theta_n, z) = \frac{1}{N_{\mathrm{syn}}(z)} \sum_{i=n-N_{syn}(\theta_n,z)/2+1}^{n+N_{syn}(\theta_n,z)/2} I_i(\theta_n, \tau_f(i,z))$$

† H. Song, **J. Kang***, *J Comput Des Eng* **9**, 1774-1787 (2022).
J. Kang, et al., US Patent 63/355,525 (2022).

✢ Frazier C. H., et al., *IEEE Trans Ultrason Ferroelect Freq Control*, **45**(1), (1998)

Design framework

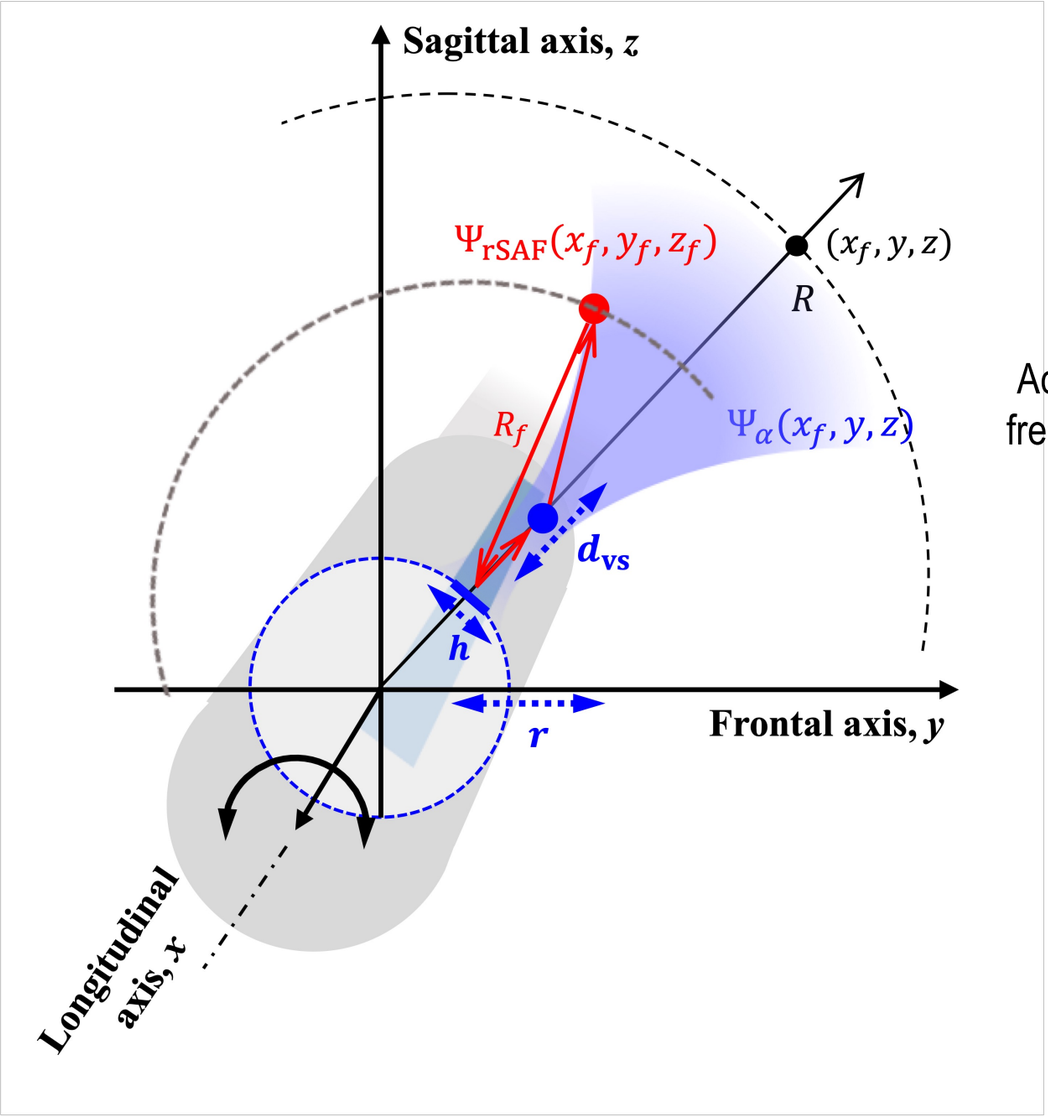

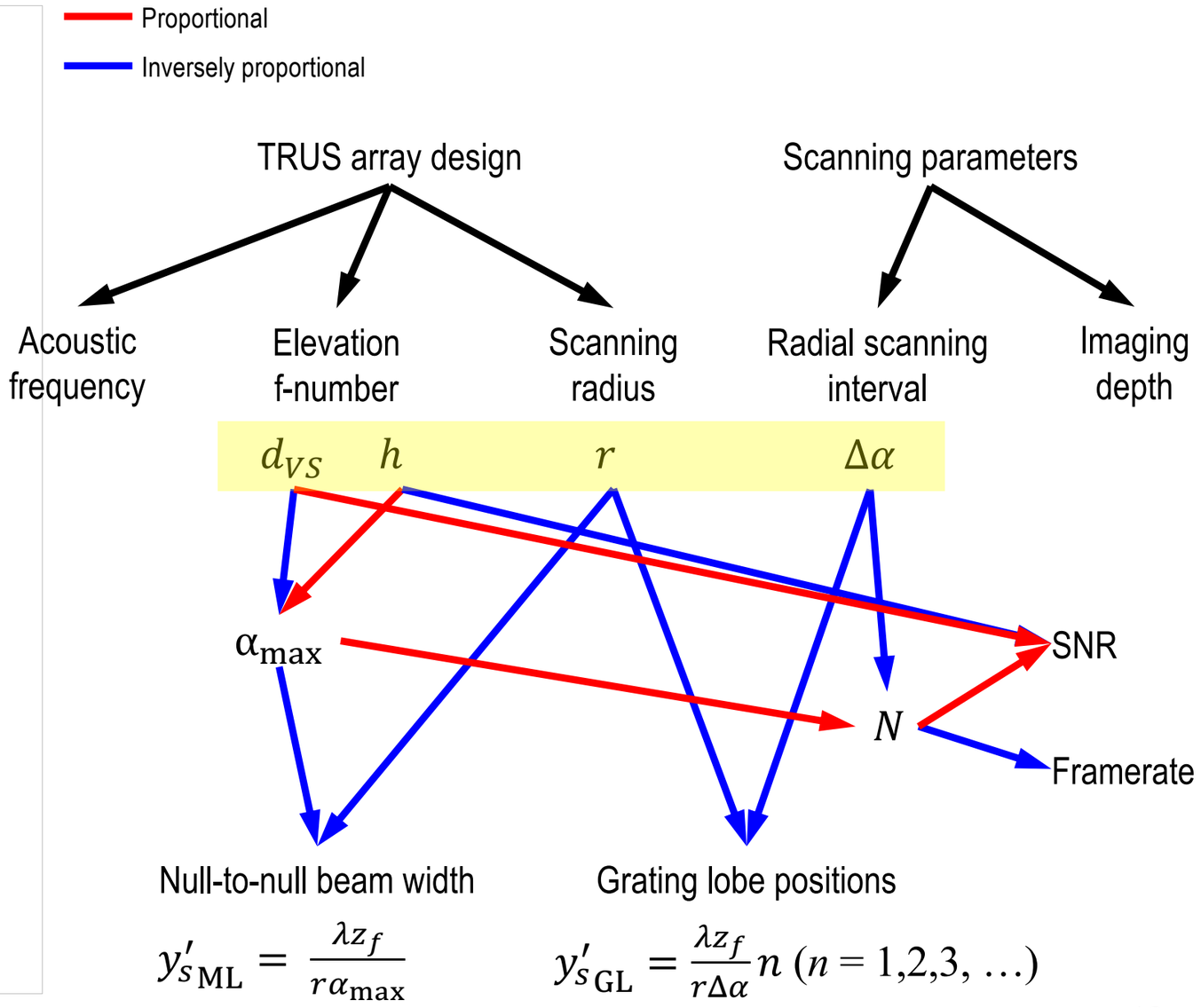

† H. Song, **J. Kang***, *J Comput Des Eng* **9**, 1774-1787 (2022).
J. Kang, et al., US Patent 63/355,525 (2022).

Spatial resolution & grating lobe

d_{VS} = 5 mm; h = 7 mm

$$y'_{s\,\mathrm{GL}} = \frac{\lambda z_f}{r\Delta\alpha} n \ (n = 1,2,3, \ldots)$$

$$y'_{s\,\mathrm{ML}} = \frac{\lambda z_f}{r\alpha_{\max}}$$

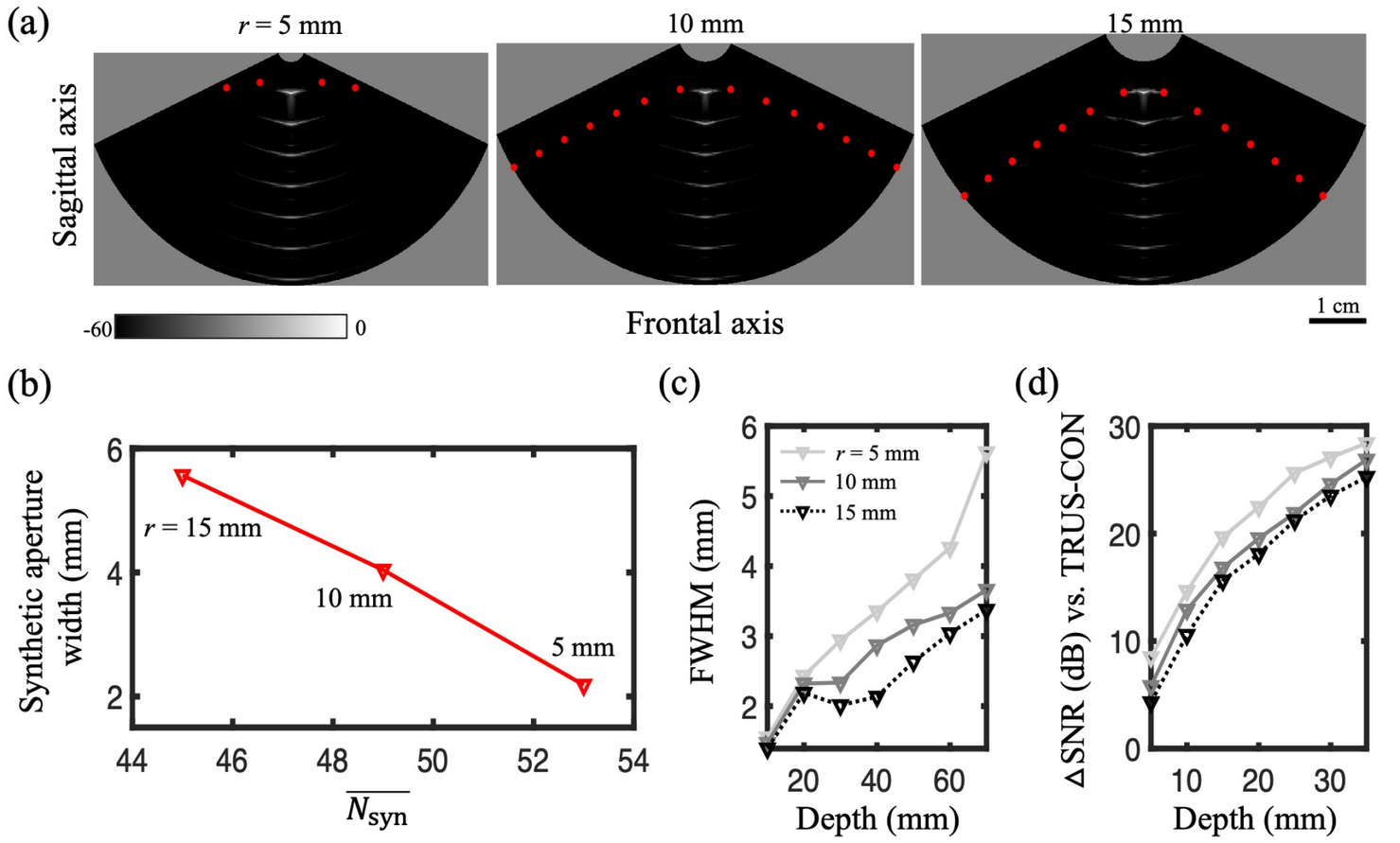

† H. Song, **J. Kang***, *J Comput Des Eng* **9**, 1774-1787 (2022).
J. Kang, et al., US Patent 63/355,525 (2022).

2D Field-II simulation – Frontal-sagittal plane

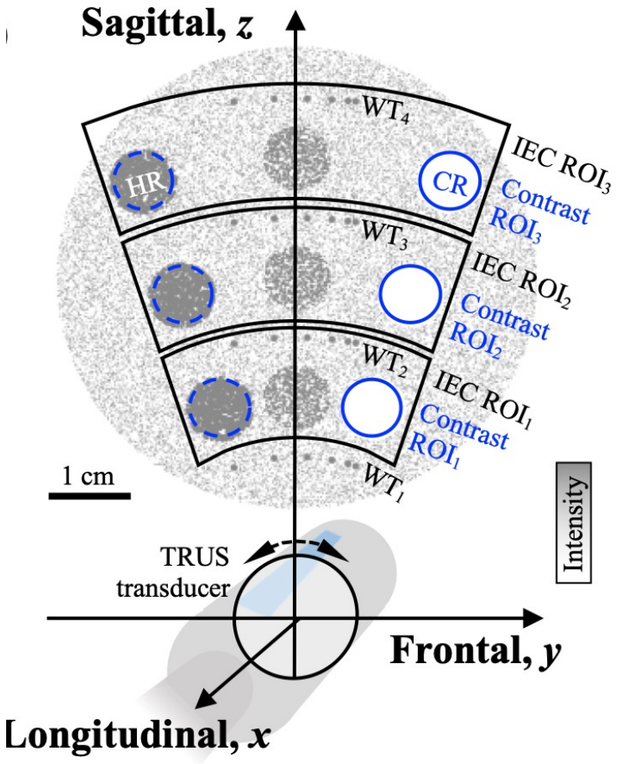

† H. Song, **J. Kang***, *J Comput Des Eng* **9**, 1774-1787 (2022).
J. Kang, et al., US Patent 63/355,525 (2022).

Comparison to clinical standard

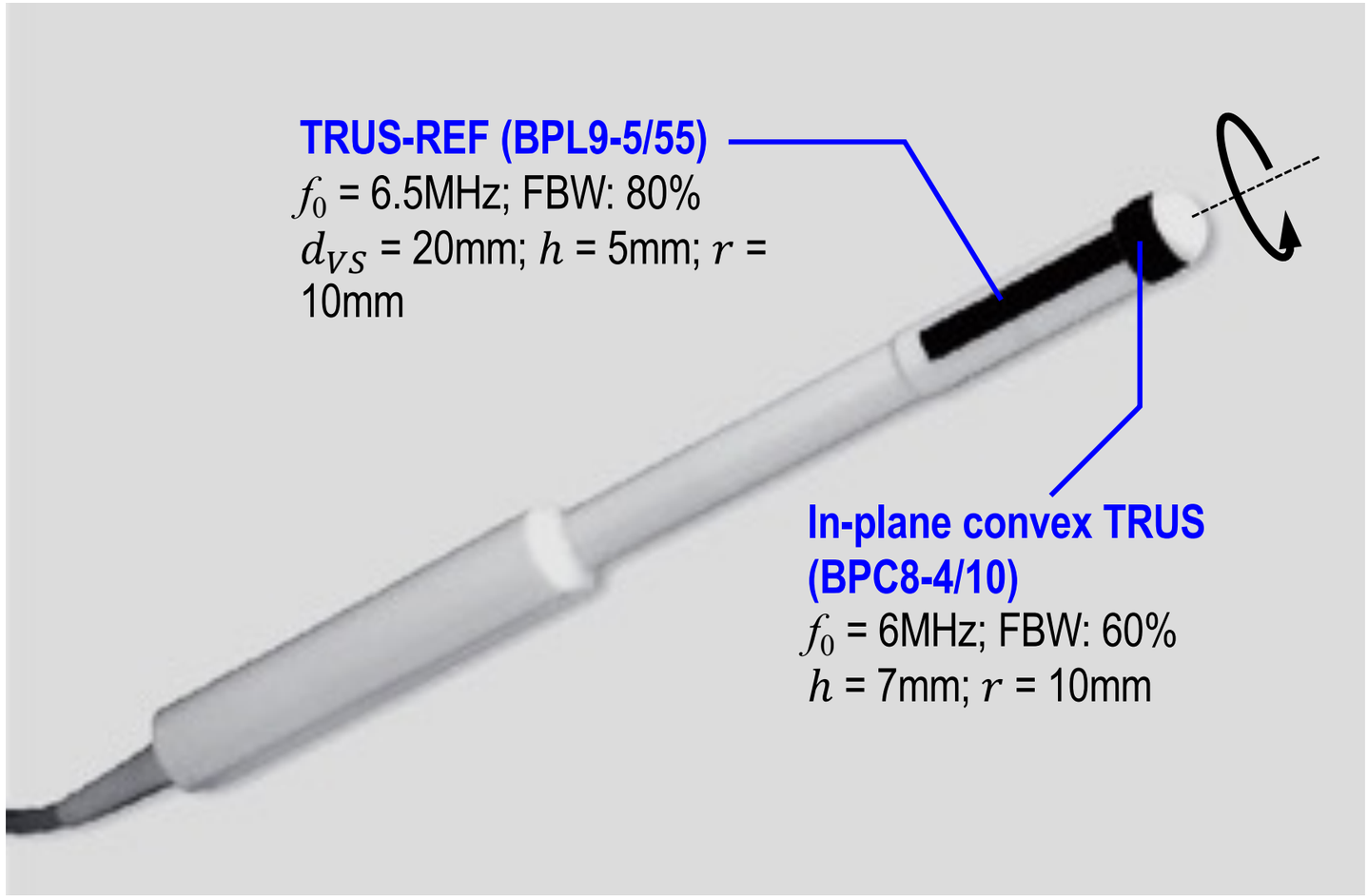

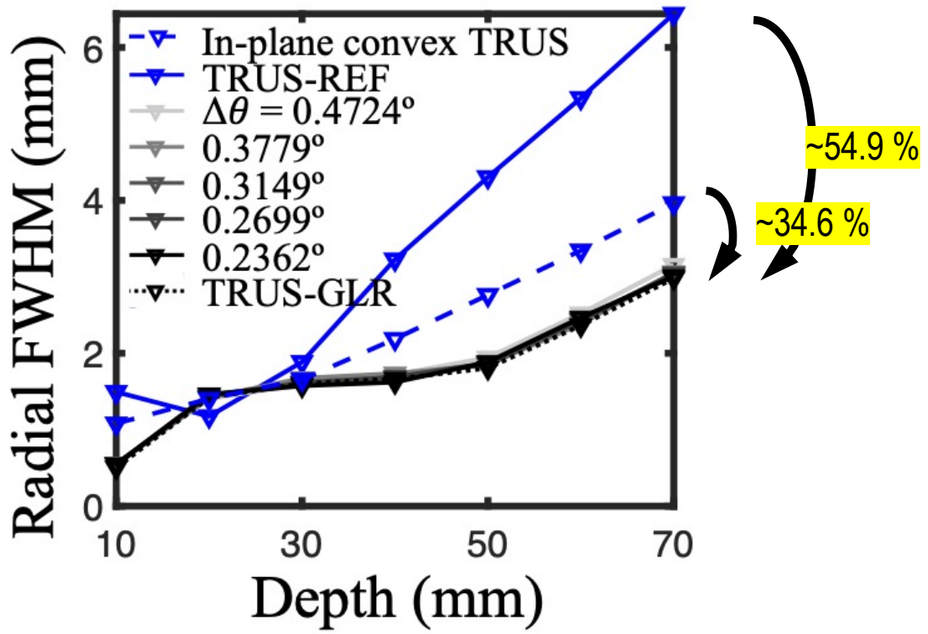

† H. Song, **J. Kang***, *J Comput Des Eng* **9**, 1774-1787 (2022).
J. Kang, et al., US Patent 63/355,525 (2022).

What's next?

Null-to-null beam width

$$y'_{s\,\mathrm{ML}} = \frac{\lambda z_f}{r\alpha_{\max}}$$

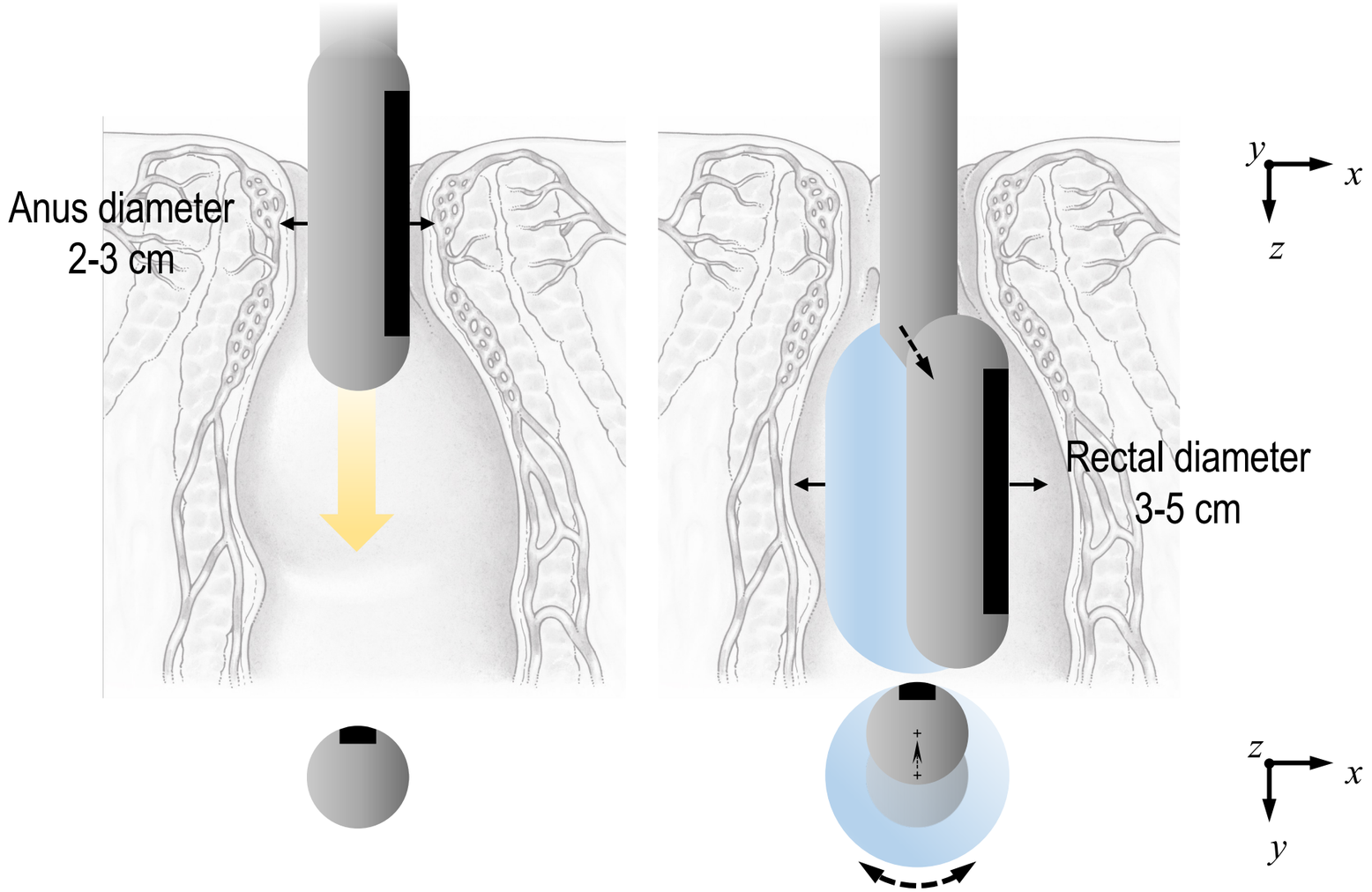

† H. Song, **J. Kang***, *J Comput Des Eng* **9**, 1774-1787 (2022).
J. Kang, et al., US Patent 63/355,525 (2022).

What's next?

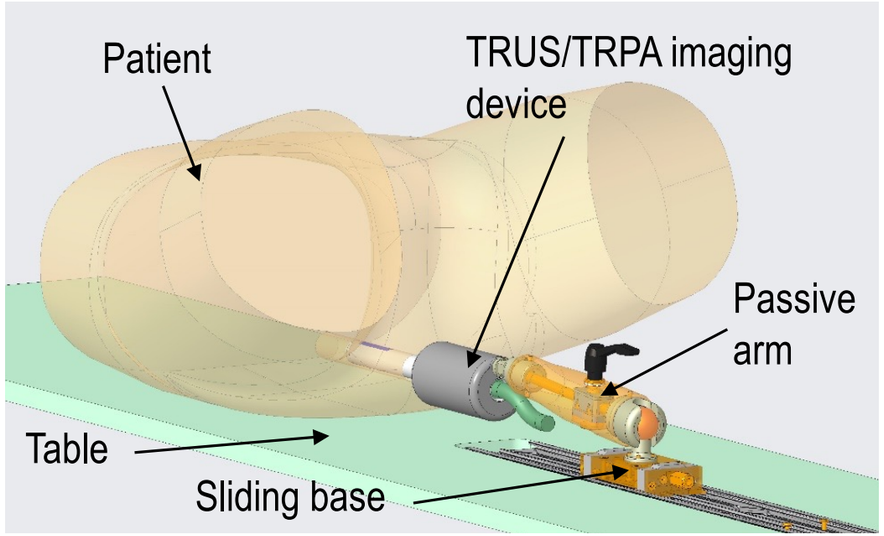

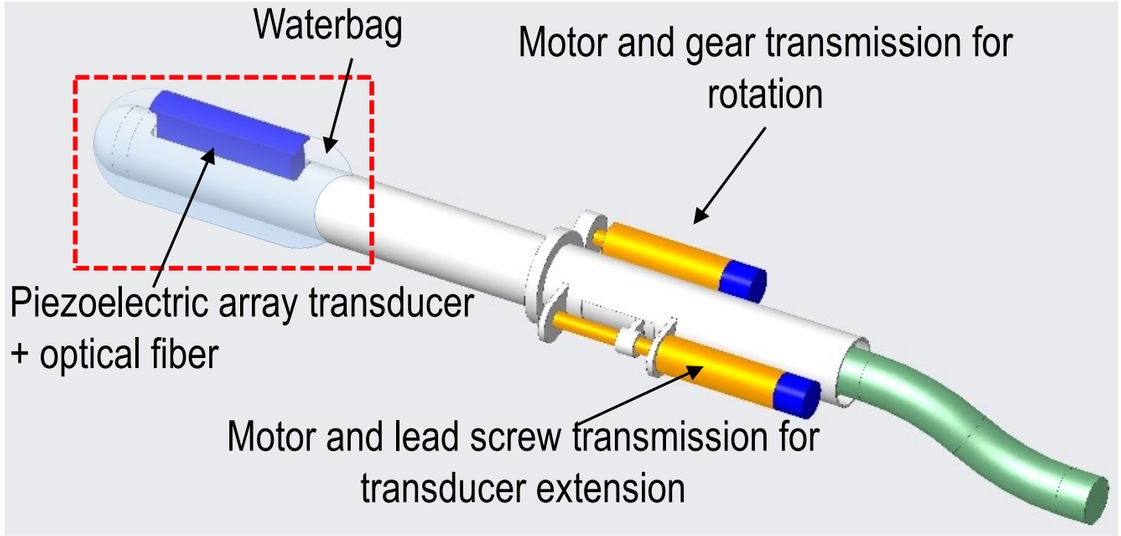

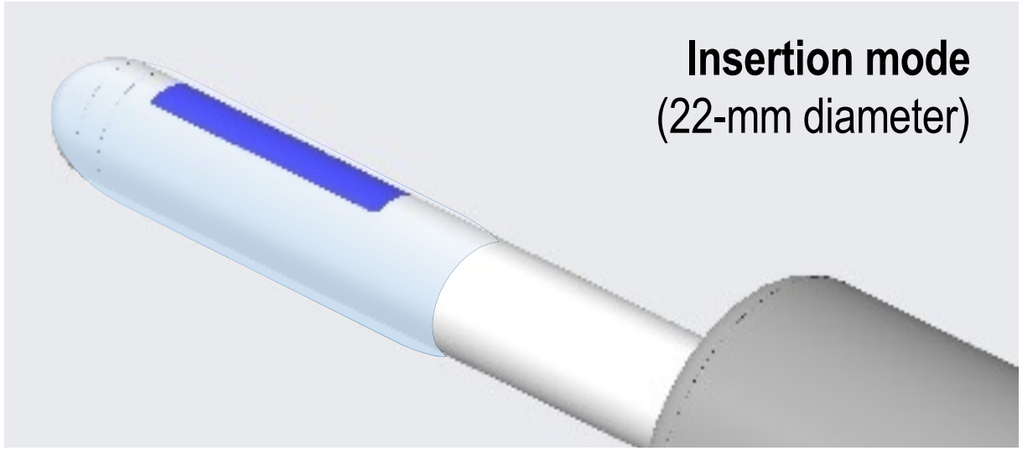

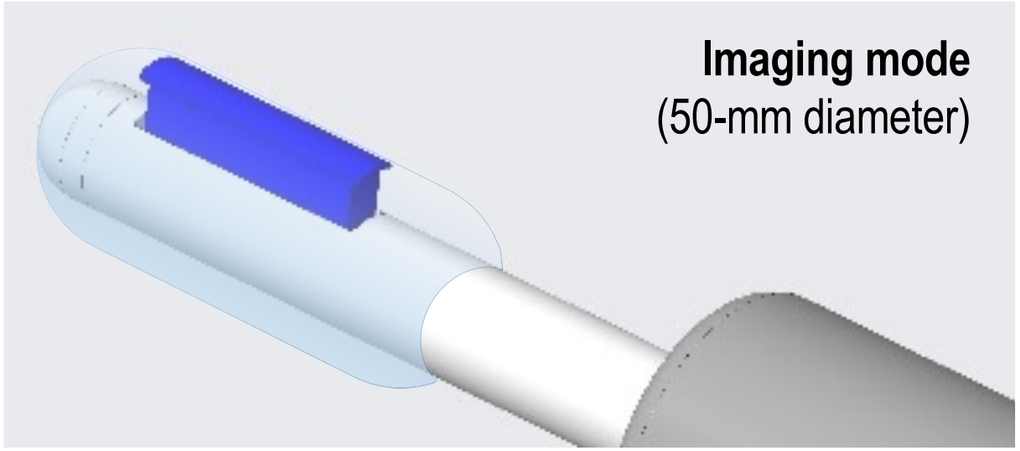

Courtesy of Dr. Iulian Iordachita

† H. Song, **J. Kang***, *J Comput Des Eng* **9**, 1774-1787 (2022).
J. Kang, et al., US Patent 63/355,525 (2022).

Summary

- TRUS-rSAF technique can provide **unprecedented volumetric spatial resolution** higher than clinical convex/linear TRUS array transducer
- Analytical description and optimization framework were developed
- Mechatronic implementation will provide a next-generation TRUS imaging for higher sensitivity and specificity to detect and diagnose PCa
- Further works: prototyping & clinical translation

Mission

Prostate-Specific Antigen (PSA) †

Transrectal US-guided biopsy

Histopathology

MRI
PET/CT

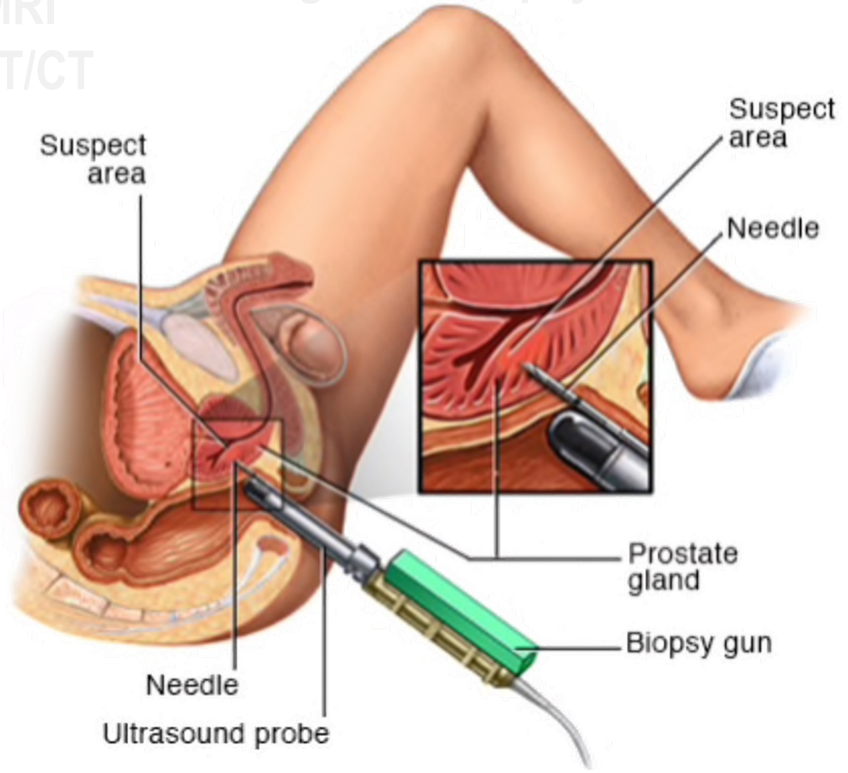

- High false-positive rate (75%) †
- The prevalence of nearly invisible PCa on TRUS ranges from 25 to 42% ♀
- **Higher spatial resolution**

Prostatectomy guidance

- **Molecular contrast**
- Post-operative complications: erectile dysfunction (59.9% at 18M); incontinence (8.4% at 18M)

† Catalona W, *et al.*, *JAMA*. **279** (19): 1542 – 7 (1998).
† Slatkoff S., et al., *J. Fam. Pract.* **60** (6): 357 – 60 (2011).
♀ Piao D., *et al.*, *IEEE J. Selec. Topics in Quantum. Electron.*, **16** (4): 715 – 29 (2009).

Prostate-Specific Membrane Antigen (PSMA)

- Type-II integral cell-surface membrane protein †
- Overexpressed in nearly all solid tumors (e.g., breast, bladder, pancreatic, testicular, or colorectal cancers) ‡
- **High correlation to PCa aggressiveness**, implying its functional role in PCa biology ♀

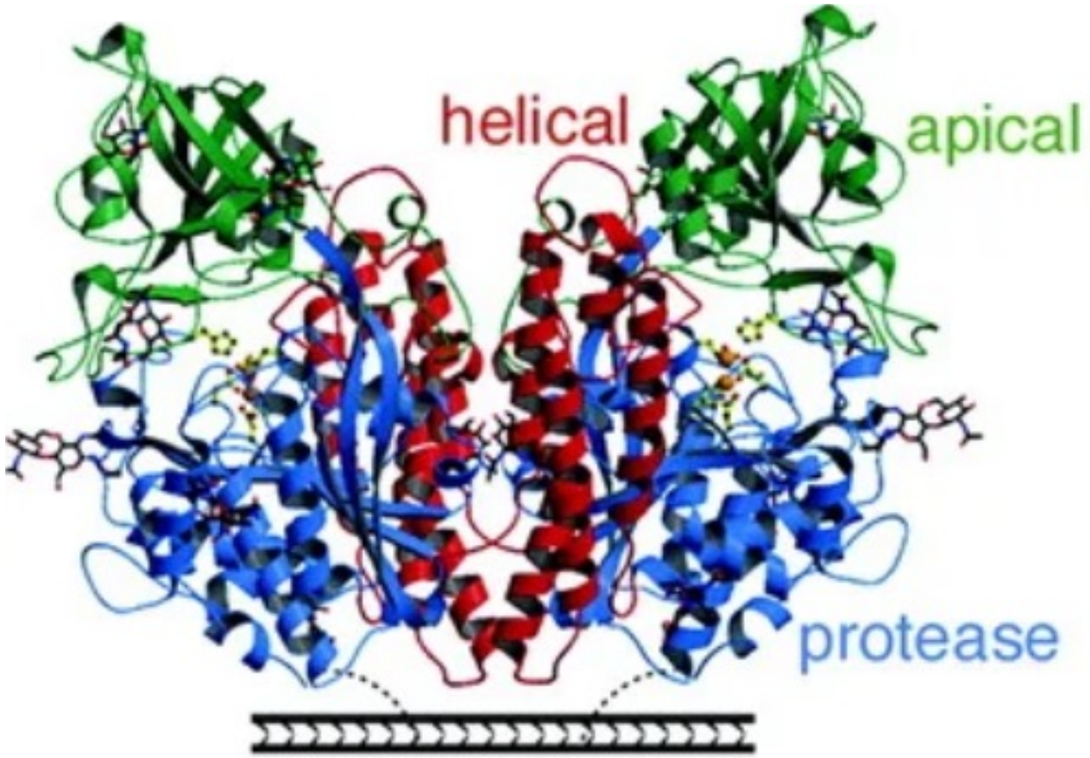

Ribbon diagrams of side view of PSMA †

† Davis M.I., et al., *PNAS* **102** (17): 5981 – 86 (2005); Balk S.P., *et al.*, *J. Clin. Oncol*. **21** (2): 383–91 (2013).
‡ Neuman B. P., et al., *Clin. Cancer Res.* **21** (4): 771 – 80 (2014).
♀ Minner S., et al., *Prostate* **71** (3), 281 – 8 (2011).

Targeting PSMA for early-PCa detection

PET/MRI/CT †

Pros: Wide field-of-view across whole-body; High specificity
Cons: Iodizing effects; Slow imaging speed; expensive

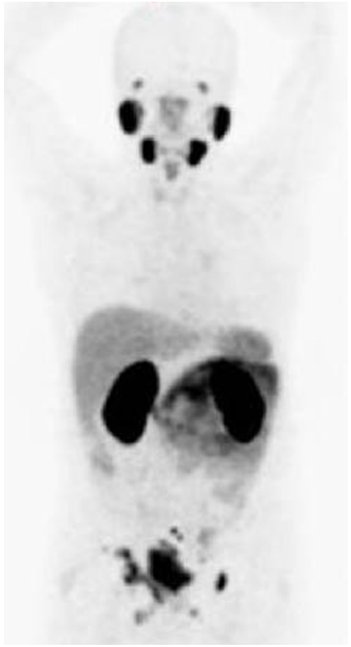

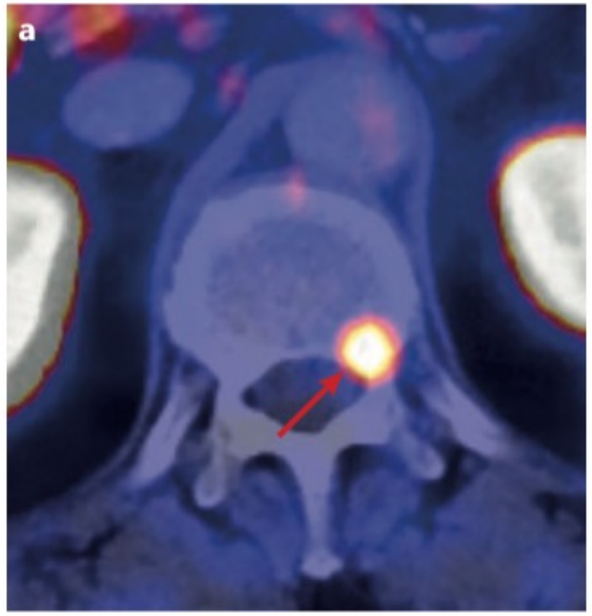

Extensive clinical trials stages I and II: NCT02282137, NCT02611882, NCT02488070, NCT02048150, NCT01173146 …

Optical imaging †

Pros: Real-time; easy to use
Cons: Superficial sensing depth

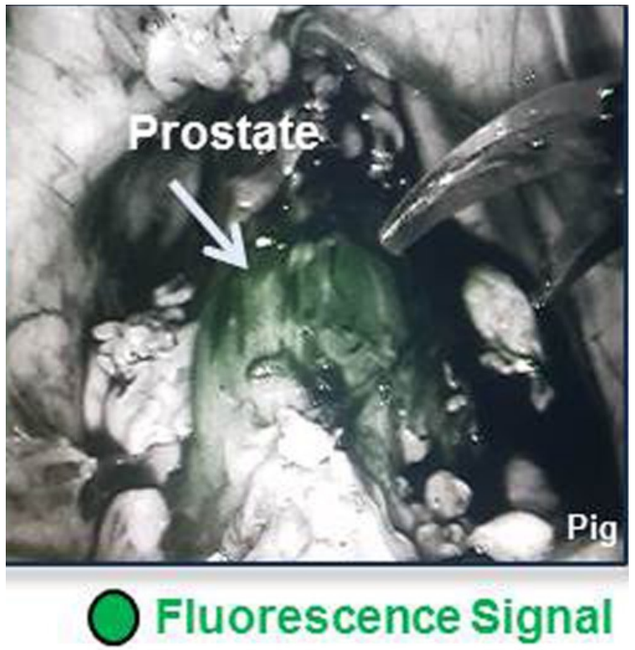

Clinical trials in IND stage: NCT01173146, NCT02048150

…

† Maurer T., et al., *Nat. Rev. Urol.* **13**: 226 – 35 (2016).
† Zhang R.R., et al., *Nat. Rev. Clin. Oncol.* **14** (6): 347 – 64 (2017); Baranski A.-C., *et al.*, *J. Necl. Med.*, **59** (4): 639 – 45 (2018).

Adding light: biomedical photoacoustics

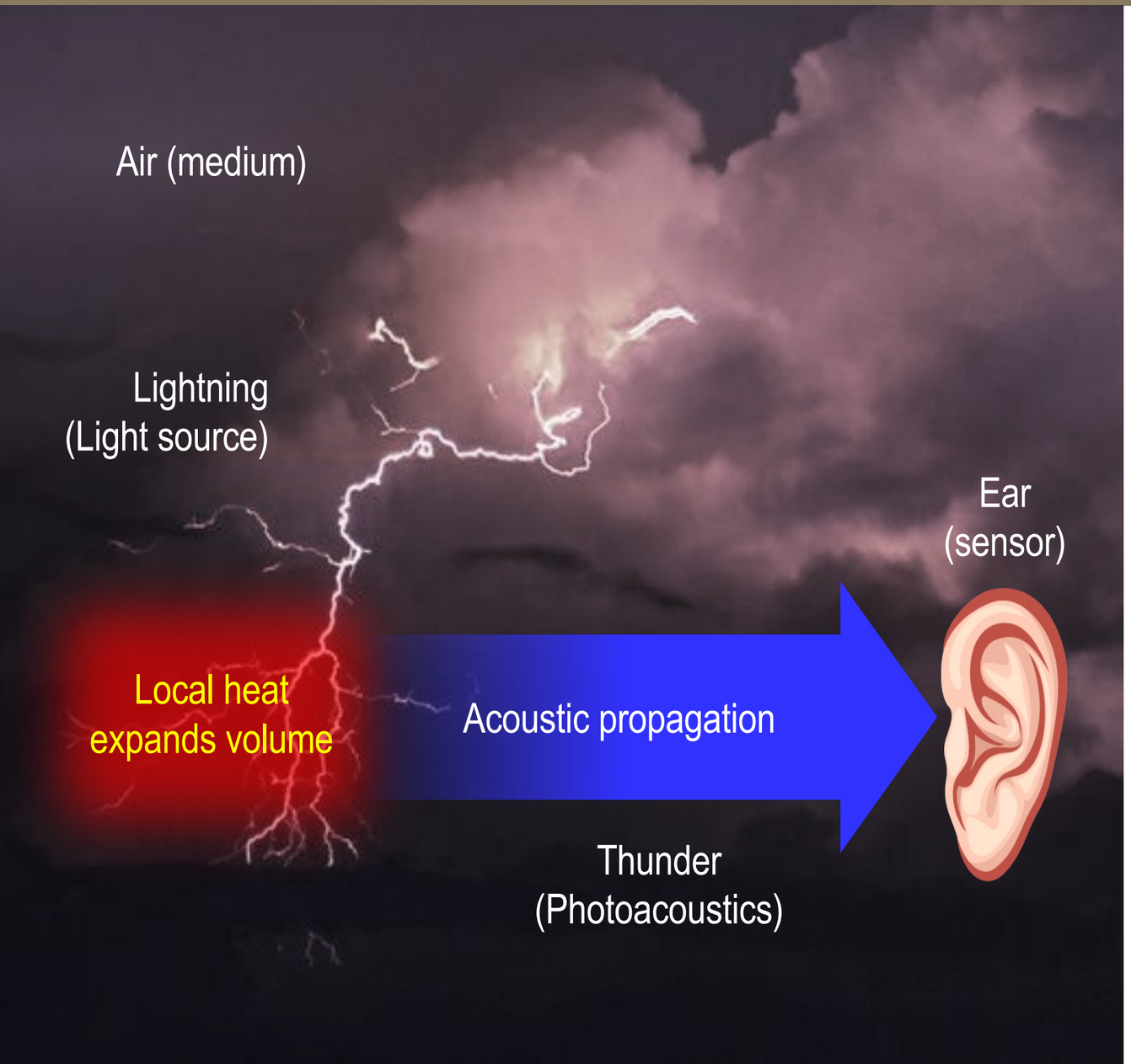

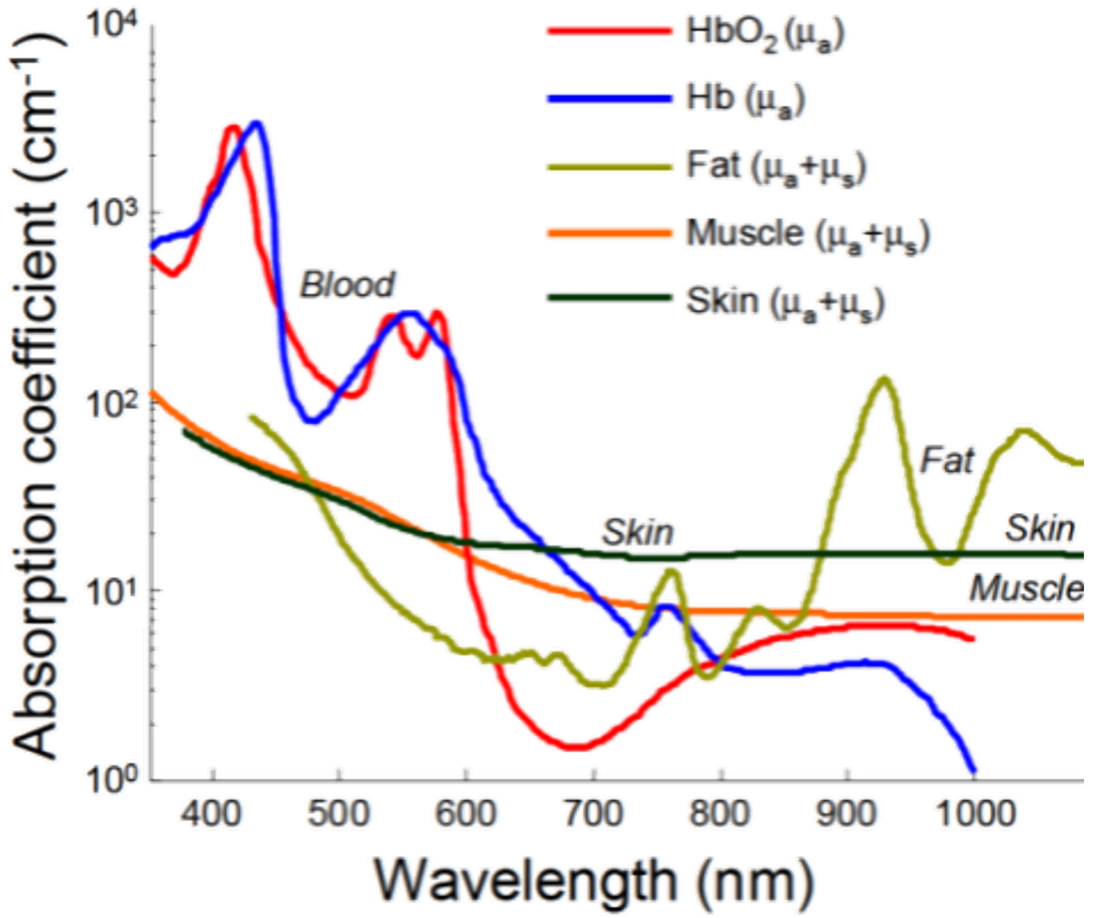

† L. V. Wang, S. Hu, *Science* **6075** (2012).
J. Kang, *et al.*, *Exp Neurol* **347** (2022).

Competitive analysis

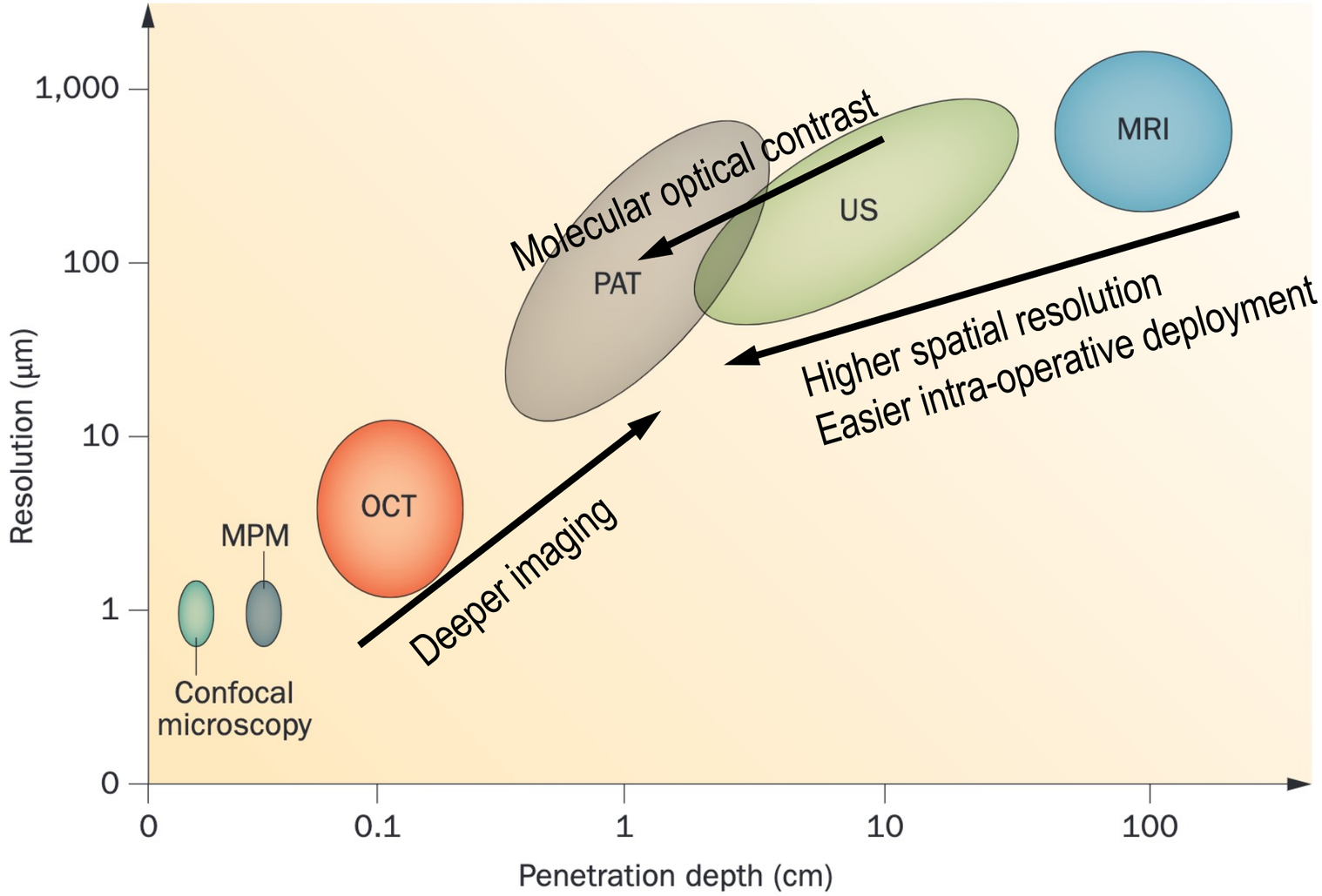

† Reproduced from
Fried N. M., Burnett A. L., Nat Urol Rev 12, 451-460 (2015).

Multi-functional PSMA-targeted platform

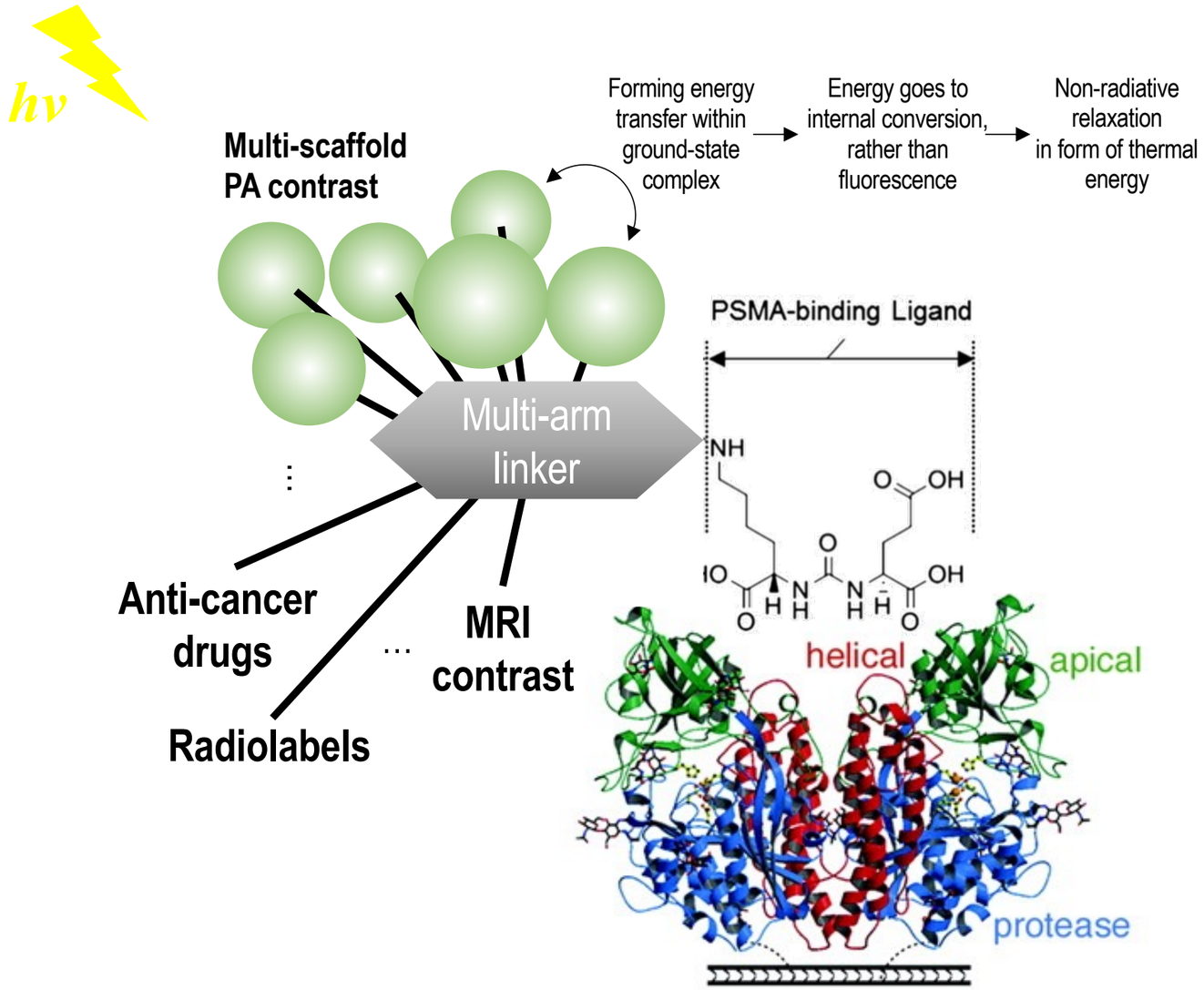

† [Zhang H.K., Chen Y.], **J. Kang**, *et al.*, *J. Biophotonics* **11**:e201800021 (2018).
[Lesniak, W., Wu, Y.], **J. Kang**, et al., *Nanoscale* **13**(20), 9217-9228 (2021).

Second-generation PSMA-targeting agent

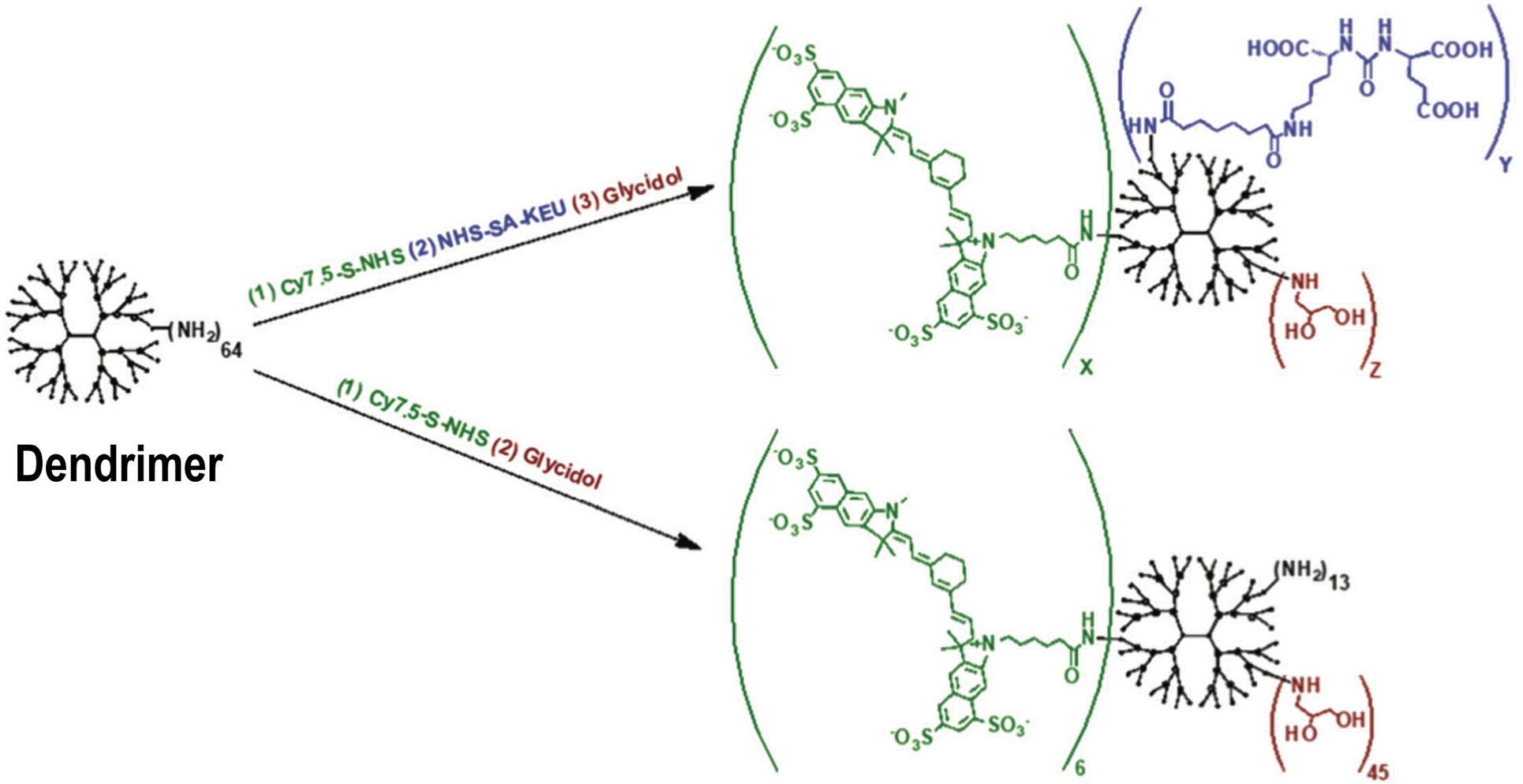

† [Zhang H.K., Chen Y.], **J. Kang**, *et al.*, *J. Biophotonics* **11**:e201800021 (2018).
[Lesniak, W., Wu, Y.], **J. Kang**, et al., *Nanoscale* **13**(20), 9217-9228 (2021).

In vivo PA-based PSMA-targeted imaging

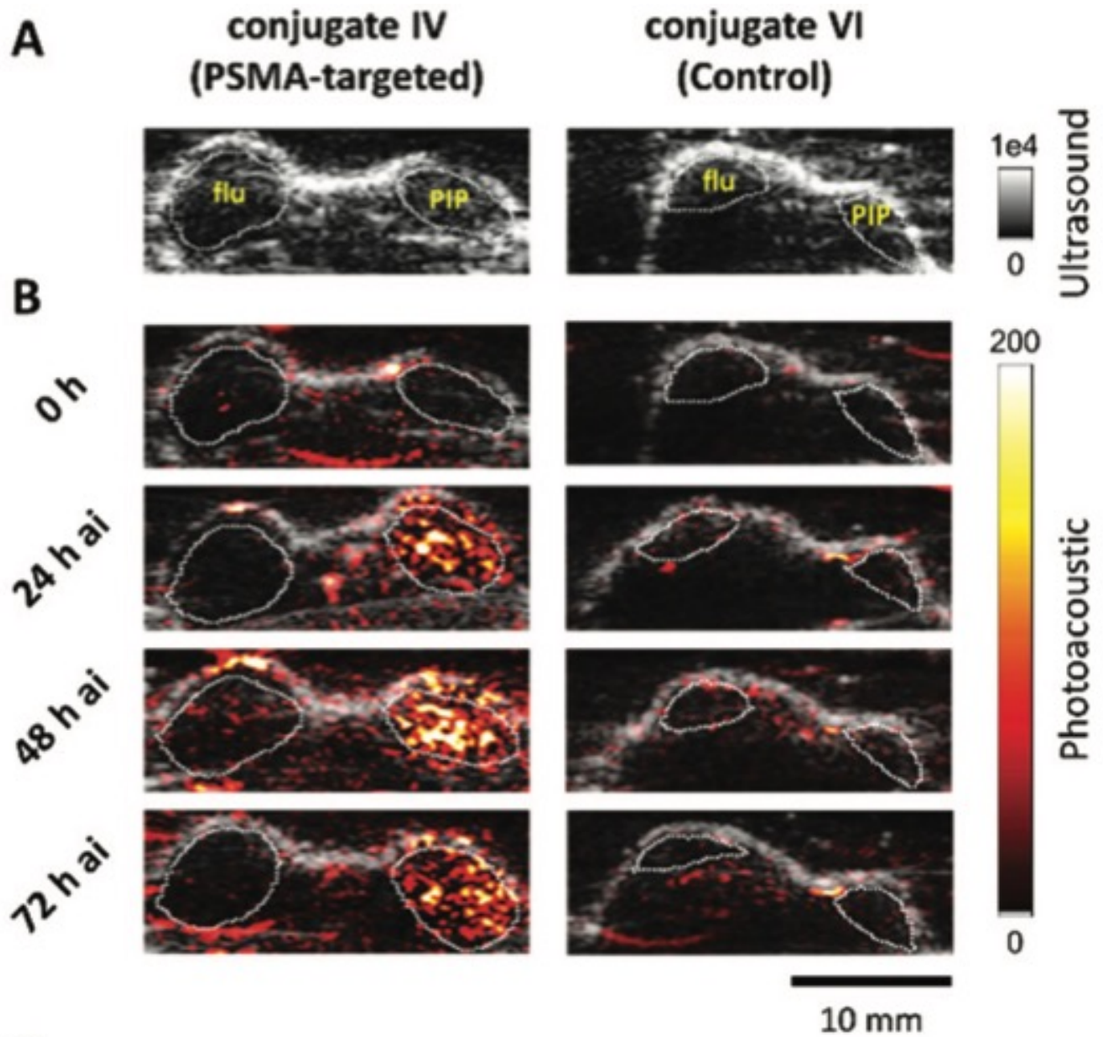

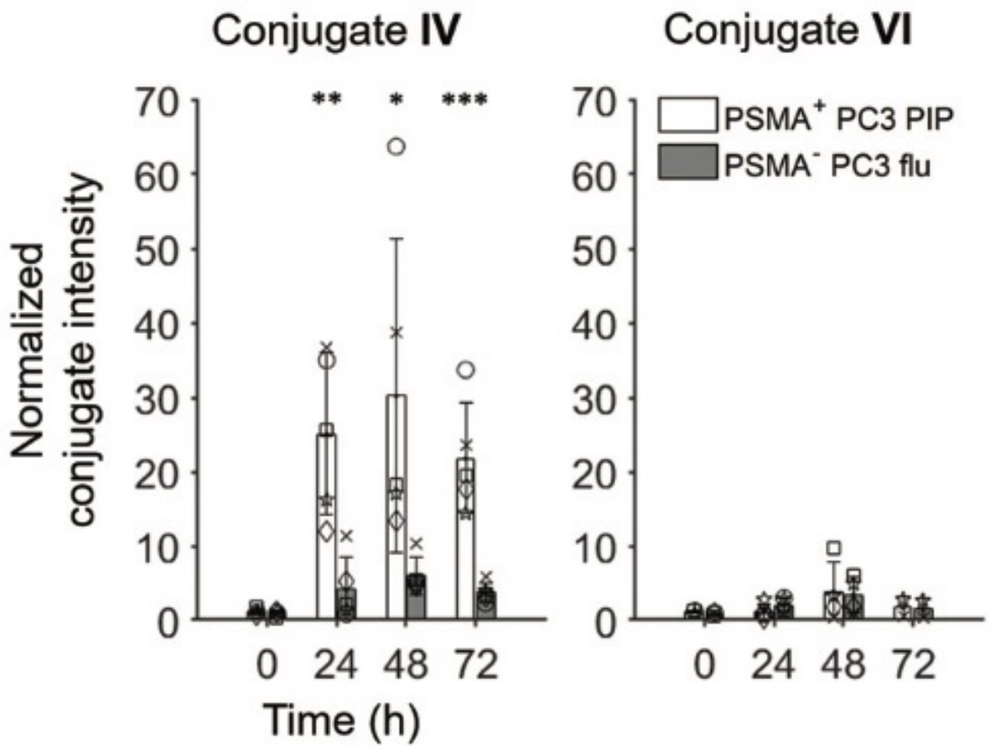

† [Lesniak, W., Wu, Y.], **J. Kang**, et al., *Nanoscale* **13**(20), 9217-9228 (2021).

Potential engineering pitfalls

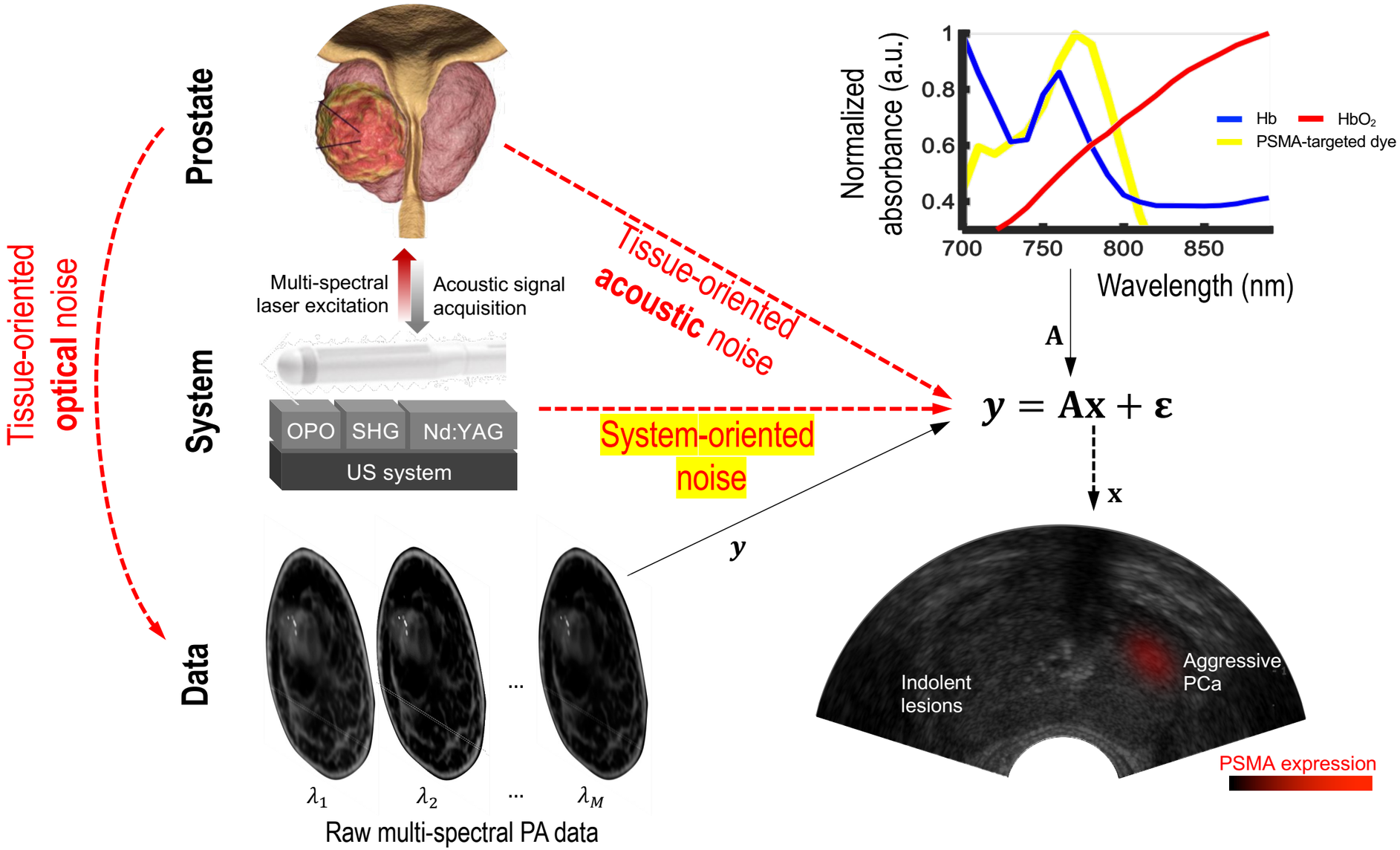

† **[Wu, Y., Kang, J.]**, *Photoacoustics* **27**, 100378 (2022).

Spectral system noise segregation

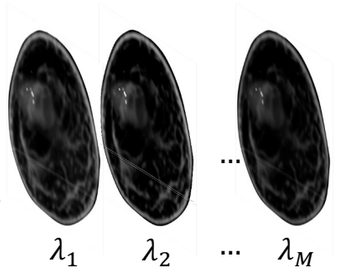

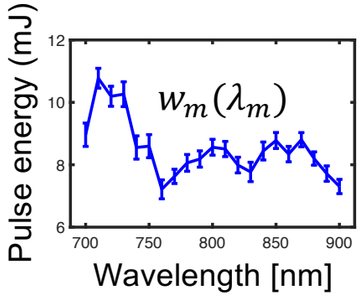

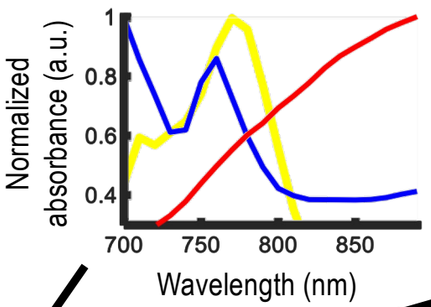

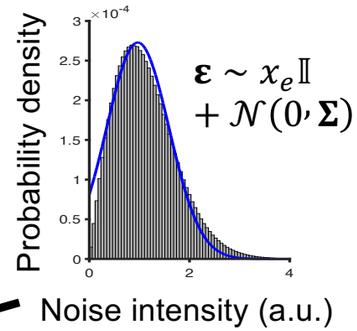

$$\boldsymbol{y} = \mathbf{A}\mathbf{x} + \boldsymbol{\varepsilon}$$

$$\bar{\mathbf{y}} = \mathbf{W}^{-1}\mathbf{y} = \mathbf{W}^{-1}(\boldsymbol{s} + \boldsymbol{\varepsilon})$$

$$\bar{\mathbf{y}} = [\mathbf{A} \mid \mathbf{v}] \begin{bmatrix} \mathbf{x} \\ x_e \end{bmatrix} + \bar{\boldsymbol{\varepsilon}} = \mathbf{Q}\bar{\mathbf{x}} + \bar{\boldsymbol{\varepsilon}}$$

Non-negative least squares (NNLS)
using quadratic programming techniques

$$\arg\min_{\mathbf{x} \geq 0} \left(\frac{1}{2} \mathbf{x}^{\mathrm{T}} \mathbf{A}^{\mathrm{T}} \mathbf{A} \mathbf{x} - \mathbf{y}^{\mathrm{T}} \mathbf{A} \mathbf{x} \right)$$

$$\arg\min_{\bar{\mathbf{x}} \geq 0} \left(\frac{1}{2} \bar{\mathbf{x}}^{\mathrm{T}} \mathbf{Q}^{\mathrm{T}} \mathbf{Q} \bar{\mathbf{x}} - \bar{\mathbf{y}}^{\mathrm{T}} \mathbf{Q} \bar{\mathbf{x}} \right)$$

$$\mathrm{diag}(\mathbf{v}) = \mathbf{W}^{-1}$$

$$\bar{\mathbf{x}} \in \mathbb{R}^{N+1}$$

$$\bar{\boldsymbol{\varepsilon}} \sim \mathcal{N}(0, \bar{\boldsymbol{\Sigma}})$$

† **[Wu, Y., Kang, J.]**, *Photoacoustics* **27**, 100378 (2022).

In vivo validation

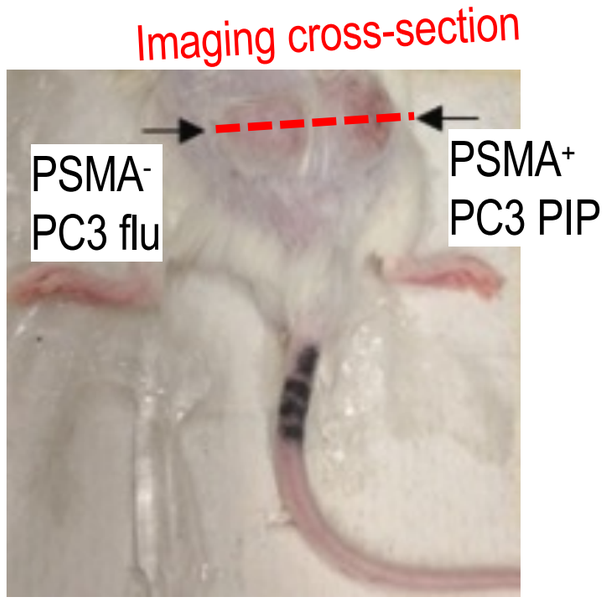

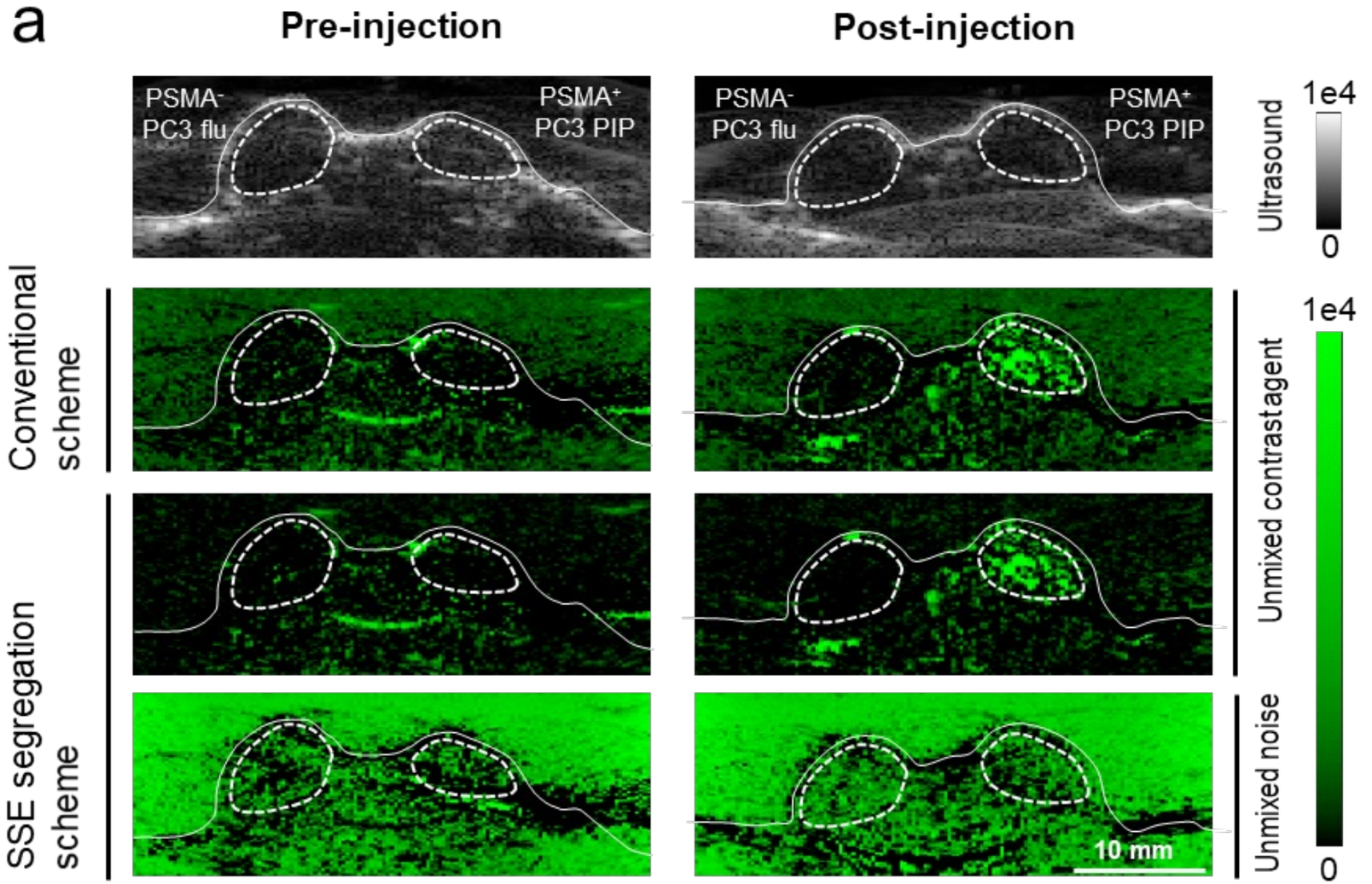

† **[Wu, Y., Kang, J.]**, *Photoacoustics* **27**, 100378 (2022).

In vivo validation

PSMA$^-$ PC3 flu PSMA$^+$ PC3 PIP

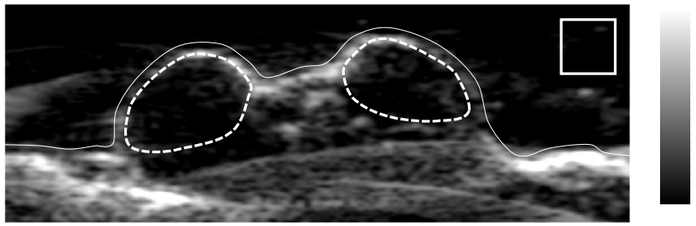

$$c_{\mathrm{SNR}} = \frac{I_{\mathrm{PSMA+}}}{I_{\mathrm{BG}}}$$

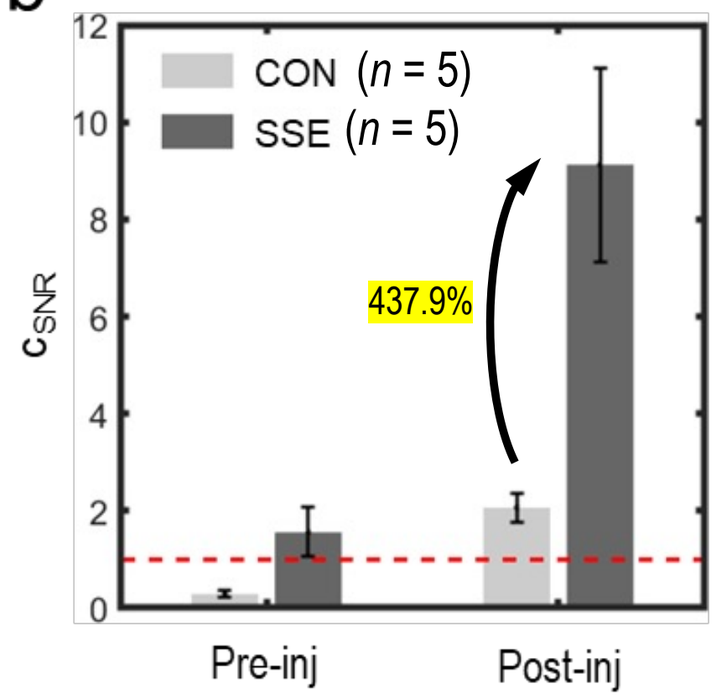

$$c_{\mathrm{PSMA}} = \frac{I_{\mathrm{PSMA+}}}{I_{\mathrm{PSMA-}}}$$

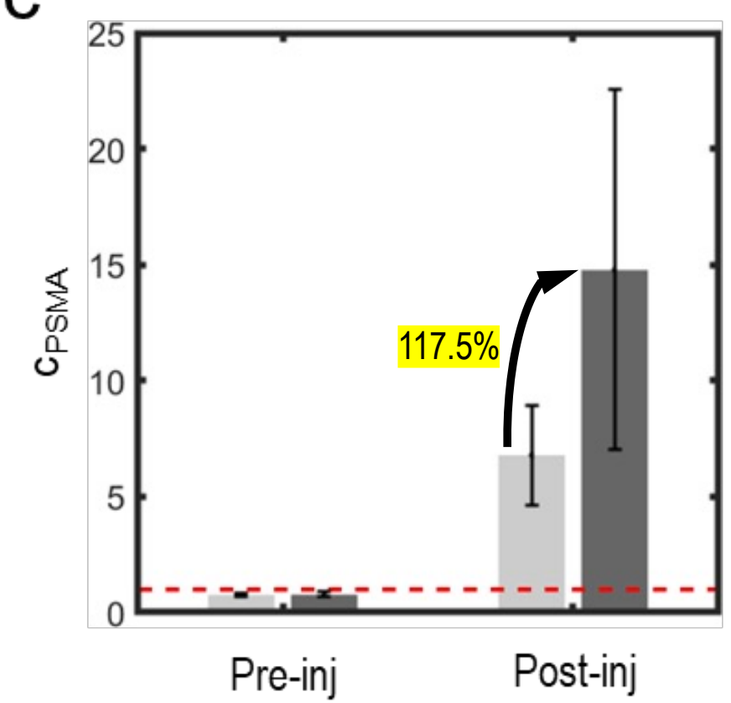

† **[Wu, Y., Kang, J.]**, *Photoacoustics* **27**, 100378 (2022).

Summary

- PSMA-targeted imaging may endow new possibility to provide **molecular contrast exclusively on aggressive PCa using TRUS/PA imaging**

- **Dedicated signal processing algorithms** (spectral system noise, wavelength optimization, frame averaging) will enhance the clinical sensitivity and specificity

- Furter works
  - Multi-functional (theranostics), multi-modal (PA/US + MRI or PET) imaging capability will be developed.
  - Multi-institutional team for animal model and clinical testing is in preparation (NIH, Hopkins).

Remarks

Transformable TRUS/PA imaging

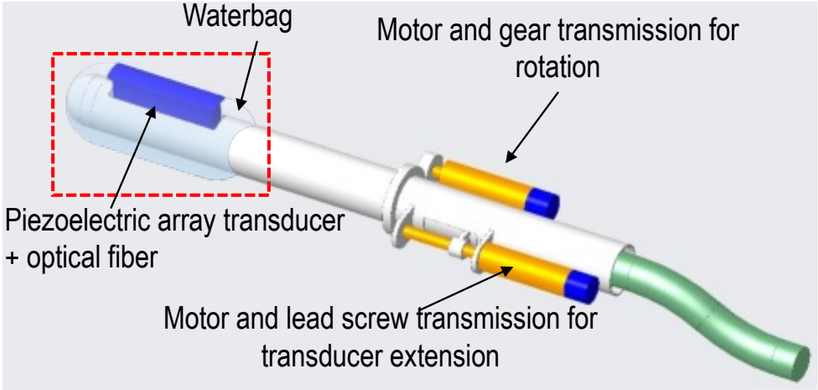

TRUS/PA diagnostics & interventional guidance

- Expanded role in PCa diagnostics
- Microtumor detection (3-5 mm → 1-2 mm)
- High-accuracy biopsy guidance, targeting PSMA expression

PSMA-targeted imaging

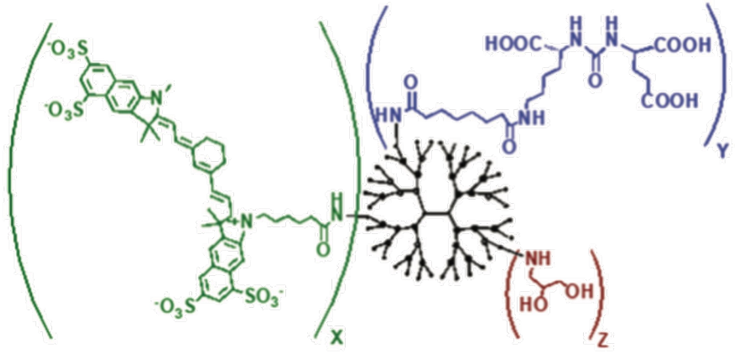

Signal processing algorithm

$$\arg\min_{\bar{\mathbf{x}} \geq 0} \left(\frac{1}{2} \bar{\mathbf{x}}^{\mathrm{T}} \mathbf{Q}^{\mathrm{T}} \mathbf{Q} \bar{\mathbf{x}} - \bar{\boldsymbol{y}}^{\mathrm{T}} \mathbf{Q} \bar{\mathbf{x}} \right)$$

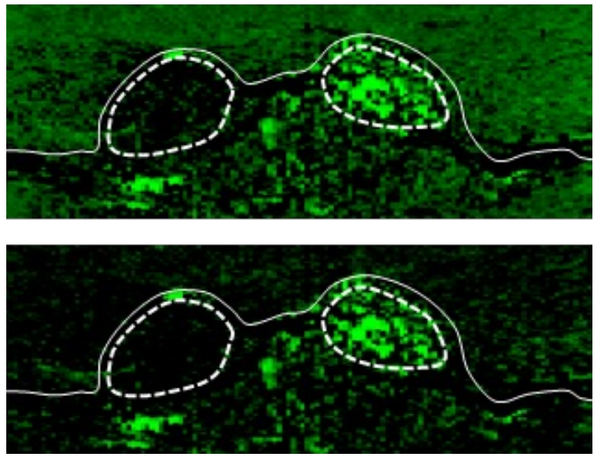

Complication of radical prostatectomy

- **Erectile dysfunction** is a post-operative complication of radical prostatectomy

- Current nerve-sparing techniques only consider neurovascular bundle (NVB), excluding cavernous nerve branches

- **Only 60-85% of PCa patients recover erectile function, and early recovery is uncommon (up to 2 years)** †

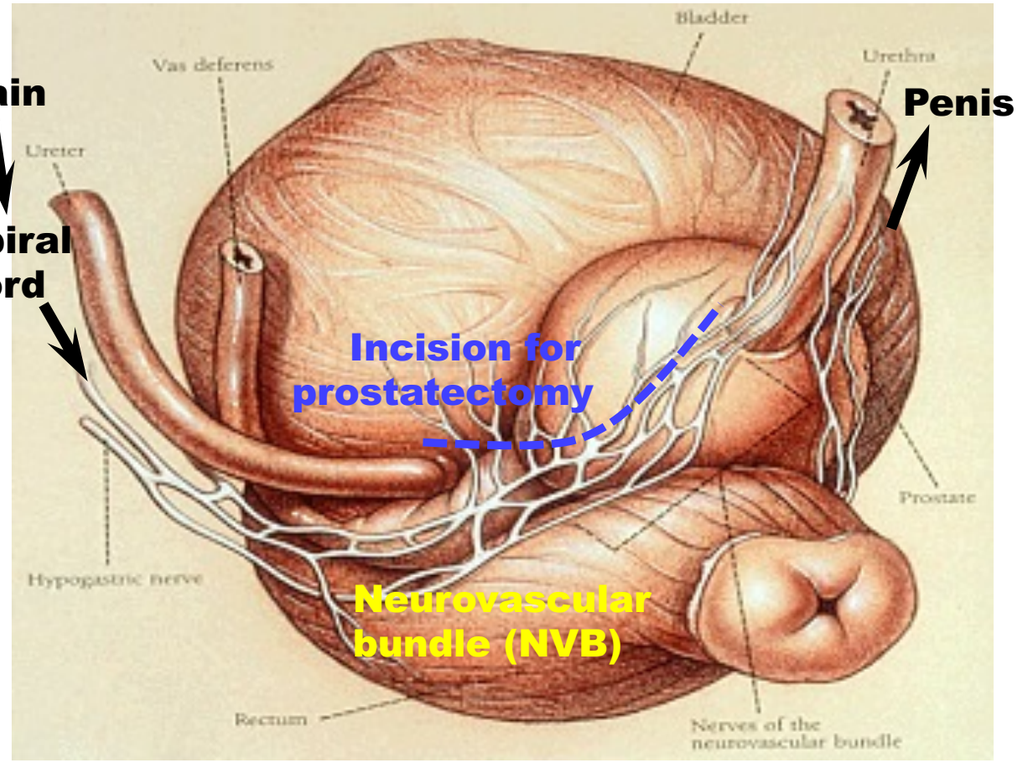

Nerve system surrounding prostatic gland ‡

† A. L. Burnett, *JAMA* **293**(21), 2648--2653 (2005).
‡ https://www.virginiamason.org/radical-prostatectomy

Current state-of-the-art

Fluorophore-based fluorescence imaging †

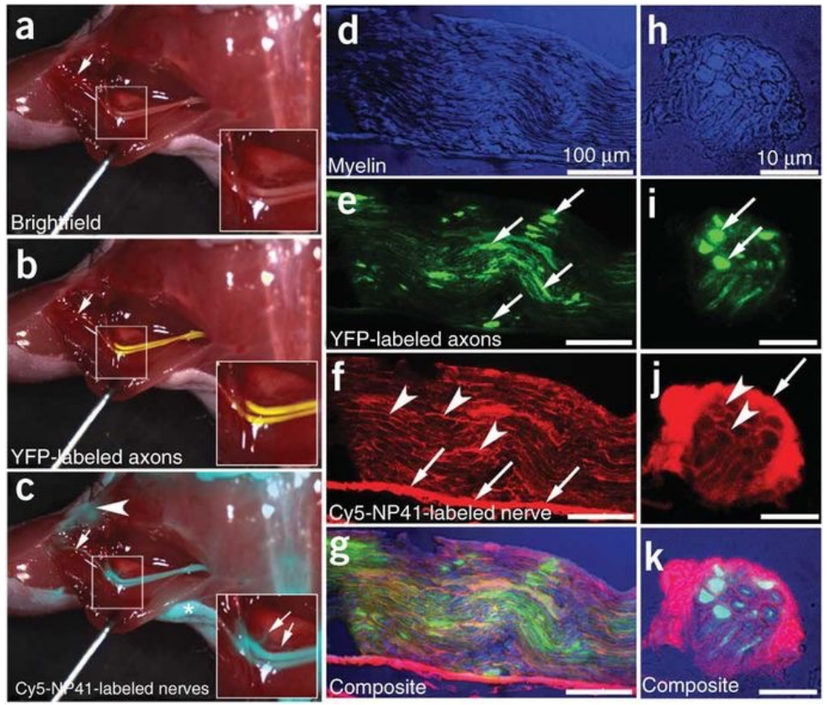

- Concern on tissue toxicity
- Long staining time (2hr – 14 days)

Coherent anti-Strokes Raman spectroscopy

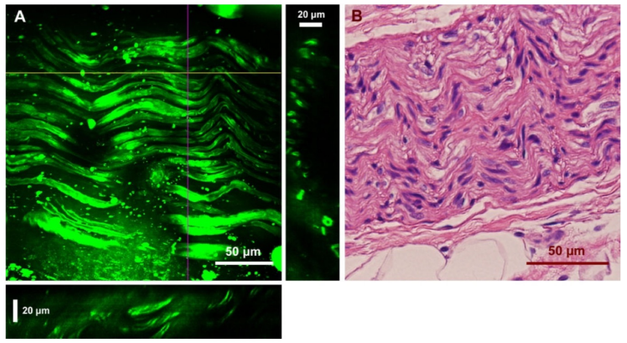

- Slow imaging
- Limited imaging depth

Confocal and Multiphoton microscopy

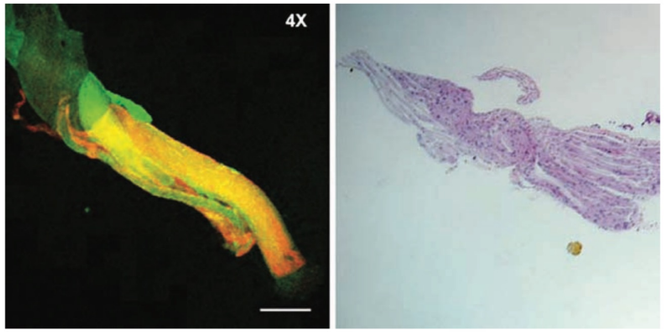

- Not optimized for intra-operative use
- Limited imaging depth

Optical coherence tomography (OCT) ‡

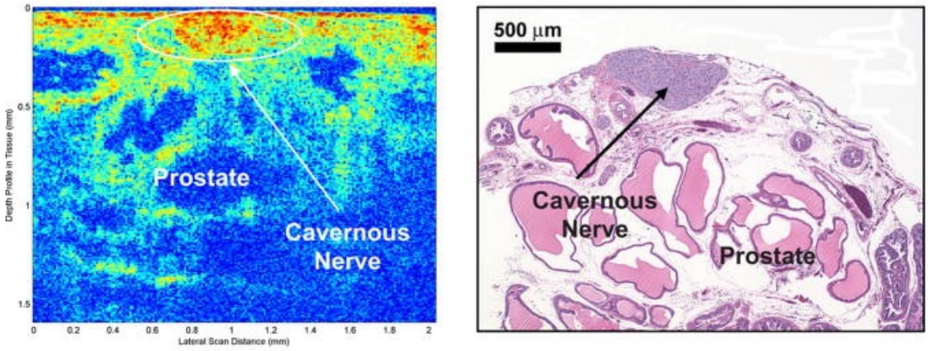

- Lack of nerve-specific contrast
- Limited contrast resolution due to speckle artifacts

Prostate MRI §

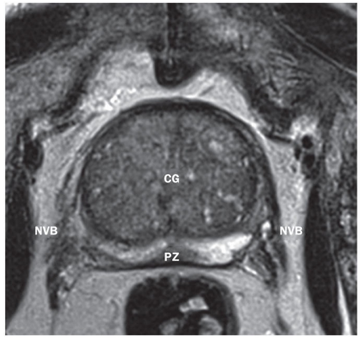

Nature Reviews | Urology

- Slow speed
- Not portable

† M. A. et al. *Nat Biotechnol* **29**, 352–356 (2011).
‡ ChiWhitneytchian, S., et al., *J. Biomed. Opt.* **14**, 014031-14-6 (2009).
§ A. L. Burnett, *Nat. Rev. Urol.* **12**, 451-460 (2015).

Near-infrared VSD mechanism

- Transmembrane redistribution mechanism †,‡

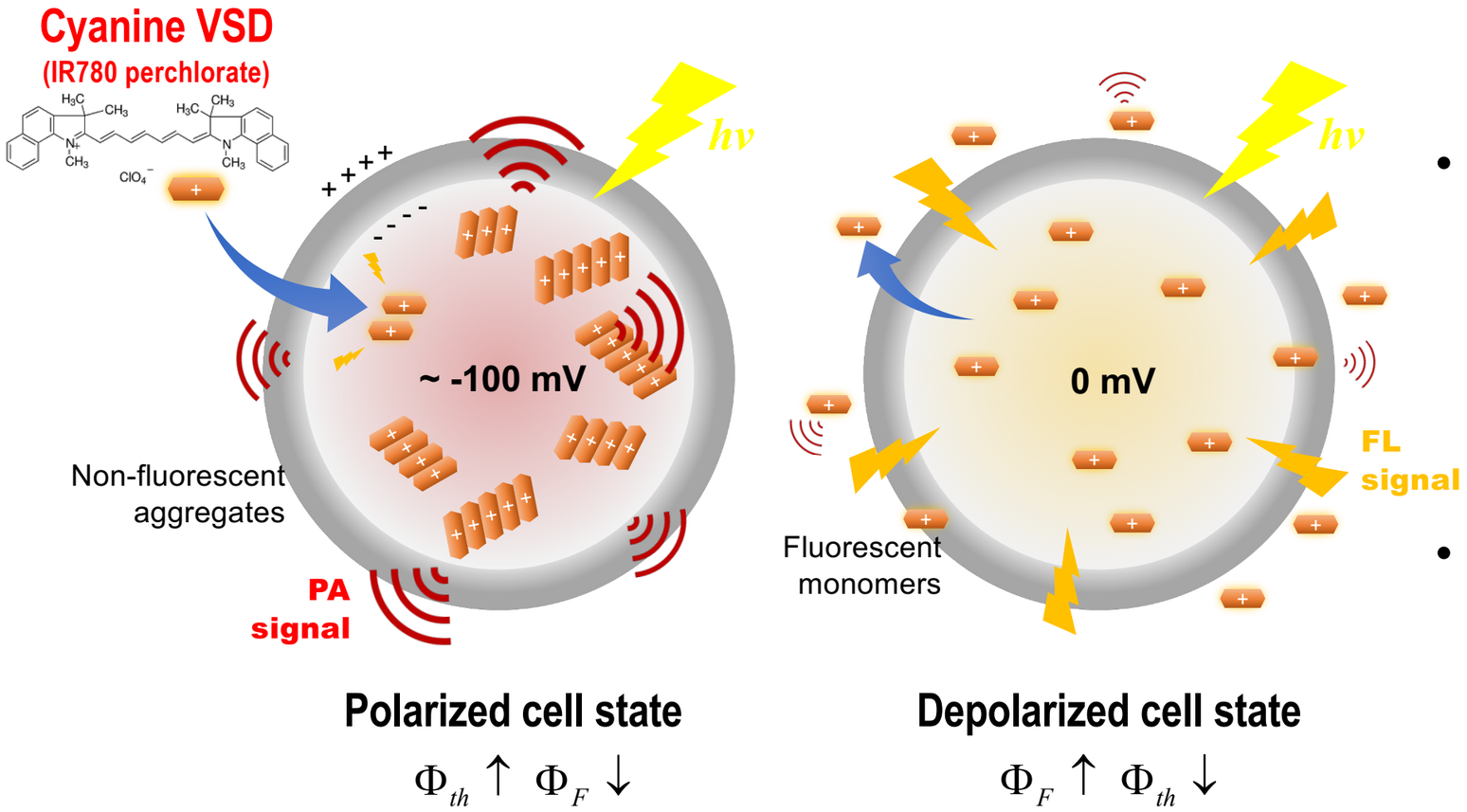

- Polarized cell state
  - Cyanine dye positively charged is attracted into cell membrane
  - The aggregation of VSD leads to fluorescence (FL) quenching, which **increases PA efficiency**
- Depolarized cell state
  - Dispersion of VSD gives **high FL efficiency**

† Zhang, H. K., **Kang, J.**, *et al. J. Biomed. Opt.* **22,** 045006 (2017).

Near-infrared VSD characterization

- Artificial membrane diffusion potential model †,‡

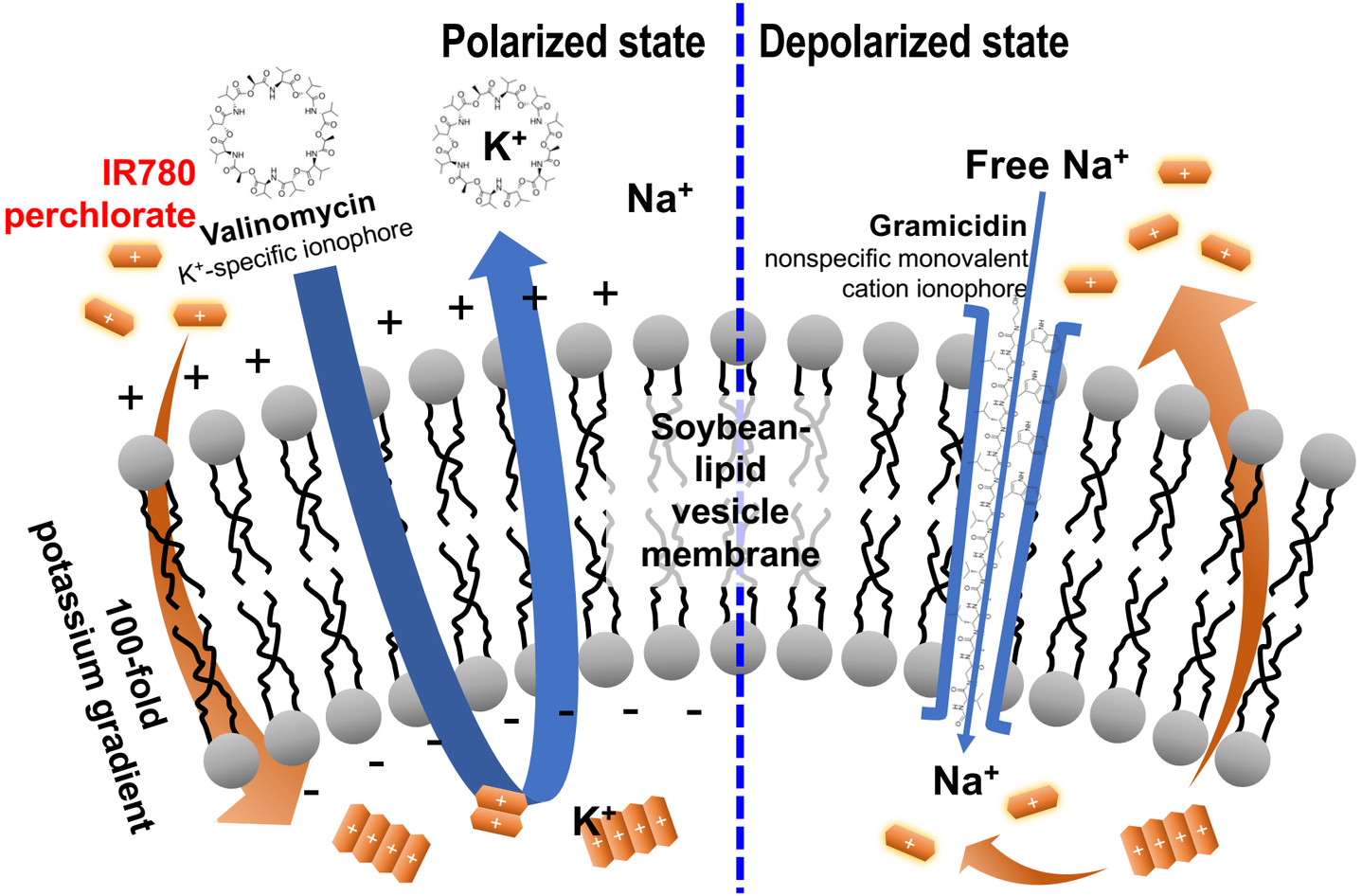

***In vitro* VSD characterization (6μM).** (A) Absorbance and fluorescence emission spectrum of near-infrared VSD. (B) Photoacoustic spectrum and intensity change at the 790 nm of peak absorbance. §

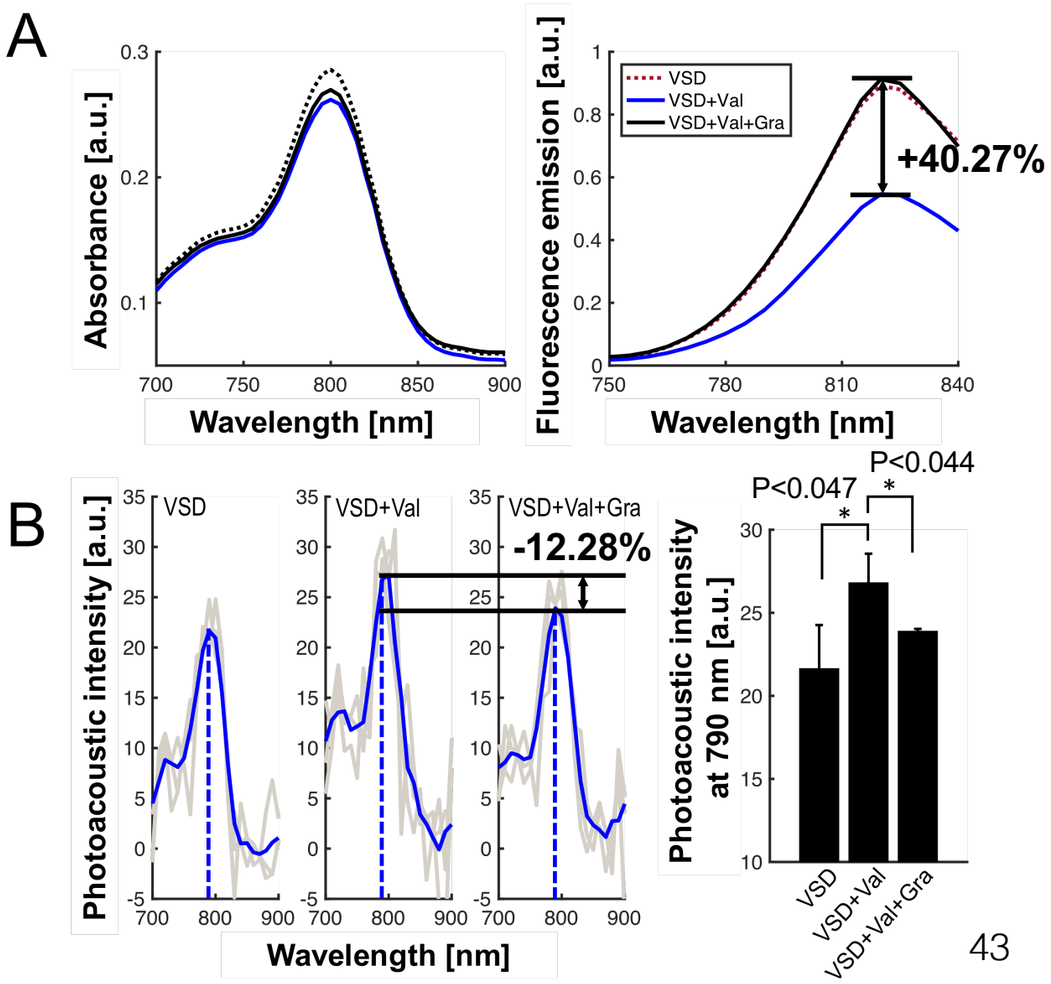

† Gross, E., et al. *Biophys. J.* **67**, 208-216 (1994)
‡ Zhang, H. K., **J. Kang**, *et al. J. Biomed. Opt.* **22,** 045006 (2017).
§ **J. Kang**, et al., *Front Neurosci* **13**(579), 1-14 (2019)

Preliminary evidence of neural sensing

Non-invasive epileptic seizure detection †

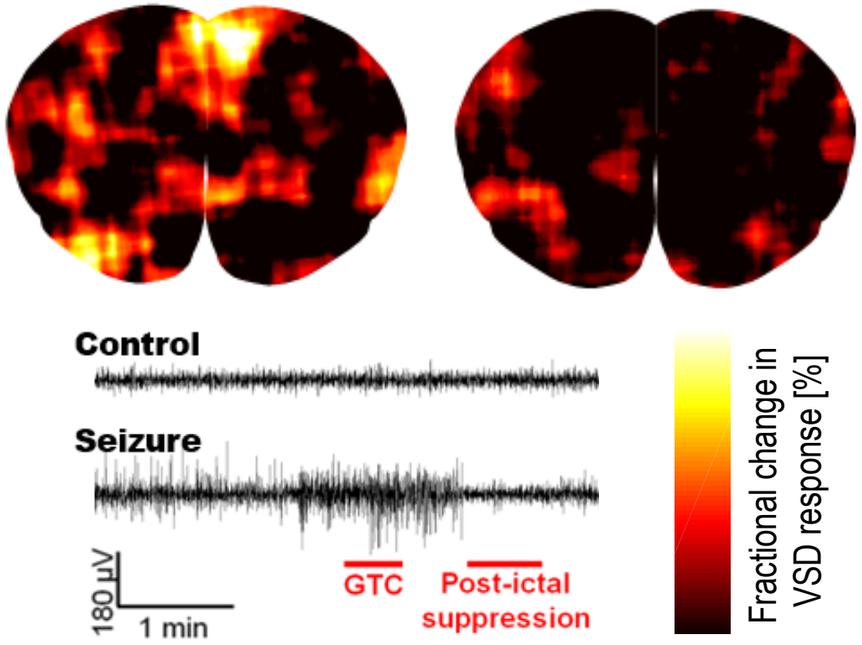

Non-invasive characterization of excitatory neurotransmittance at rat hippocampus ‡

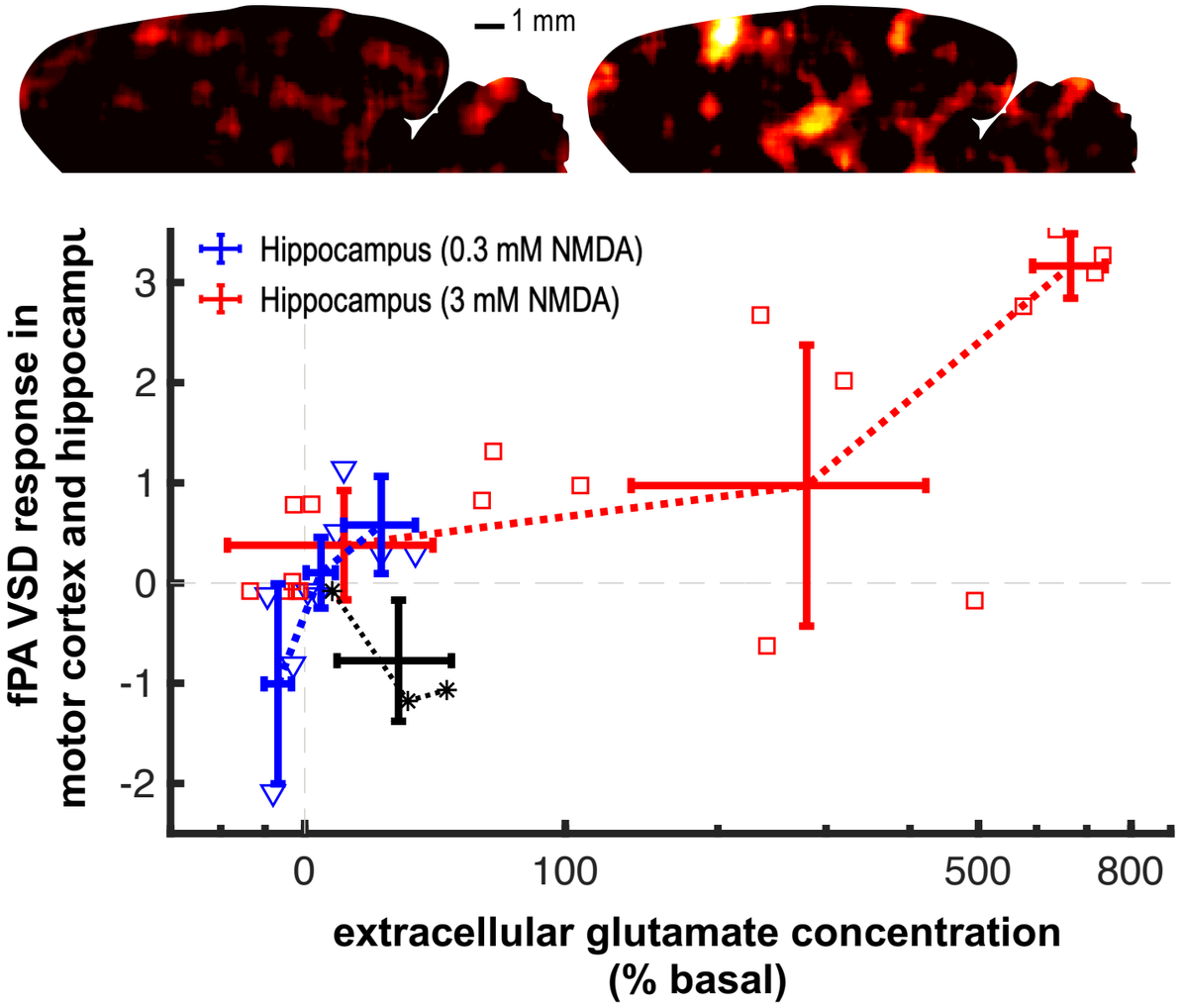

† **J. Kang**, *et al.*, *Front Neurosci* **13**(579), 1-14 (2019)
‡ **J. Kang**, *et al.*, *J Neural Eng* **17**(2), 025001 (2020).

Proposed image-guided nerve-sparing laparoscopic radical prostatectomy

- **Objective:** Image-guided nerve guidance with:
  - **(1) Real-time functional nerve localization** with high specificity,
  - **(2) Short VSD staining duration** (~10 min)
  - **(3) Wide field-of-view** familiar with surgeons, and
  - **(4) Near-infrared imaging** for better transfascial nerve localization

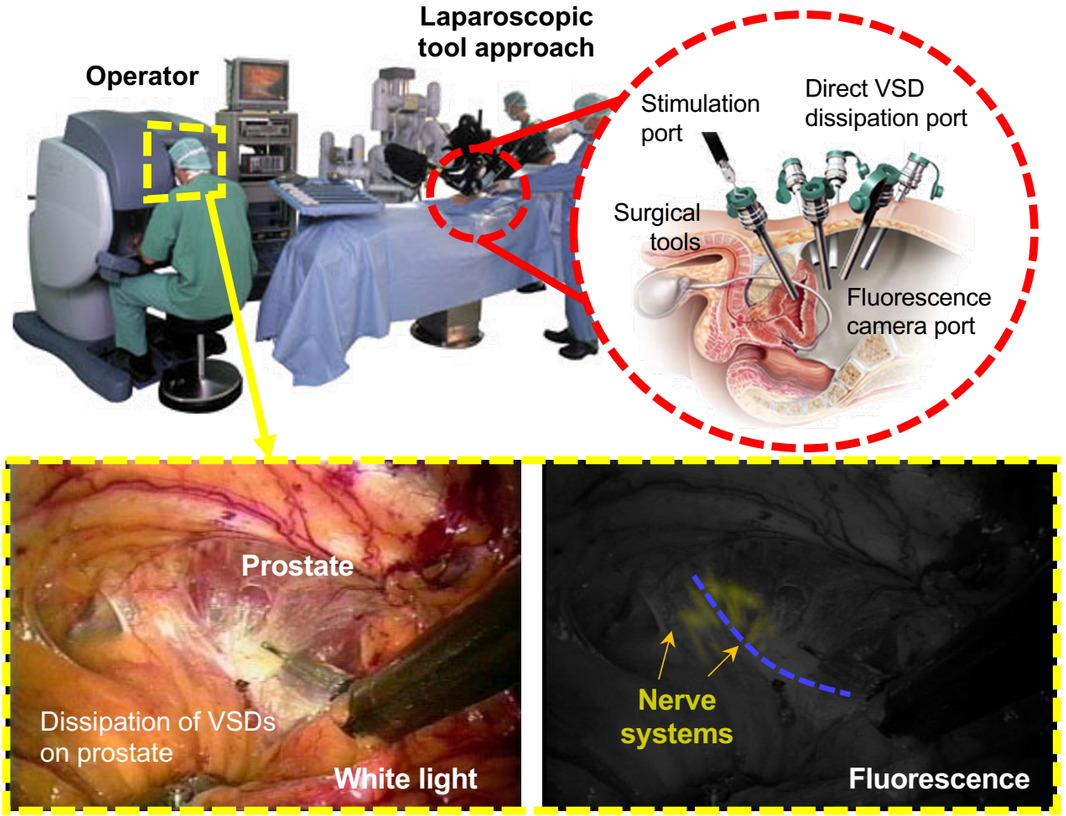

Step 1: Robotic tool approach through the ports on the abdominal incisions,

Step 2: Direct transfascial VSD staining within a time limit up to 10 min,

Step 3: Flushing out of the VSD on the prostate surface which is not bound at tissue membrane,

Step 4: Nerve stimulation for nerve-selective VSD contrast, and

Step 5: Nerve-sparing prostatectomy with the augmented nerve map using intra-operative FL imaging solution

† **J. Kang**, *et al.*, *Sci Rep* **10**, 6618 (2020).

In vivo experimental setup: Imaging system and animal preparation

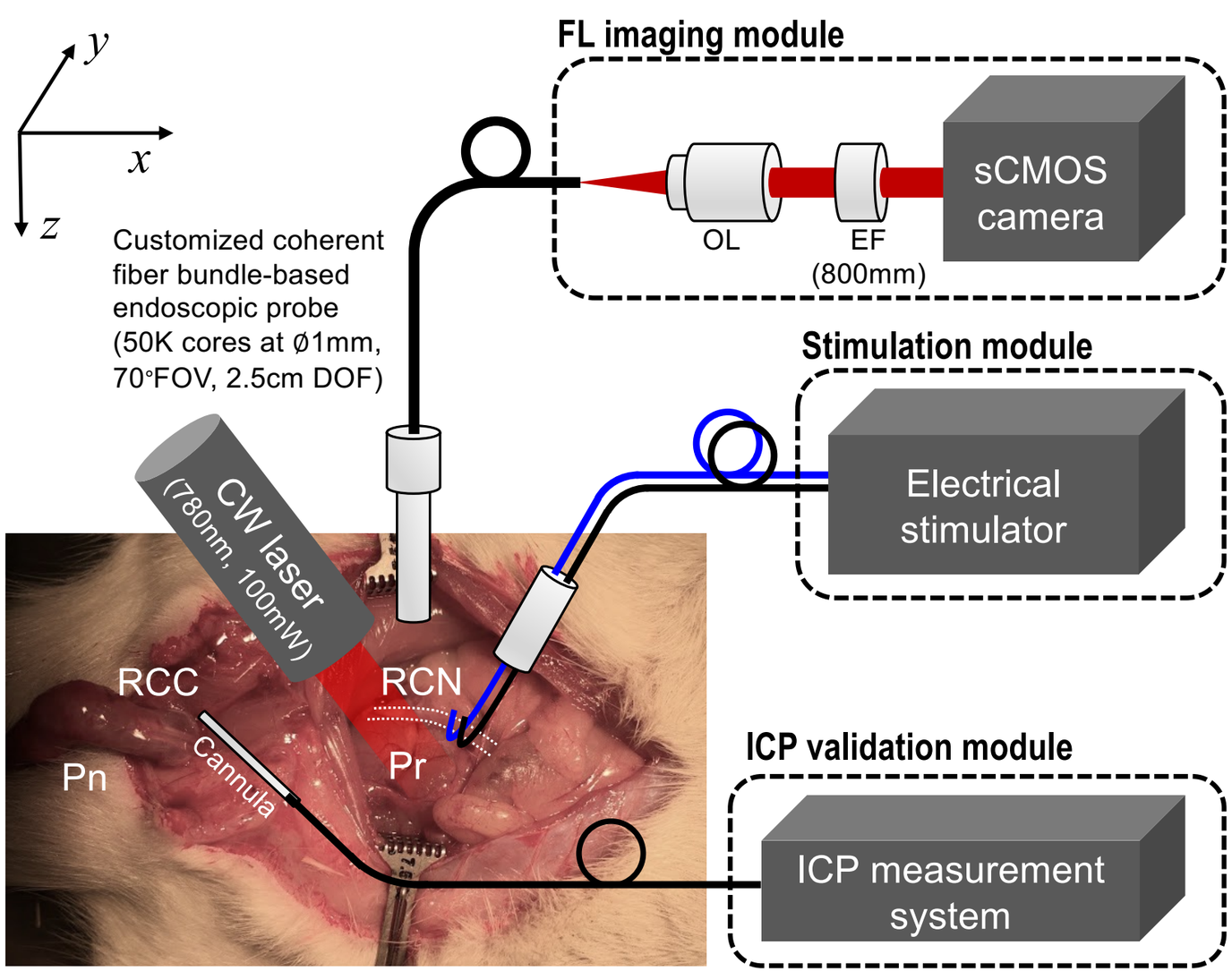

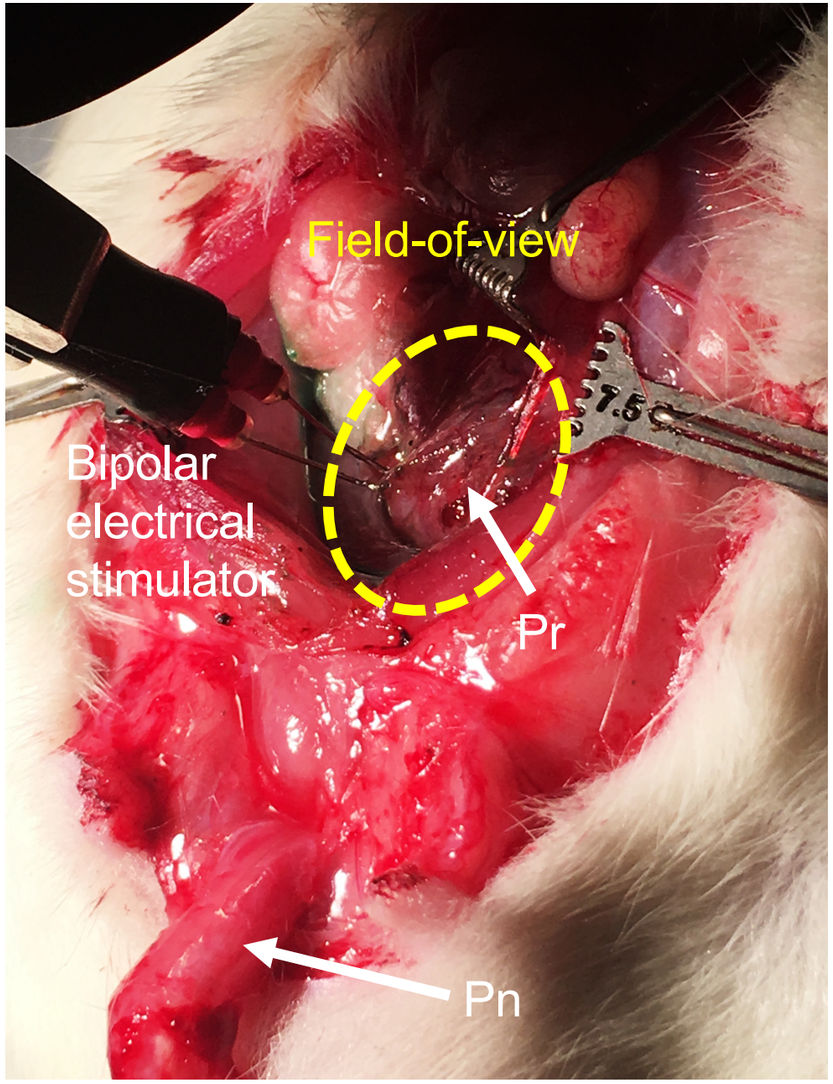

† **J. Kang**, *et al.*, *Sci Rep* **10**, 6618 (2020).

Pr: prostate; Pn: penis; CN: cavernous nerve; RCC: right corpus caverosum; ICP: Intracavernosal pressure

In vivo experimental setup: Imaging and stimulation protocol

- Experimental protocol

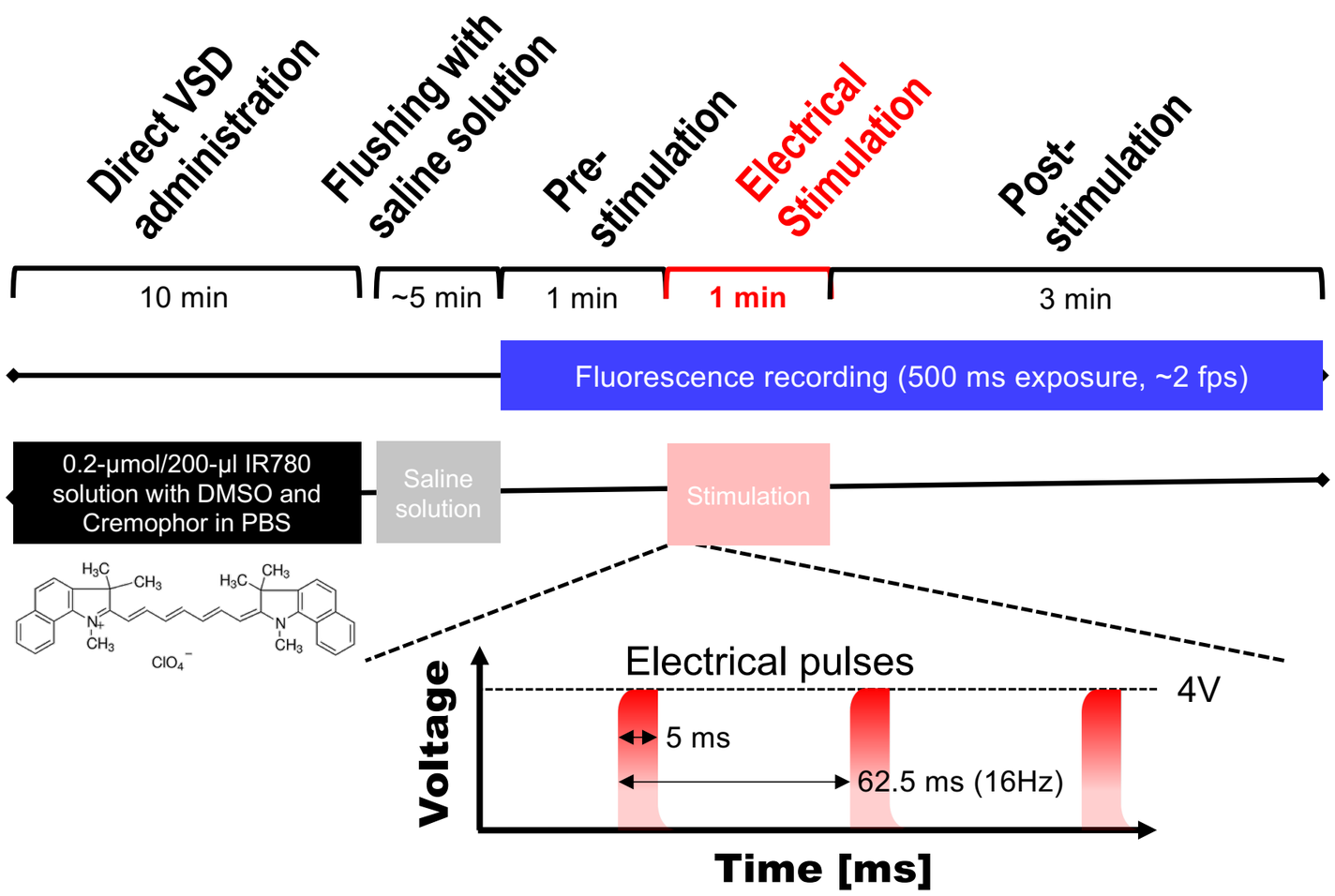

Validation of erectile stimulation

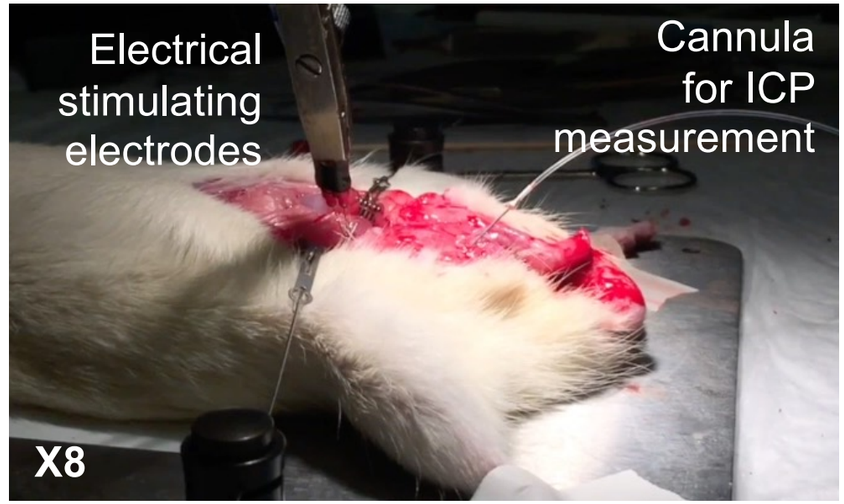

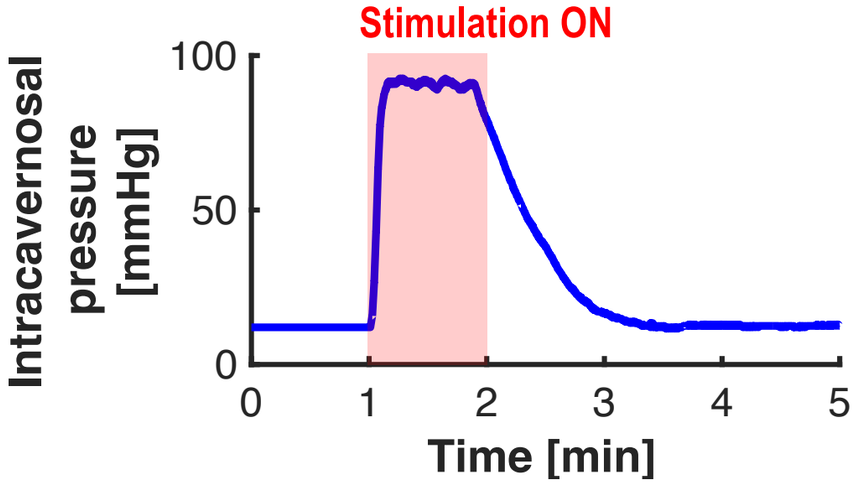

† **J. Kang**, *et al.*, *Sci Rep* **10**, 6618 (2020).

Real-time trans-fascial functional prostate nerve mapping *in vivo*

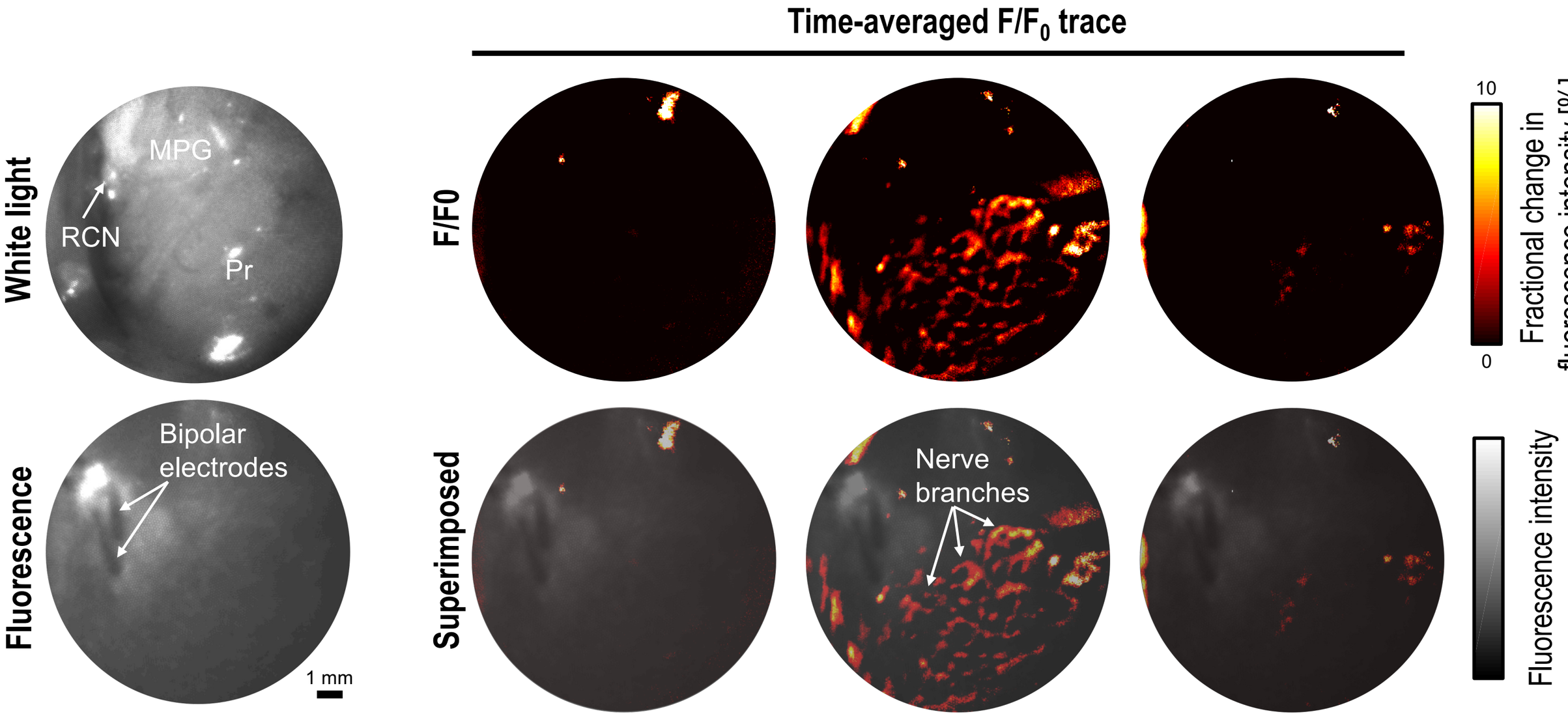

† **J. Kang**, *et al.*, *Sci Rep* **10**, 6618 (2020).

Histological validation of direct VSD delivery

- Successful direct VSD staining on nerve layer below prostatic fascia

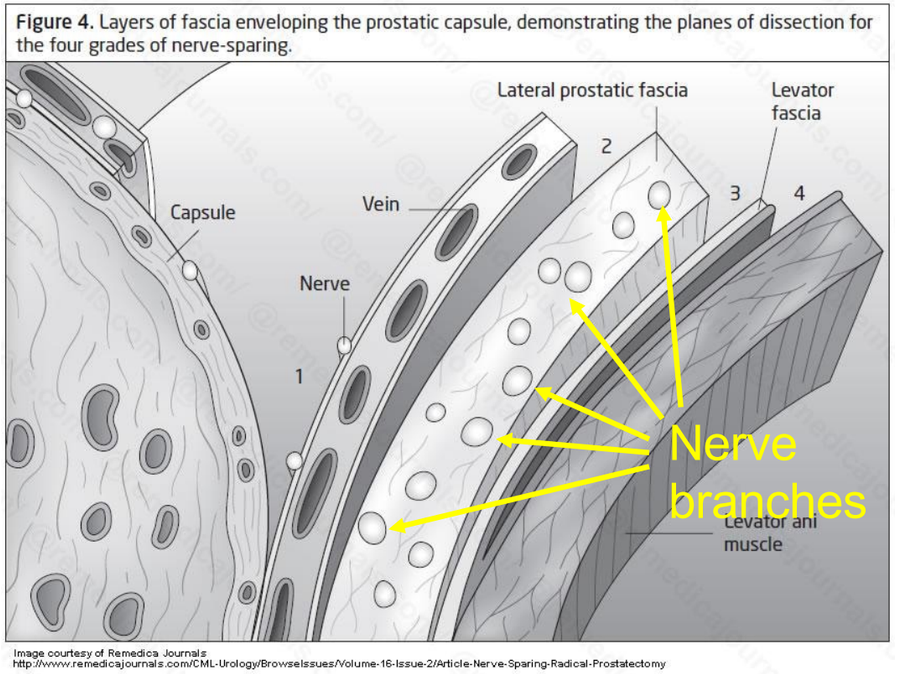

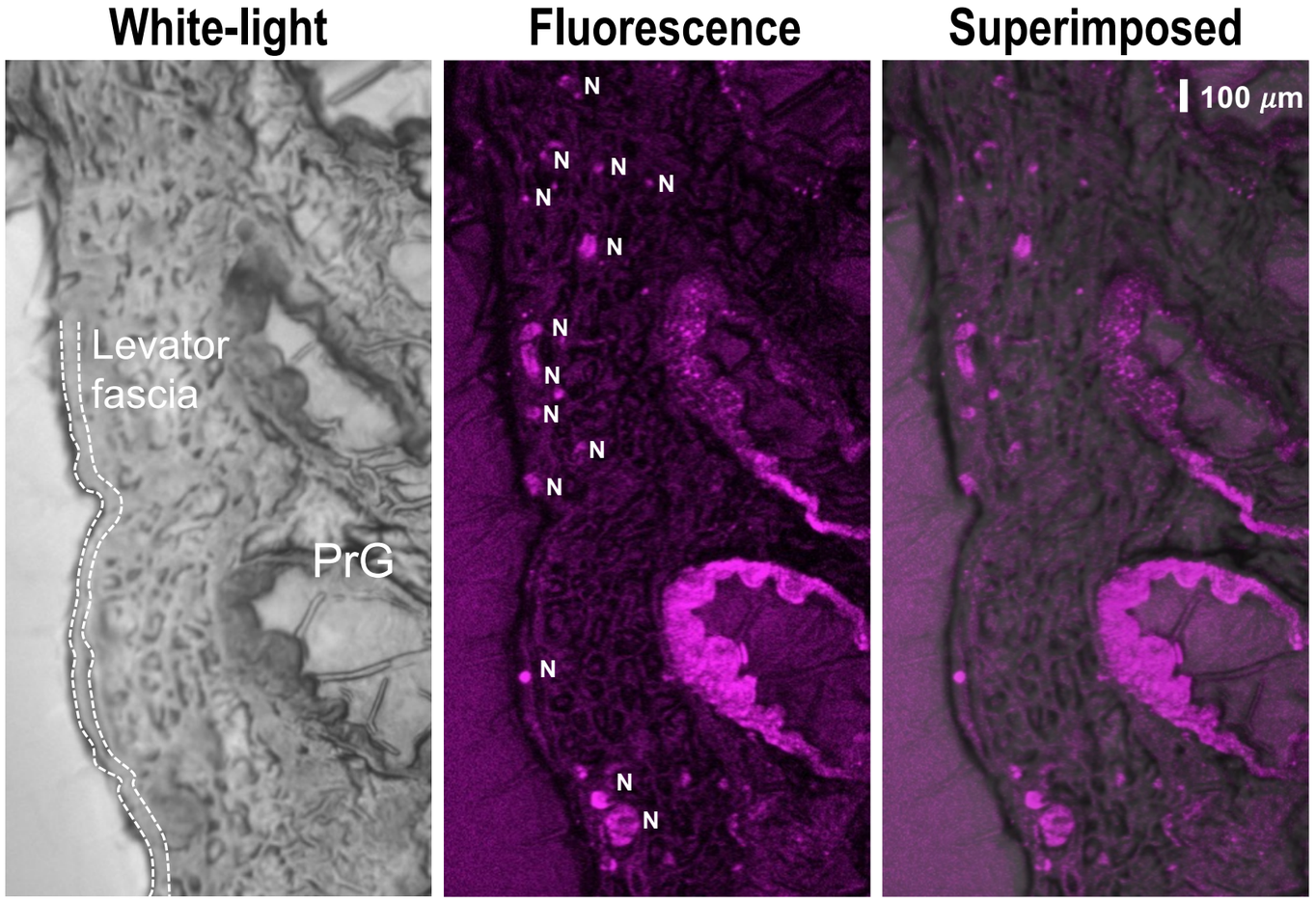

† **J. Kang**, *et al.*, *Sci Rep* **10**, 6618 (2020).

Discussion

- We presented the preliminary results of real-time nerve guidance using dual-modal VSD and near-infrared FL imaging
- Our further works will be focused on
  - Collecting more data for statistical rigor
  - Toxicity study and efficiency evaluation with various VSD concentrations
  - Advance experimental setup to induce selective cavernous nerve blocking
  - Developing pulsed laser-based dual-modal intra-operative guidance system
  - *In vivo* large-scale animal study for evaluating clinical outcome (post-operative erectile dysfunction with functional guidance vs. no imaging guidance)

Defining the right form of “the sixth sense”

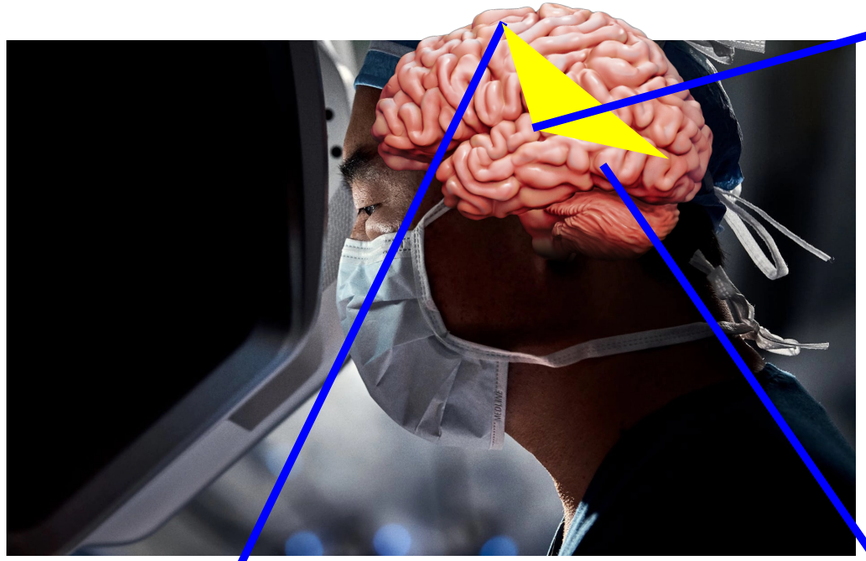

Knowledge in anatomy & surgery

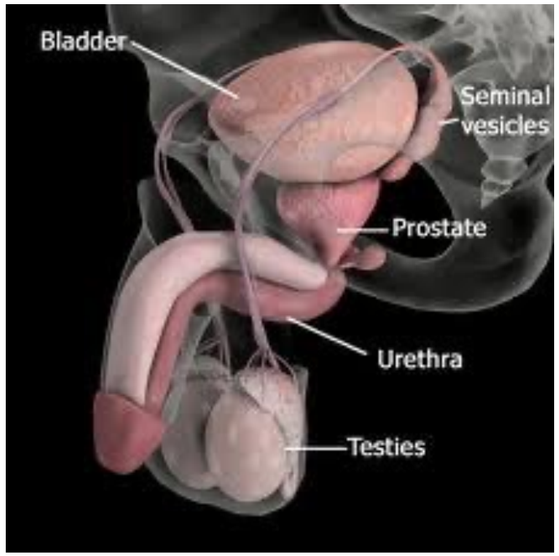

Vision: a dynamic input

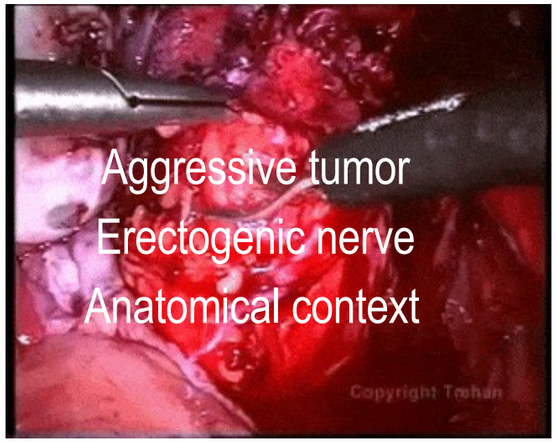

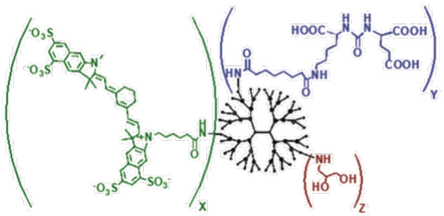

PSMA-targeting agents

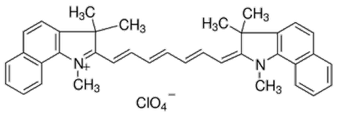

Voltage-sensitive dye

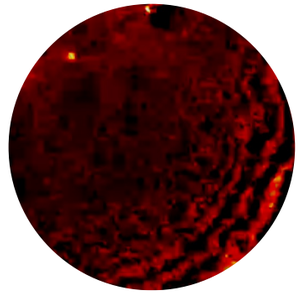

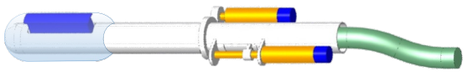

Transformable TRUS/PA x signal processing

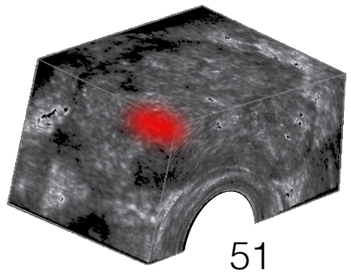

Acknowledgement

- CDMRP PCRP W81XWH-18-1-0188 **(PI)**
- NIH Blueprint MedTech Pilot program **(PI)**
- NIH R41 EB033758 **(MPI)**
- NIH R01 HL139543; R24 MH106083
- Discovery award, Johns Hopkins University

National Institutes of Health
Turning Discovery Into Health

CDMRP

Thank you

JOHNS HOPKINS UNIVERSITY

LABORATORY FOR Computational Sensing + Robotics

MUSiiC Research Laboratory